

**MODELS FOR INTERACTION OF THE TEAR FILM WITH THE
CORNEAL AND CONJUNCTIVAL EPITHELIA**

by

Jennifer L. Bruhns

A thesis submitted to the Faculty of the University of Delaware in partial fulfillment of the requirements for the degree of Bachelor of Science in Quantitative Biology with Distinction

Spring 2013

© 2013 Jennifer L. Bruhns
All Rights Reserved

**MODELS FOR INTERACTION OF THE TEAR FILM WITH THE
CORNEAL AND CONJUNCTIVAL EPITHELIA**

by

Jennifer L. Bruhns

Approved: _____
Richard Braun, Ph.D.
Professor in charge of thesis on behalf of the Advisory Committee

Approved: _____
Christopher Raymond, Ph.D.
Committee member from the Department of Mathematical Sciences

Approved: _____
James Glancey, Ph.D.
Committee member from the Board of Senior Thesis Readers

Approved: _____
Michelle Provost-Craig, Ph.D.
Chair of the University Committee on Student and Faculty Honors

ACKNOWLEDGMENTS

I want to thank my research advisor Dr. Richard Braun for his help and guidance throughout everything.

I also want to thank my parents, Maria and Thomas Prignano, for their continual support.

This material is based upon work supported by the National Science Foundation under Grant No. 1022706 (RJB), the National Institutes of Health R01-EY017951 (PEKS) and the Howard Hughes Medical Institute (JLB).

TABLE OF CONTENTS

LIST OF TABLES	vii
LIST OF FIGURES	ix
ABSTRACT	xii
 Chapter	
1 INTRODUCTION	1
1.1 Tear Film and Dry Eye	2
1.2 Anatomy of the Eye	4
1.2.1 Ocular Surface	4
1.2.2 Eyelids and Eyebrows	4
1.2.3 Lacrimal System	5
1.2.4 The Conjunctiva	5
1.2.5 The Cornea	7
1.2.5.1 Corneal Metabolism	8
2 MODELS FOR THE TEAR FILM AND WATER TRANSPORT IN THE EPITHELIA	11
2.1 Theoretical Models	13
2.1.1 Tear Film Model	13
2.1.2 Corneal Epithelial Cells and Model	15
2.1.3 Conjunctival Epithelial Cells and Model	16
2.2 Results	18
2.2.1 Experimental results	18

2.2.2	Theory for the Tear Film Alone	20
2.2.3	Theory with the Corneal Epithelium	21
2.2.3.1	Single Interblink	21
2.2.3.2	Multiple Interblinks	24
2.2.3.3	Permeability Study	27
2.2.4	Theory with Conjunctival Epithelium	30
2.2.4.1	Single Interblink	30
2.2.4.2	Multiple Interblinks	32
3	INCLUDING METABOLIC REACTIONS: TEAR FILM AND EPITHELIUM	36
3.1	Introduction	36
3.2	Proposed Model	37
3.2.1	Initial Conditions	38
3.2.2	Inner Cell Equations	39
3.2.3	Tear Film Equations	45
3.2.4	Boundary Fluxes	48
3.2.4.1	Tear Film/Air Interface	49
3.2.4.2	Tear Film/Epithelial Cell Interface	51
3.2.4.3	Epithelial Cell/Epithelial Cell Interface	53
3.2.4.4	Epithelial Cell/Stroma Interface	55
4	DISCUSSION	57
4.1	Cornea and Conjunctiva	57
4.2	Corneal Metabolism	59
Appendix		
A	PARAMETERS FOR CHAPTER 1	62
B	CODES FOR CHAPTER 1	64
B.1	Equations for Cornea	64
B.2	Permeability Studies Single Blink	65
B.3	Permeability Studies Multiple Blink	70

B.4	Single Blink Cornea	78
B.5	Multiple Blink Cornea	83
B.6	Equations for Conjunctiva	88
B.7	Single Blink Conjunctiva	88
B.8	Multiple Blink Conjunctiva	93
C	PARAMETERS FOR CHAPTER 3	99
	BIBLIOGRAPHY	103

LIST OF TABLES

2.1	Results for the tear film and epithelial thicknesses and osmolarities at the end of a single 90s interblink. The osmolarity c has units of mOsM; the thickness ratios h_i (cornea) and y_i (conjunctiva) are dimensionless. Dimensional thicknesses for the tear film and the cell layers are given in the parentheses in μm	23
2.2	Results for the corneal epithelium showing ending values of the decrease fraction for the tear film $h(t_{\text{end}})$, each cell layer $h_i(t_{\text{end}})$ and the osmolarity $c(t_{\text{end}})$. The osmolarity c has units of mOsM; the thickness ratios are dimensionless. The dimensional thickness of each layer is given in μm in parentheses.	27
2.3	Results for the conjunctival epithelium showing ending values of the decrease fraction for the tear film $y(t_{\text{end}})$, each cell layer $y_i(t_{\text{end}})$ and the osmolarity $c(t_{\text{end}})$. The osmolarity c has units of mOsM; the thickness ratios are dimensionless. The dimensional thicknesses are given in parentheses in μm	33
A.1	Parameter definitions and values. Unless otherwise noted, these values were used to generate the computational results. K and \bar{K} are chosen to satisfy the experimentally measured thinning rate. α and A^* are recovered from the nondimensional parameters in Winter <i>et al</i> [1]. Ajaev and Homsy [2] discuss α and K	63
C.1	Initial Concentrations in the tear film. These values were taken from the initial concentrations in [3]. The initial osmolarity in the tear film is 300 mOsm. Note: Osmolarity is the sum of the concentrations of sodium, chloride, bicarbonate, and lactate.	99
C.2	Henry's Constants and valence values.	100
C.3	Initial Concentrations in the epithelial cells. Here $j = 1$ to $j = 7$. These values were taken from the steady state results in [3].	100

C.4	Constants concentrations in the stroma. These values where taken from the steady state results in [3].	101
C.5	Parameters in proposed model. These values where taken from [3].	102

LIST OF FIGURES

1.1	This shows the layers of the tear film. The most posterior to anterior layers are; the mucin layer, aqueous layer and the lipid layer. Their relative thickness is specified in the picture.	2
1.2	This figure shows the anatomy of the eye. In our model, we focus on the cornea and conjunctiva. This picture was taken from [4].	4
1.3	Corneal metabolism in the epithelial cells. Three metabolic processes can occur; glycolysis, fermentation or the Krebs cycle.	9
2.1	Schematic drawing for the corneal model. In this figure, $c(t)$ represents the concentration in the tear film, $h(t)$ represents the thickness of the tear film and $h_i(t)$ represents the thickness of the epithelial cell layers such that $i = 1$ through 7.	13
2.2	Fluorescent images at, A, 2 s and, B, 57 s after a blink. Arrows in A show circular areas used for averaging intensities over the cornea and conjunctiva. [5]	19
2.3	(A) Examples of fits of models for thinning of the pre-corneal tear film in two subjects. (B) Average thinning curve for the pre-corneal tear film together with a least squares fit of the model. [5]	19
2.4	(A) Examples of fits of a model for thinning of the pre-conjunctival tear film in two subjects. (B) Average thinning curve for the pre-conjunctival tear film together with a least squares fit of the model. [5]	20

2.5	This figure models a single interblink over a 90 second interval for the corneal model. Plots (a) and (b) are for a thinning rate of $2.5 \mu\text{m}/\text{min}$. Plot (a) shows the tear film concentration and thickness. The upper curve is the concentration increase in the tear film and the curve on the bottom is the tear film thickness decrease. Plot (b) shows the fractional thickness of each layer in the epithelium. The curves from bottom to top represent the anterior to posterior layers of the cornea, respectively. Plots (c) and (d) show the variables but the thinning rate is $10\mu\text{m}/\text{min}$	22
2.6	Results for the corneal model with multiple blinks are shown here for the $2.5\mu\text{m}/\text{min}$ thinning rate. Plots (a) and (b) represent the thickness decrease fraction in the epithelial cells and the osmolarity increase in the tear film and epithelium for repeated 6s interblinks over 4 hours. In plot (b) the top curve is the osmolarity of the tear film and the curves below it are the osmolarity in the layers. Plots (c) and (d) are similar results for 30s interblink intervals.	25
2.7	This is the final decrease fraction in each corneal epithelia layer (h_1 to h_7) after 90 seconds while varying \bar{P}_f	28
2.8	While varying \bar{P}_f , this is the final osmolarity in the tear film(h) and layers (h_1 to h_7) after after 4 hours of blink intervals of 6 seconds. The tear film is the top blue line and the epithelium layers from anterior to posterior are under the tear film curve.	29
2.9	While varying \bar{P}_f , this is the final osmolarity in the tear film (h) and layers (h_1 to h_7) after after 4 hours of blink intervals of 30 seconds. The tear film is the top blue line and the epithelium layers from anterior to posterior are under the tear film curve.	29
2.10	This figure models a single interblink over a 90 second interval for the conjunctival model. Plots (a) and (b) are for a thinning rate of $1.4 \mu\text{m}/\text{min}$. Plot (a) shows the tear film concentration and thickness. The curve on top is the concentration increase in the tear film and the curve on the bottom is the tear film thickness decrease. Plot (b) shows the fractional thickness of the epithelium. The curves from bottom to the top represent the anterior to posterior layers of the cornea.	31

2.11	Results for the conjunctival multiple blink model are shown. Plots (a) and (b) show the thickness decrease fraction in the epithelium and the osmolarity increase in the tear film and epithelium for repeated interblinks of 6 s and a thinning rate of 1.4 $\mu\text{m}/\text{min}$ over a period of 4 hours. In plot (b) the top line is the osmolarity of the tear film and the lines below are the osmolarity in the layers. Plots (c) and (d) are the same results but for repeated interblinks of 30 s each.	32
3.1	This is the schematic drawing of the proposed model. There is a tear film layer ($j = 0$), with seven epithelial layers ($j = 1$ to $j = 7$) and the stroma. The cells will be referred to as the j^{th} cell with the j^{th} membrane located anteriorly and the $(j + 1)^{\text{st}}$ membrane located posteriorly in regards to the j^{th} cell.	38
3.2	Inside Cell j	40
3.3	A schematic drawing of the tear film. This includes the equations that are applied in the tear film. There are two cases each for oxygen and carbon dioxide concentrations and the pH. If one choose to keep the variable constant (C_O , C_C or C_H) constant then the equations that are used for that conditions are under that constant choice. If one choose to allow the variable to change (C_O , C_C or C_H) then the equations that are used for that condition are under that change choice.	46
3.4	Tear Film/ Air Interface $j = 0$. There is a flux of water (J_V) out of the tear film due to evaporation. Solutes and metabolites have no flux between the tear film/air interface. The equation for the flux of oxygen and carbon dioxide at this boundary are still to be determined. The $\Delta\psi$ value was taken from [3].	50
3.5	Tear Film/ Epithelial Cell Boundary $j = 1$	52
3.6	Epithelial Cell/Epithelial Cell Interface ($j = 2, 3, 4, 5, 6, 7$)	54
3.7	Epithelial Cell/Stroma Interface ($j = 8$)	56
4.1	A sketch of the locations decribed by the theoretical models and the experimental measurements. The central cornea (A) and the conjunctiva not far from the limbus (B) are locations considered. C denotes the meniscus in the temporal canthus and represents the location used for TearLab or similar measurements.	58

ABSTRACT

Mathematical models that connect the tear film with the underlying epithelia of the cornea and conjunctiva were developed. The tear film is assumed to be a spatially uniform evaporating aqueous layer with a concentration variable representing the osmolarity in the tear film. In the first model, the underlying epithelia are approximated as in Levin and Verkman [6], with a few layers of cells of varying thickness that are linked via osmosis between each of the cells and with the tear film. Loss of water due to evaporation from the tear film causes increased osmolarity there, leading to osmotic flow from the epithelium to the tear film, and between the epithelial cells. The parameters are set by comparison with thinning rate measurements from human subjects *in vivo*. In those experiments, 5% fluorescein solution is instilled in the tear film, and the thickness of the tear film is deduced from subsequent intensity measurements in the concentrated fluorescein regime. These measurements were used to calibrate the model parameters for osmosis. A second model is proposed that includes the molecules involved in metabolism in the epithelial cell of the cornea. This model is based on the Leung *et al* model [3]. The proposed model includes differential and algebraic equations to represent the concentrations of the metabolites in the cells and their effects over time. Both models are used to predict tear film thickness and osmolarity, as well as epithelial cell layer thicknesses and osmolarities. The first model predicts thickness and osmolarity changes for single interblinks and for extended periods of many blink cycles with constant interblink duration. Cumulative effects from multiple blink cycles are seen that are significantly more than for single interblinks. We interpret the results in light of biochemical response and the rate of progression of apoptosis in squamous cells.

Chapter 1

INTRODUCTION

This thesis consists of two models for the tear film on the ocular surface and the tissue beneath it. The models focus on the tear film and the cornea. The first model in Chapter 2 is based on one model by Levin and Verkman [6] for the epithelial cells of mice. In the Levin and Verkman model, a fixed concentration perfusate was placed after a stack of mice epithelial cells to measure the water transport through the cell membranes. They used their experimental data to determine the permeability of water through the epithelial membranes. Their model used a system of ordinary differential equations for five cell layers with their measured permeability to determine the thickness changes due to water transport in each cell layer. In our model, the Levin and Verkman model is converted to a human model by increasing the number of cellular layers and also incorporates a tear film driven by evaporation [7]. This first model yields the osmolarity and thickness changes in the cells and tear film which are a result from water permeation through the cell membranes.

The second model in Chapter 3 is based on a model by Leung *et al* [3] that includes corneal metabolism and water transport in the presence of a contact lens. There were no distinct cellular layers present in their model, ordinary differential equations for concentrations as a functions of a continuous space variable across the epithelium, stroma and contact lens were used. The Leung *et al* model focused on corneal swelling from simulating which metabolic molecules and ions would be present throughout the cornea. The epithelium and stroma were treated as continuous variables in space. In our proposed model, we created discrete cellular layers in the epithelium and convert the stromal conditions to boundary conditions for the ordinary differential equations in the epithelial. Thus we consider the

changes in metabolism at a cellular level. In addition, the proposed model also incorporates a tear film driven by evaporation [7]. The resulting thinning and increased osmolarity in the tear film are expected to cause changes throughout the epithelial cell layers.

1.1 Tear Film and Dry Eye

A tear film covers the surface of the eye and is exposed to air. There are three layers to the tear film. The layer exposed to the air is a lipid layer of meibomian lipids provided from the meibomian glands in the tarsal plates in the eyelids [8,9]. The lipid protects the aqueous layer beneath from evaporation and creates a smooth surface to enhance the refractive power. The layer posterior to the lipid layer is an aqueous layer. This layer consists primarily of water, but also has small concentrations of various proteins and salts [8]. Immunoglobulins are also present in the aqueous layer, which strongly inhibits infections from occurring [8]. The layer posterior to the aqueous layer is a mucus layer formed mostly by transmembrane glycoconjugate proteins but also from secretions of goblet cells. The mucus layer provides a lubrication to the epithelial cells beneath it which then protects the cells and provides comfort.

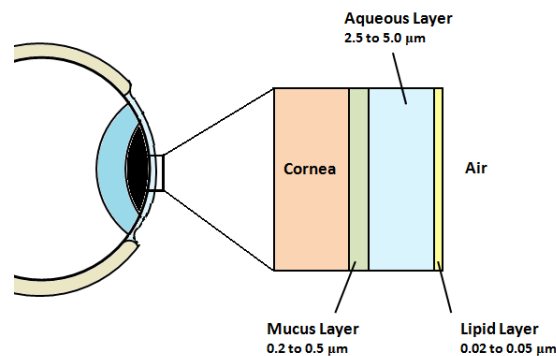


Figure 1.1: This shows the layers of the tear film. The most posterior to anterior layers are; the mucin layer, aqueous layer and the lipid layer. Their relative thickness is specified in the picture.

Dry eye is a disease that causes discomfort to the eye. About 3.23 million women and 1.68 million men which adds to about 4.91 million Americans above the ages of 50 years old suffer from dry eye [10]. Dry eye impairs and degrades visual performance [10]. Therefore, by understanding the tear film thinning and osmolarity increase in the tear film and underlying cells, one can better understand how to diagnose it accurately and better cure it.

Osmolarity is the measure of ion solute concentration in a solution. In the tear film that covers the eye the solution is water and some of the many solutes are sodium ions, chloride ions, and bicarbonate ions. An osmolarity that is increasing means that the ratio of solute per solution is increasing. Hence, the amount of solute is increasing or the amount of solution is decreasing. We assume in our models that the amount of solution is decreasing through evaporation. In the second model, we allow the ion concentration to change in the tear film due to metabolic reactions in the epithelium. The normal osmolarity of the tear film is about 300 mOsm. An osmolarity of above 318 mOsm is considered high enough for diagnosis of dry eye. The threshold to feel discomfort and pain in the eye is equal to or above 450 mOsm according to Liu *et al* [11].

1.2 Anatomy of the Eye

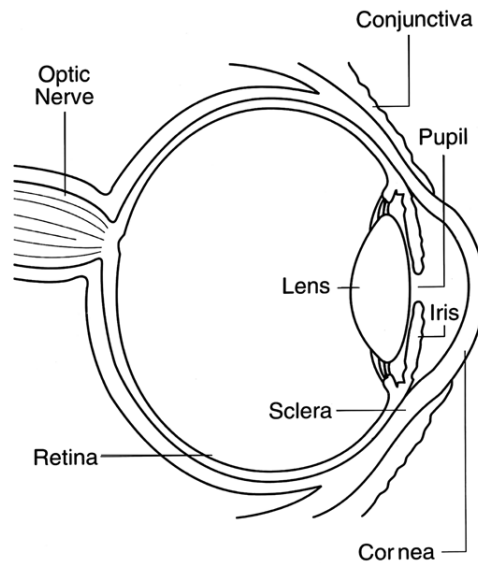


Figure 1.2: This figure shows the anatomy of the eye. In our model, we focus on the cornea and conjunctiva. This picture was taken from [4].

1.2.1 Ocular Surface

The ocular surface is made up of surface and glandular epithelia of the cornea, conjunctiva, lacrimal gland, and meibomian gland, and the nasolacrimal duct. All components of the system are linked functionally by continuity of the epithelium, by innervation, and by the endocrine, vascular, and immune systems [12].

1.2.2 Eyelids and Eyebrows

There is an upper and lower eyelid for each eye. The upper eyelid is larger and more mobile compared to the lower eyelid. They meet at a medial and lateral corners known as the canthi. The opening of the eyelids is known as the palpebral fissure and the maximal opening of the sagittal plane is roughly 8 to 11 mm. Together the eyelids provide lubrication to the surface of the eye. When the eye is fully closed, the entire cornea should be covered. The eyelid margins are about 2 mm thick and 30 mm long. The lateral portion

is squared off, whereas the medial portion is rounded. The anterior border of the margins have 2 to 3 layers of eyelashes. The eye lashes on the superior lid curl up and the eye lashes on the bottom lid curl down. They help protect the eye from foreign particles and debris entering into the tear film onto the ocular surface. There is also a punctum on each margin near the medial canthus. The punctum is about 0.3 mm and is an outlet that drains excess tears. In addition there are also tarsal gland or meibomian gland which open onto the eyelid margin [8]. The meibomian gland is the primary source of the lipid layer on the ocular surface.

The eyebrows lie above each eye. They are positioned where the forehead and the upper lid meet. They are composed of thick hair which helps protect things from entering the ocular surface [8].

1.2.3 Lacrimal System

There are two subsections to the lacrimal system. The first is the secretory system which delivers tears via the tarsal gland to the eye. The second is the excretory system which disposes of excess tears via the punctum from the eye [8].

1.2.4 The Conjunctiva

The conjunctiva is a vascular mucous membrane that covers the anterior globe and inner surfaces of the eyelids. The bulbar conjunctiva covers the globe of the eye. The palpebral conjunctiva covers underneath the eyelids which meets at the fornix [8]. We will focus on the bulbar conjunctiva.

The bulbar conjunctiva is loosely attached and has a continuous stroma and epithelium that sits anterior to the sclera. The stroma is made up of two distinct parts; loose connective tissue and a deeper fibrous layer of elastic tissue, nerves, lymphatics, blood vessels and glands [13]. The epithelium is comprised of about four cell layers. It can range from 20 cells thick near the limbus and two cell layers thick medially and temporally. Posteriorly, cells are basal cells then anteriorly cells are squamous. There are goblet cells that are not

uniformly distributed through the conjunctiva. These goblet cells secrete mucus by bursting into the tear film that sits on top of the epithelial layer. The mucus lubricates the epithelial cells' anterior surface and provides protection from foreign objects and the moving upper lid [14]. Goblet cells are about 10 to 20 μm in diameter and become larger as they approach the anterior surface [15].

The bulbar conjunctival epithelium (BCE) varies thickness in different quadrants of the eye. The inferior quadrant has the largest mean thickness of about 47 microns. The nasal, temporal and superior quadrants have BCE thicknesses of about 40 μm , 40 μm and 42 μm respectively. In dry eye and other diseases such as glaucoma, the thickness of the BCE increases significantly [16].

In the epithelium the deepest cells are cylindrical cells. The intermediate layer of cells are polyhedral cells and the most superficial are squamous cells [15]. From the limbal conjunctiva to the nasal region and from the limbal conjunctiva to the temporal region, the number of cellular layers decreases. However, the deepest layer always contains cylindrical basal cells. The conjunctiva epithelia cells are attached by desmosomes like corneal epithelial cells, but the intracellular space is wider than the corneal cells [17]. In addition, the squamous epithelial cells have microvilli on the surface [15]. These microvilli are between 0.5 and 1 μm in height and about 0.5 μm thick. The apical side of the microvilli contain glycocalyx, a transmembrane protein, on their surface which is responsible for the wettability of the surface and binding to mucin [14, 17].

The episclera is posterior to the conjunctiva. It is a loose connective tissue that makes up the outermost layer of the sclera. The episclera provides the blood supply from the anterior ciliary arteries [8]. The sclera is posterior to the episclera. The function of the sclera is to a protective coat for interocular contents and provides structural support for the globe of the eye [8]. It is made up of collagen fibers and is hydrated. It depend on the episclera for vascular nutrition [8].

1.2.5 The Cornea

The cornea is located in the center of the eye anterior to the pupil and is the most sensitive part of the eye. It makes up about one sixth of the external globe and contributes about two thirds of the refractive power of the eye [8]. The developed cornea is translucent which is essential for clear vision. The blood supply to the cornea is minimal. It comes from the subconjunctiva, episclera, and sclera. The tiny capillaries just barely cross into the limbus and loop into the cornea tissue [8]. Hence, the cornea is mostly avascular. The limbus is where the cornea and conjunctiva meet and is ten or more cells layers thick. The cornea is about 5.3 mm thick in the center in humans and is made of five layers from anterior to posterior; there is the epithelium, Bowman's membrane, stroma, Descemet membrane, and endothelium [8].

The epithelium is one of the fastest healing tissues in the body. The turnover for the epithelial cells is less than 14 days. This means that no epithelial cells on the cornea are more than two weeks old. The corneal epithelium consists of 5 to 7 layers of cells. The most anterior cells are squamous cells which directly interact with the tear film. The tear film provides most of the oxygen to the corneal epithelial cells. There are about two to three layers of squamous cells on average in the cornea [17]. Proceeding posteriorly, the next layer of cells are wing cells. These cells are slightly thicker than the squamous cells [17]. The most posterior layer of cells are a single layer of basal cells. Basal cells migrate from the limbus and are the thickest cell layer [8]. These cells are responsible for mitosis and they migrate upwards [18]. So a basal cell will turn into a wing cell which will migrate anteriorly and become a squamous cell. As basal cells become wing cells, they begin to enter apoptosis or cell death. When they reach the anterior surface they are further in apoptosis and will finally be shed from the epithelium when they have died [8]. By creating a model of the osmolarity increase throughout the entire cornea driven by evaporation of the tear film would help predict and understand the symptoms due to osmolarity increase associated with dry eye. It is believed that an increase in osmolarity can accelerate apoptosis [19].

The Bowman's membrane is acellular and anchors the basal cells of the epithelium [8]. The stroma is posterior to this layer. The stroma makes up about 90% of the cornea's thickness. This layer is made up of collagen fibers like the conjunctiva, however, the collagen fibers are not hydrated and are arranged in a regular pattern that allow light transmission. This dehydration contributes to the clarity of the cornea [8]. Over hydration of the stroma causes corneal swelling and decreases the ability for the person to see properly.

1.2.5.1 Corneal Metabolism

It is believed that metabolism contributes to the hydration of the stroma [3]. As stated in the previous section, when the stroma becomes improperly hydrated the pattern of collagen fibers is altered causing poor vision. It is thought that when cells are under hypoxic conditions or deprived of oxygen, then improper hydration of the stroma will occur [3]. This can be modeled using anaerobic and aerobic processes described more in depth below.

Energy in the form of adenosine triphosphate (ATP) is used for cellular function and maintenance. ATP is generated from the breakdown of glucose. The cornea obtains most of its glucose from the aqueous humor [18]. Most of the metabolic activity occurs in the epithelium and the endothelium in order to protect the visual functions of the cornea [18]. The epithelial contains about 2000 $\mu\text{mol}/\text{kg}$ wet weight of ATP whereas the stroma which is not high in metabolic activity contains about 10 to 15 $\mu\text{mol}/\text{kg}$ of ATP [18].

Glucose can be broken down by different cycles. The break down of glucose by these cycles is dependent of the supply of oxygen. If oxygen is present then the cell will use aerobic processes and if oxygen is not present the cell will use anaerobic processes. The epithelium gets most of its oxygen supply from the tear film and the endothelium gets most of its oxygen supply from the aqueous humor.

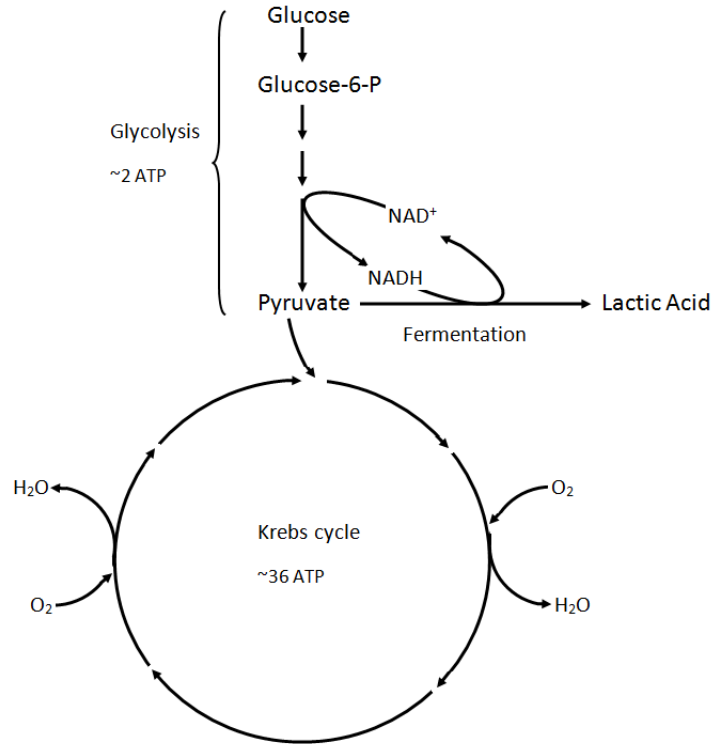


Figure 1.3: Corneal metabolism in the epithelial cells. Three metabolic processes can occur; glycolysis, fermentation or the Krebs cycle.

Glucose is broken down into pyruvate by a process called glycolysis [20]. This is independent of oxygen. Under aerobic conditions, pyruvate will further be broken down into water and carbon dioxide through the Krebs Cycle [20]. Under anaerobic conditions, pyruvate will be converted to lactic acid through fermentation [20]. Glycolysis produces 2 moles of ATP whereas the Krebs cycle produces 36 moles of ATP [18]. In fermentation, the formation of lactic acid conserves NADH which is an important cofactor in reactions in glycolysis [20]. As shown in Figure 1.3, the cofactor NADH is used to produce lactic acid and NAD⁺. This NAD⁺ is then used in reactions in glycolysis. Therefore, in anaerobic conditions, glycolysis is still able to function because of this conservation. However, aerobic conditions produce a lot more energy making it more favorable because of their relative

efficiency.

As stated before, the epithelium contains much more ATP than the stroma [18]. Therefore, by focusing on the epithelium at a cellular level, the changes in certain metabolic species could help understand the causes for corneal swelling or the stages in which the cells are. Simulating the epithelia at a cellular level with metabolic reaction has not been done before. Looking at the results could help understand why corneal swelling occurs, which is caused from hydration [3, 8]. If the stroma is overly hydrated then the tissue will swell leading to loss of transparency. In addition, the stroma is rich in sodium ions compared to the epithelium [18]. For all these reason, the cornea epithelium plays an important role in maintaining normal vision by the proper hydration and balance of ions in the stroma.

Chapter 2

MODELS FOR THE TEAR FILM AND WATER TRANSPORT IN THE EPITHELIA

This chapter will begin with the formulation of the model. It will then discuss the experimental results from The Ohio State College of Optometry for the tear film thickness which is used to obtain parameters. Then progress to the computational results for the combined tear film and epithelium models.

In this Chapter, we focus on the dynamics at a single point on either the cornea or the conjunctiva. At the Ohio State College of Optometry, experiments using fluorescence imaging was used to determine the thickness of the tear film as a function of time. Mathematical models for the tear film were developed and used to fit the thickness change to determine the thinning rate and the water permeability via osmosis. The permeability is similar to, but smaller than, that reported by Fatt and Weisman in their Ch. 7 [21] using combined *in vitro* animal data. We then develop and solve ordinary differential equations (ODEs) for the tear film thickness and osmolarity in the tear film at these locations. This kind of model is inspired in part by the compartment model of Gaffney *et al* [22], which simplified various parts of the tear film as spatially-uniform yet interconnected compartments with different compositions and volumes. They studied the dynamics of osmolarity, tear film thickness and volume under different conditions. They did not incorporate osmosis between the tear film and epithelium in their model; however, in this work we include this effect based on our experimental evidence and that obtained from murine models that we discuss next. A cumulative effect well beyond that expected for a single interblink period is found in some cases when even a small rate of osmosis is included.

Levin and Verkman [6] used knockout and wild-type mice to study the role of aquaporins in water transport in the corneal and conjunctival epithelium. In their experiments, a hypo-osmolar solution was perfused over the epithelial surface with and the swelling of each layer of the epithelium was measured. The swelling was due to osmosis, as water traveled into the cells with higher osmolarity than the perfusate. They also developed a mathematical model in which the idealized epithelial layers interacted via water transport in response to osmosis across cell boundaries. Their murine model consisted of five cell layers with a thick basal layer progressing to the thinnest squamous layer at the anterior surface. Using appropriate choices for the input parameters for the model, they were able to fit the experimental results for the swelling of the two most anterior layers of the epithelium.

In this work, a model for the tear film is combined with osmosis from an ideally semipermeable cornea with measured *in vivo* thinning rates to find permeabilities for the cornea and conjunctiva. We then adapt Levin and Verkman's model [6] to the human corneal and conjunctival epithelia by adjusting the permeability of the cell boundaries and the number and sizes of the epithelial cells. And, rather than perfuse a hypo-osmolar solution, we instead use a model for the evaporating tear film, which will induce a hyperosmotic state adjacent to the epithelium, which will respond by losing water to the tear film and shrinking.

In the human cornea, there are 5 to 7 layers of cells (e.g., [23]). The most posterior layer is a basal cell layer which is the thickest of the epithelial cells. Proceeding anteriorly, the next few layers are wing cells followed by squamous cells. We altered the Levin and Verkman model by adding two layers and changing the initial thickness of the cells to correspond to human epithelial cell thicknesses. We also set lower cell-cell permeabilities than for mice to match human data. We proceeded similarly with the conjunctiva. It consists of about four cell layers on the average, though the number and type of cells varies by location [24]; we neglect this variation here. The conjunctival cell thicknesses also decreases as one proceeds anteriorly as described in more detail below. For either the cornea or the conjunctiva, the overall model incorporates evaporation from the tear film, leading to an osmolarity increase

in the tear film, and the epithelial cells decrease in thickness because of water transport to the tear film. Our model uses a system of simultaneous ODEs to determine the tear film and epithelial quantities of interest. We explore the dependence of the tear film and epithelial thicknesses, as well as the osmolarities in each location, on the parameters in the model. We then interpret the results in the context of clinical measurements and of squamous cell apoptosis. This interpretation is in Chapter 4.

2.1 Theoretical Models

Figure 2.1 shows the tear film plus corneal epithelium is approximated as layers as shown layers with the same cross-sectional area. The top (anterior) layer is the tear film. The variables $h(t)$ and $c(t)$ represent the thickness of the post corneal tear film (PCTF) and the concentration of the PCTF. The variables $h_i(t)$ represent each layer in the cornea. The most anterior cell thickness is $h_1(t)$ and the numbering continues to the most posterior cell thickness, $h_7(t)$. The conjunctiva is labeled similarly but there are only four layers of cells. In the both the corneal and conjunctival models, the cell thickness increases from anterior to posterior cells which will be described in Section 2.1.2 and Section 2.1.3.

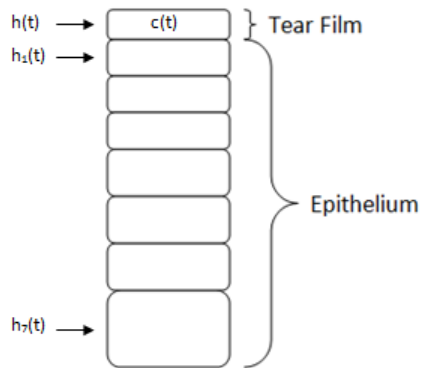


Figure 2.1: Schematic drawing for the corneal model. In this figure, $c(t)$ represents the concentration in the tear film, $h(t)$ represents the thickness of the tear film and $h_i(t)$ represents the thickness of the epithelial cell layers such that $i = 1$ through 7.

2.1.1 Tear Film Model

In the tear film model, we used equations for both the thickness and the concentration. The equation for the non-dimensional tear film thickness ($h(t)$) that we used was adapted

from Winter *et al* [1], as described by Braun [7]:

$$\frac{dh}{dt} = P_c(c - 1) - EJ \quad (2.1)$$

Here $c(t)$ is the osmolarity in the tear film, P_c is the non-dimensional permeability of the corneal surface, E is a non-dimensional constant and $J(t)$ is the non-dimensional evaporation flux from the tear film surface [1]. The dimensional and non-dimensional parameters are given in Table A.1. Proceeding from left to right in Eqn. (2.1), the terms represent the rate of change of the thickness, the supply of water from the cornea via osmosis, and the loss of water at the air/tear film interface via evaporation. An equation for the osmolarity may be obtained through manipulating conservation of mass enforced by $\frac{d}{dt}(hc) = 0$ (assuming a fixed area of the cell in the frontal plane). We obtain $\frac{dc}{dt} = -\frac{c}{h}\frac{dh}{dt}$, and eliminating $\frac{dh}{dt}$, one finds

$$\frac{dc}{dt} = -\frac{c}{h} [P_c(c - 1) - EJ]. \quad (2.2)$$

The terms in this equation have a similar interpretation.

Alternatively, integrating conservation of mass with respect to time results in

$$c(t)h(t) = c(0)h(0) = 1, \quad (2.3)$$

where $h(0) = 1$ and $c(0) = 1$ are the respective initial (nondimensional) values. One may eliminate c from Eqn. (2.1) to obtain a single equation for h . Making the further assumption that $EJ = E_0$ is a constant, one obtains

$$\frac{dh}{dt} = P_c(h^{-1} - 1) - E_0 \quad (2.4)$$

This equation was used in conjunction with the experimental evidence to determine the permeability in some cases [5]. We note that the initial conditions for these equations are $h(0) = 1$, corresponding to a dimensional thickness of $d = 3.5\mu\text{m}$ and $c(0) = 1$ corresponding to an isotonic osmolarity of $c_0 = 300$ mOsM.

A spatially-non-uniform version of the thickness and concentration equations can be found in [7].

The evaporation mass flux, $J(t)$, appears in both equations (2.1) and (2.2) and is dependent on $h(t)$. It represents the flux of water out of the tear film into the air:

$$J(t) = \frac{1}{\bar{K} + h}(1 - A\delta h^{-3}). \quad (2.5)$$

Here δ measures the effect of the film surface curvature on the rate of evaporation, and A measures the size of hypothesized van der Waals effects that represent the wettability of the glycocalyx and epithelial surface [1]. Values of these parameters for the tear film were estimated by Winter *et al* [1] using estimates of glycocalyx thickness and tear film breakup dynamics. The constants that appear in the nondimensional equations above, and the dimensional quantities that are inputs for them, are given in Table A.1 [7, 25].

The equations for the tear film thickness and osmolarity, together with their initial conditions, are thus

$$\frac{dh}{dt} = P_c(c - 1) - EJ, \quad h(0) = 1; \quad (2.6)$$

$$\frac{dc}{dt} = \frac{c}{h}[EJ - P_c(c - 1)], \quad c(0) = 1, \quad (2.7)$$

and J is given in Eqn. 2.5. The parameter values are given in Table A.1 in the appendix. Next, we will put these equations together with equations for the epithelial cell thicknesses.

2.1.2 Corneal Epithelial Cells and Model

In the corneal model, the equations from [6] were adjusted to make a human model by adding two layers of cells, and changing the initial thicknesses of the layers. In the human cornea, there are five to seven layers to the epithelium; we converted the Levin and Verkmann model to a model with seven layers and appended the epithelium model to the tear film model. There are two to three layers of wing cells in the corneal epithelium according to confocal microscopy as described in [26]. According to [8], there are two to three layers of squamous cells. Both state that the epithelium squamous cells were $4 \mu\text{m}$ thick and the

basal cells where $20 \mu\text{m}$ thick. On this basis, we chose initial thicknesses of the cells from anterior to posterior, as follows: [26]

$$h_1(0) = h_2(0) = h_3(0) = 4\mu\text{m}, \quad h_4(0) = h_5(0) = h_6(0) = 6\mu\text{m}, \quad h_7(0) = 20\mu\text{m}. \quad (2.8)$$

We nondimensionalize each of the equations for the cell thicknesses with the initial values above. The resulting equations are as follows.

$$\frac{d\bar{h}_1}{d\bar{t}} = \lambda \left[2 \left(\frac{1}{\bar{h}_1} - c \right) - \frac{1}{2} \left(\frac{1}{\bar{h}_2} - \frac{1}{\bar{h}_1} \right) \right], \quad \bar{h}_1(0) = 1; \quad (2.9)$$

$$\frac{d\bar{h}_i}{d\bar{t}} = \frac{\lambda h_1(0)}{2h_i(0)} \left[\left(\frac{1}{\bar{h}_i} - \frac{1}{\bar{h}_{i-1}} \right) - \left(\frac{1}{\bar{h}_{i+1}} - \frac{1}{\bar{h}_i} \right) \right], \quad \bar{h}_i(0) = 1, \quad i = 2, 3, 4, 5, 6; \quad (2.10)$$

$$\frac{d\bar{h}_7}{d\bar{t}} = \frac{\lambda h_1(0)}{h_7(0)} \left[\frac{1}{2} \left(\frac{1}{\bar{h}_7} - \frac{1}{\bar{h}_6} \right) - \left(1 - \frac{1}{\bar{h}_7} \right) \right], \quad \bar{h}_7(0) = 1. \quad (2.11)$$

The complete corneal model is Eqns. (2.6), (2.7) and (3.26), together with Eqns. (2.9)–(2.11).

The nondimensionalization factor for the equations is λ , such that

$$\lambda = \frac{dP_f V_w \phi_0}{100y_1(0)\epsilon U_0}. \quad (2.12)$$

The value of the permeability (P_f) in Equation 2.12 was determined by the fit of the data from The Ohio State College of Optometry. The constant d represents the thickness of the tear film and V_w is the molar volume of water. The constant ϕ_0 is the isotonic condition of 300 mOsm. The constant ϵ is a dimensionless parameter and ϵU_0 is the thinning rate. These values can be found in Table A.1.

2.1.3 Conjunctival Epithelial Cells and Model

For the conjunctival model, the model from [6] was converted to a four layer model, corresponding to a typical number of cells in the conjunctival epithelium [24]. According to Nichols *et al* [27], the surface projections exposed on the conjunctiva were twice the length of those on the surface of the cornea. Therefore, we assumed that the anterior-most cell membrane will have twice the amount of surface exposed to the tear film, and that the permeability of the anterior-most boundary of the conjunctival cells was twice the

permeability of corresponding boundary of the cornea. The conjunctival model was combined with the tear film model. This combined model is again driven by evaporation from the tear film. There are two to ten layers of cells in on in the conjunctiva epithelia depending on the location in the conjunctiva. We will focus on the central bulbar conjunctiva; hence, we assume there are four cells. Once again, the deepest layer are made up cylindrical basal cells as described in [15], each about $20 \mu\text{m}$ thick. The epithelial cells are thinner the more anterior they are. Thus, we assumed thicknesses for squamous and wing cells equal to $6 \mu\text{m}$ and $8 \mu\text{m}$, respectively. The initial thicknesses, denoted y_i , for the conjunctiva layers are then

$$y_1(0) = 6\mu\text{m}, y_2(0) = 8\mu\text{m}, y_3(0) = 8\mu\text{m}, y_4(0) = 20\mu\text{m}. \quad (2.13)$$

Proceeding in manner similar to that for the cornea, the set of ordinary differential equations for the conjunctival epithelium are

$$\frac{d\bar{y}_1}{d\bar{t}} = \lambda \left[4 \left(\frac{1}{\bar{y}_1} - c \right) - \frac{1}{2} \left(\frac{1}{\bar{y}_2} - \frac{1}{\bar{y}_1} \right) \right], \bar{y}_1(0) = 1, \quad (2.14)$$

$$\frac{d\bar{y}_i}{d\bar{t}} = \frac{\lambda y_1(0)}{2y_i(0)} \left[\left(\frac{1}{\bar{y}_i} - \frac{1}{\bar{y}_{i-1}} \right) - \left(\frac{1}{\bar{y}_{i+1}} - \frac{1}{\bar{y}_i} \right) \right], \bar{y}_i(0) = 1, \quad i = 2, 3 \quad (2.15)$$

$$\frac{d\bar{y}_4}{d\bar{t}} = \frac{\lambda y_1(0)}{y_4(0)} \left[\frac{1}{2} \left(\frac{1}{\bar{y}_4} - \frac{1}{\bar{y}_3} \right) - \left(1 - \frac{1}{\bar{y}_4} \right) \right], \bar{y}_4(0) = 1. \quad (2.16)$$

The permeability at the conjunctival surface was doubled relative to the cornea due to its roughness, which results in the indicated value of P_c ; see Table A.1.

The initial conditions for the epithelial cell thicknesses is $y_i(0) = 1$, $i = 1, 2, 3, 4$, since each thickness is made non-dimensional with the corresponding thickness in Eqn. 2.13. The complete conjunctival model is Eqns. (2.6), (2.7) and (3.26) together with Eqns. (2.14)–(2.16).

The cornea and conjunctival models were solved two ways. First, results were found for a single interblink. This case modeled an eye that was held open for a 90s interval, which the results can be found experimentally in a controlled experiment in the clinic. We then solved the models for a period of four hours with multiple interblinks of either 6s and 30s.

The 6s interblink models the normal conditions lacking any concentrated task or focus. The 30s interblink models intense activity, such as intense work or video games, such that the eye does not blink as often. The multiple interblinks were approximated as follows. All variables began with unit initial conditions, and one interblink was computed. Then the tear film thickness and osmolarity *only* were reset to unit initial values while the cell concentrations remain unchanged, and the process repeated until a four hour span was completed. The values at the end of each interblink are shown in the plots for these cases.

2.2 Results

We begin with experimental results from the Ohio State College of Optometry for the tear film thickness, then progress to computational results for the combined tear film and epithelium models.

2.2.1 Experimental results

The experimental results were obtained and analyzed by Dr. Ewen King-Smith and Dr. Padmapriya Ramamoorthy at the Ohio State College of Optometry. Images for one subject are shown in Figure 2.2 (A) and (B) at two and 57 s after the blink [5]. (The first two seconds was ignored in our analysis because of the upward drift after a blink.) Fluorescent intensity and hence thickness was analyzed in circular areas over the cornea and conjunctiva indicated by arrows in Figure 2.2 (A). The intensity decay, and hence thinning, over the conjunctiva can be seen to be much less than over the cornea.

In Figure 2.3(A) two examples of pre-corneal thinning rates are shown [5]. There is a slower and faster thinning rate. A slower thinning rate will result from less evaporation. The dashed lines in the figure show the fits of a model based on constant evaporation and increasing osmotic flow through the corneal surface [5]. Figure 2.3(B) show the average thinning curve for the pre-corneal tear film together with a least squares fit of the model [5]. The “initial thinning rate” is thought to be mainly due to evaporation. The thinning rate found from this experiment was 2.5 microns per minute over the pre-corneal tear film.

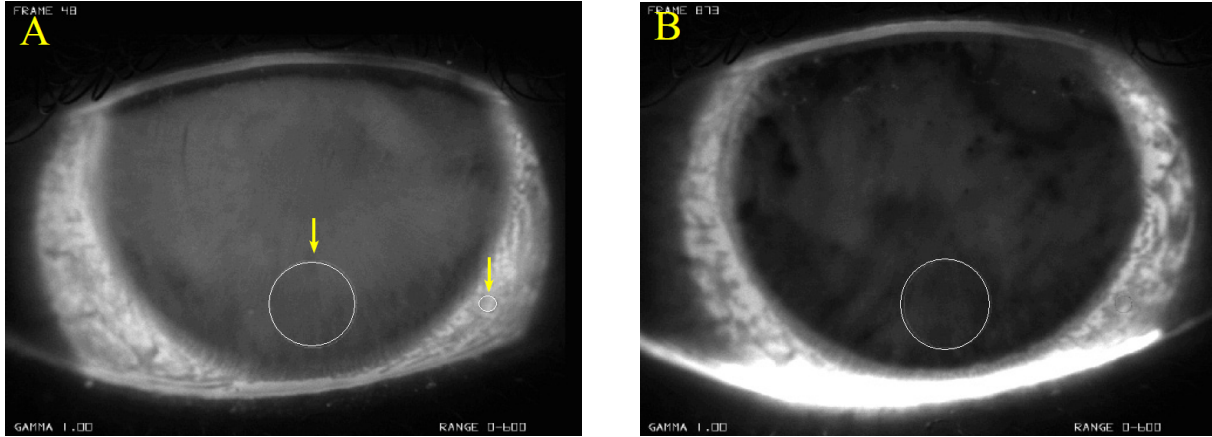


Figure 2.2: Fluorescent images at, A, 2 s and, B, 57 s after a blink. Arrows in A show circular areas used for averaging intensities over the cornea and conjunctiva. [5]

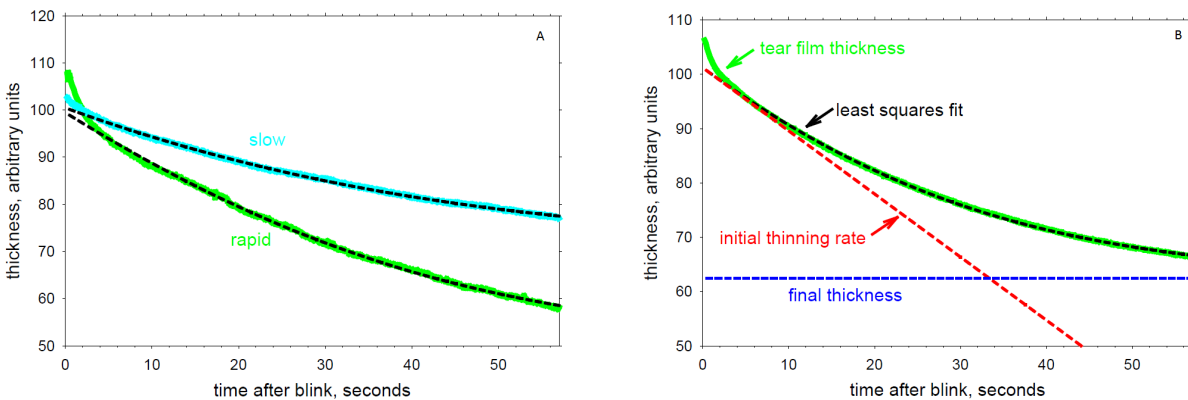


Figure 2.3: (A) Examples of fits of models for thinning of the pre-corneal tear film in two subjects. (B) Average thinning curve for the pre-corneal tear film together with a least squares fit of the model. [5]

The same was done for the pre-conjunctiva tear film. Figure 2.4(A) two examples of pre-conjunctival thinning rates are shown [5]. There again is a slower and faster thinning rate. The dashed lines in the figure show the fits of a model based on constant evaporation

and increasing osmotic flow through the conjunctiva surface. Comparing the pre-conjunctival tear film thinning rates, in both the slower and faster thinning rates the thickness of the tear film become constant relatively quickly. Also, in the slower thinning rate the thickness become constant very quickly and varies only slightly from the original thickness. The average thinning curve with a least squares fit of the model for the pre-conjunctival tear film and is shown in Figure 2.4(B) [5]. The thinning rate found from this experiment was 1.4 microns per minute over the pre-conjunctival tear film. The initial thinning rate is less than for the pre-corneal tear film - Fig. 2.3(B). This could be perhaps because of increased outward osmotic flow relative to the cornea.

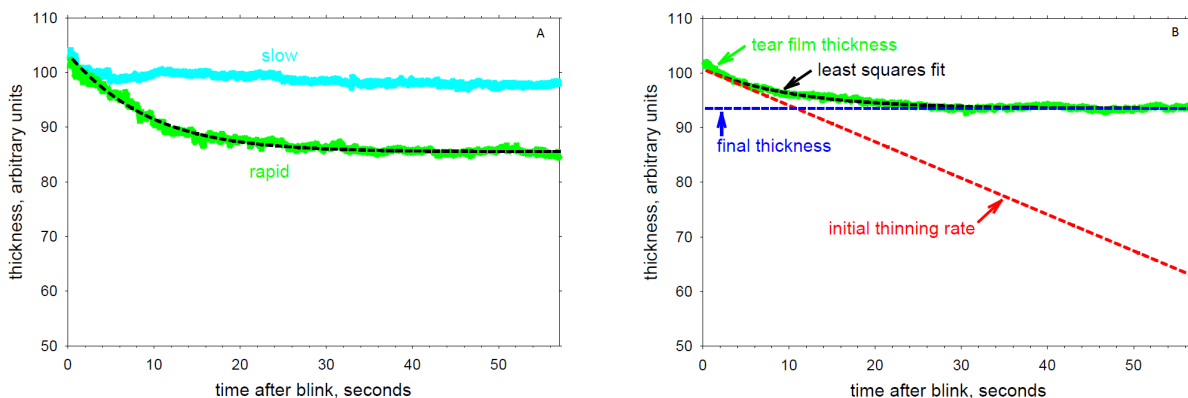


Figure 2.4: (A) Examples of fits of a model for thinning of the pre-conjunctival tear film in two subjects. (B) Average thinning curve for the pre-conjunctival tear film together with a least squares fit of the model. [5]

2.2.2 Theory for the Tear Film Alone

We first solve the mathematical model for the pre-corneal tear film alone, namely Equation 2.4 subject to $h(0) = 1$, for a single interblink of 60s. The dimensional initial tear film thickness was $3.5\mu\text{m}$. The osmolarity may then be found using mass conservation, Equation 2.3. The (numerically) computed solution for the thickness $h(t)$ are the dashed curves shown in Figures 2.3 and 2.4. To obtain these curves, a least squares fit is performed

using the initial thinning rate and the permeability of the cornea as parameters. In terms of the parameters, from Levin and Verkmann [6], the permeability is $P_f = 12\mu\text{m/s}$ when treating the cornea as single zero-thickness semi-permeable membrane, as reported in [5]. We can express this permeability using the notation of Fatt and Weissman ([21], Ch. 7) as well, in that case, the total flow resistance for the cornea is $R_t = 8.06 \times 10^{11} \text{ dyn s cm}^{-1}$. This value is more than three times the resistance given in [21] for a composite model from various animal tissues measured *in vitro*. The rapid or slow thinning cases are based on the initial thinning rates, which are determined from the initial slopes of the solution curves. From Figure 2.3, the initial thinning rate for the pre-corneal tear film was $2.5\mu\text{m/min}$; from Figure 2.4, the thinning rate for the pre-conjunctival tear film was $1.4\mu\text{m/min}$.

The theory is clearly able to fit the data very well, and to give a good estimate for the permeability that is of the correct size compared to previous measurements.

2.2.3 Theory with the Corneal Epithelium

We now turn to solving the mathematical model for the pre-corneal tear film and the underlying corneal epithelium for a typical initial (dimensional) tear film thickness of $d = 3.5\mu\text{m}$. We solve the model for slower and faster thinning rates for a single interblink, then go on to solve the case over many interblinks for two different interblink times.

2.2.3.1 Single Interblink

The thinning rate used in the first case was the value fitted in Figure 2.3 at $2.5\mu\text{m/min}$ and the duration of the single simulated interblink was 90s. In the simulated interblink in Figure 2.3(B), the tear film thickness decrease to 66% of its original thickness after 90s. In this figure the pre-corneal thinning rate was $2.5 \mu\text{m/min}$. To obtain this thinning rate with the addition of Equations 2.9 to 2.11 to the tear film Equations 2.6 and 2.7, the permeability of the cell membranes had to be adjusted. In the terminology of [6], the value $P_f = 7.56 \mu\text{m/s}$ was chosen to match the data of Figure 2.3; in particular, this choice recovers the final thickness of 66% of its original thickness as seen in Figure 2.5(a). After 90s, the tear film

thickness, h , is 66% of its original thickness or $2.33\mu\text{m}$. In this case, the concentration of the tear film increases by about 50% as shown in Figure 2.5(a); therefore, the osmolarity in the tear film rises to 450 mOsM. The cornea epithelium decreases in thickness as shown in Figure 2.5(b). The most anterior epithelial cell layer thickness decreased by a factor of 0.735, so the thickness of the cell decreased from $4\mu\text{m}$ to $2.94\mu\text{m}$. The next cell has a decreased by a factor of 0.94 and thereby decreased to $3.76\mu\text{m}$ thick. The other five layers did not change significantly. The total decrease in corneal epithelial thickness was about $1.3\mu\text{m}$ to 48.7μ thick from an initial total thickness of $50\mu\text{m}$. The results for the single interblink cases are summarized in Table 2.1.

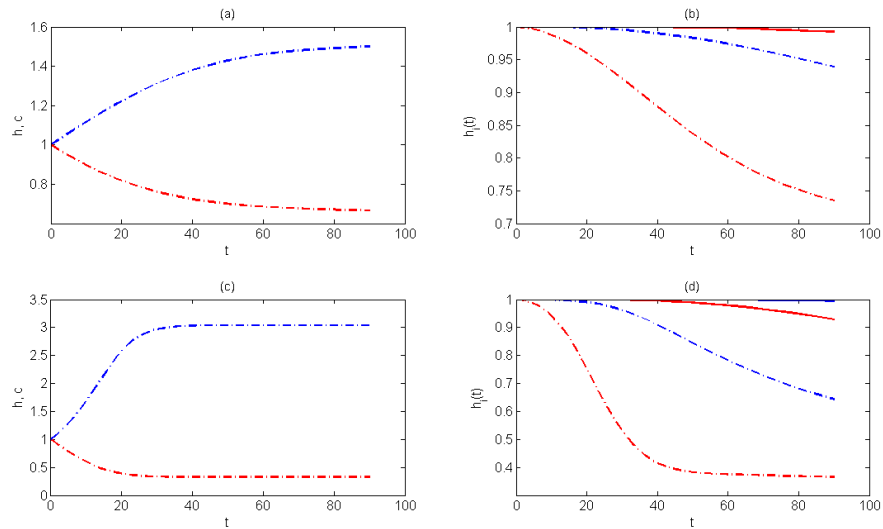


Figure 2.5: This figure models a single interblink over a 90 second interval for the corneal model. Plots (a) and (b) are for a thinning rate of $2.5\mu\text{m}/\text{min}$. Plot (a) shows the tear film concentration and thickness. The upper curve is the concentration increase in the tear film and the curve on the bottom is the tear film thickness decrease. Plot (b) shows the fractional thickness of each layer in the epithelium. The curves from bottom to top represent the anterior to posterior layers of the cornea, respectively. Plots (c) and (d) show the variables but the thinning rate is $10\mu\text{m}/\text{min}$.

	Cornea				Conjunctiva			
	2.5 $\mu\text{m}/\text{min}$		10 $\mu\text{m}/\text{min}$		1.4 $\mu\text{m}/\text{min}$		2.5 $\mu\text{m}/\text{min}$	
	h_i (μm)	c	h_i (μm)	c	y_i (μm)	c	y_i (μm)	c
Tear Film	0.66 (2.33)	450	0.329 (1.15)	912	0.8 (2.79)	375	0.88 (3.08)	342
Cell 1	0.735 (2.94)	408	0.37 (1.46)	810	0.82 (4.95)	342	0.9 (4.5)	333
Cell 2	0.95 (3.76)	319	0.64 (2.57)	469	0.98 (7.81)	306	0.99 (7.92)	303
Cell 3	~ 1 (4)	300	0.93 (3.72)	323	~ 1 (8)	300	~ 1 (8)	300
Cell 4	~ 1 (6)	300	~ 1 (6)	300	~ 1 (20)	300	~ 1 (20)	300
Cell 5	~ 1 (6)	300	~ 1 (6)	300	—	—	—	—
Cell 6	~ 1 (6)	300	~ 1 (6)	300	—	—	—	—
Cell 7	~ 1 (20)	300	~ 1 (20)	300	—	—	—	—

Table 2.1: Results for the tear film and epithelial thicknesses and osmolarities at the end of a single 90s interblink. The osmolarity c has units of mOsM; the thickness ratios h_i (cornea) and y_i (conjunctiva) are dimensionless. Dimensional thicknesses for the tear film and the cell layers are given in the parentheses in μm .

As can be seen from Figure 2.5, if the simulation was stopped at 6 s (a typical spontaneous interblink time), there would be little effect on changes in the thickness and osmolarity increase in both the tear film and epithelial cells from a single interblink. This is a reasonable expectation given that the permeability of the corneal epithelium is small [21, 22]. Continuing the simulation to longer times can show some noticeable effect, which may correspond to some subjects in experiments or other situations holding the eye open for extended periods. The level of osmolarity at the end of the simulation is approaching that where the subject would feel discomfort [11].

In some patients, a faster thinning rate of 10 $\mu\text{m}/\text{min}$ can occur. This was also simulated in Figure 2.5(c) and (d). Using the same permeability as before, for a single 90s interblink, the tear film osmolarity increases by a factor of 3.04 as shown in Figure 2.5(c) resulting in an osmolarity of 912 mOsM. The tear film decreases to about one third of its original thickness, or 1.15 μm . The cornea epithelium decreases more rapidly and significantly in this case as shown in Figure 2.5(d). The most anterior layer decreases to 0.37 time the original thickness or 1.46 μm . The next cell also decreases significantly unlike the

case with the slower thinning rate. This cells decreases to 0.64 of its original thickness or $2.57\mu\text{m}$. The third layer also is effected with a faster thinning rate. This layer decreases by 0.93 to $3.72\mu\text{m}$. This third cell layer cell thickness change is similar to the thickness change of the second cell layer in the slower thinning rate. The other four layers did not change significantly. The total decrease in the cornea epithelial thickness was about $4.25\mu\text{m}$ to $45.75\mu\text{m}$ thick. The increased level of osmolarity in this situation would cause irritation in a subject [11], and repeated exposure to this level of osmolarity would very likely lead to ocular surface damage. For the single interblink simulation, only the anterior cells are affected; we now turn to a multiple interblink simulation where cumulative effects will extend throughout the epithelium.

2.2.3.2 Multiple Interblinks

In the multiple interblink model, a single blink was simulated repeatedly over a specified interval. After the first blink, the initial conditions for the next interblink in the epithelial cells were set to the end values of the previous interblink. The initial condition for the tear film in each interblink was set to unit thickness and the isotonic condition of 300 mOsM ($c = 1$ nondimensionally). This process was repeated for each interblink over the entire interval.

In the multiple blink model of the cornea, the interblinks used were 6s and 30s and the results were looked at over a four hour duration; the interblink was a constant in each simulation. The shorter interblinks of 6s are realistic for many subjects, and the extended 30s interblink simulated in this section may approximate extended work or study periods. The thinning rates of $2.5\mu\text{m}/\text{min}$ and $10\mu\text{m}/\text{min}$ were both simulated. The results for both interblinks and the slower thinning rate are shown in Figure 2.6 and the results for both interblinks and thinning rates are summarized in Table 2.2. All of the variables tend to constant, steady state values as time increases. In the corneal model with the interblink of 6 s and a thinning rate of $2.5\mu\text{m}/\text{min}$ is shown in Figure 2.6(a) and (b). The tear film osmolarity increases to about 321 mOsM after four hours as shown in Figure 2.6(b).

The most anterior cells decrease by a factor of 0.97 to $3.86\mu\text{m}$ resulting in 311 mOsM as shown in Figure 2.6(a). This layer experiences greatest osmolarity change. The next layers end the simulation with decreased thicknesses of $3.89\mu\text{m}$, $3.91\mu\text{m}$, $5.90\mu\text{m}$ and $5.92\mu\text{m}$, respectively. The corresponding cells' osmolarities decrease from 311 mOsM to 303 mOsM as one progresses posteriorly, as listed in Table 2.2. The two posterior-most layers ($i = 6, 7$) was essentially unchanged in thickness and osmolarity; this last outcome is most likely because we specified that the most posterior cell ($i = 7$) was exposed to a constant isomolar condition. The final epithelial thickness decreased by $0.56\mu\text{m}$ to about $49.44\mu\text{m}$ over four hours.

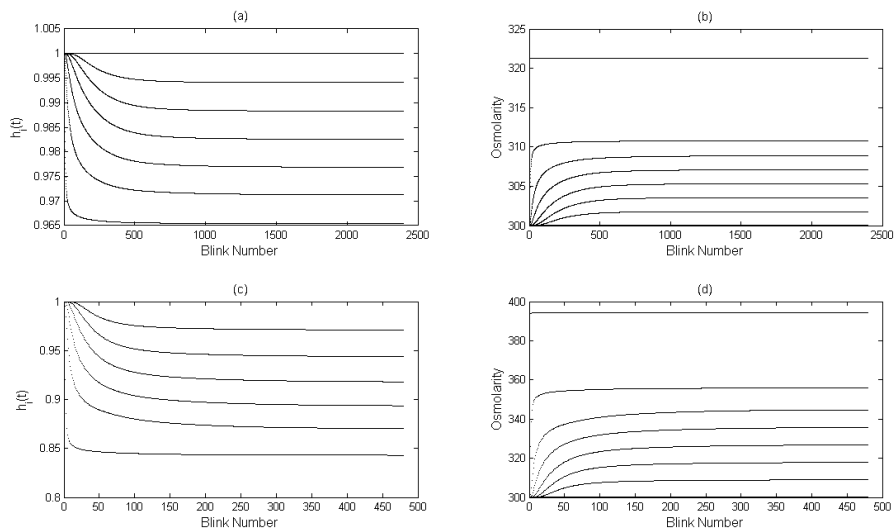


Figure 2.6: Results for the corneal model with multiple blinks are shown here for the $2.5\mu\text{m}/\text{min}$ thinning rate. Plots (a) and (b) represent the thickness decrease fraction in the epithelial cells and the osmolarity increase in the tear film and epithelium for repeated 6s interblinks over 4 hours. In plot (b) the top curve is the osmolarity of the tear film and the curves below it are the osmolarity in the layers. Plots (c) and (d) are similar results for 30s interblink intervals.

When the thinning rate was increased to $10\mu\text{m}/\text{min}$, the simulation showed more significant changes in thickness and osmolarity. For an interblink of 6 s over four hours,

the thicknesses and osmolarities again tend to constant values. However, for the larger thinning rates, the cells took significantly longer to approach their steady states. The tear film osmolarity increases much higher than the slower thinning rate to about 406 mOsM as shown in Table 2.2. This result makes sense, because the increase in thinning rate increased the evaporation loss of water through the tear film which in turn increases the osmolarity more than the case before. The most anterior cell layer thickness decreased by a factor of 0.85 to $3.40\mu\text{m}$ resulting in 351 mOsM. Again, the thickness decrease and accompanying osmolarity increase becomes less as one progresses posteriorly through the epithelial layers. In this faster thinning rate case, six of the seven cell layers are affected by the repeated blink cycles and but the seventh layer is not significantly effected. The final epithelial thickness decreased by $2.58\mu\text{m}$ to about $47.42\mu\text{m}$ over four hours with this thinning rate.

For an interblink of 30 s over four hours for a thinning rate of $2.5\mu\text{m}/\text{min}$, the thicknesses and osmolarities again tend to constant values. In this case, the tear film osmolarity increases to about 394 mOsM as shown in Figure 2.6(d) and in Table 2.2. This is similar to the 6s interblink with the faster thinning rate. The osmolarity also increases to about 356 mOsM in the most anterior cell layer. This is also significantly high and can have negative effects on cellular function. Again, the thickness decrease and accompanying osmolarity increase becomes less as one progresses posteriorly through the epithelial layers. Again like the 6s interblink with the faster thinning rate six of the seven cell layers are affected by the repeated blink cycles. The final epithelial thickness decreased by $2.58\mu\text{m}$ to about $47.42\mu\text{m}$ over four hours. In this case, the increase of the osmolarity in the tear film and epithelial layers is significantly higher than for the 6s interblink repeated over four hours with the same thinning rate.

	6s interblink				30s interblink	
	2.5 $\mu\text{m}/\text{min}$		10 $\mu\text{m}/\text{min}$		2.5 $\mu\text{m}/\text{min}$	
i	h_i (μm)	c	h_i (μm)	c	h_i (μm)	c
TF	0.93 (3.33)	321	0.74 (2.59)	406	0.76 (2.66)	394
1	0.97 (3.86)	311	0.85 (3.40)	351	0.84 (3.37)	356
2	0.97 (3.89)	309	0.88 (3.52)	342	0.87 (3.48)	345
3	0.98 (3.91)	307	0.90 (3.60)	333	0.89 (3.56)	336
4	0.98 (5.90)	305	0.92 (5.52)	325	0.92 (5.52)	327
5	0.99 (5.92)	302	0.95 (5.70)	317	0.94 (5.64)	318
6	~ 1 (6)	300	0.97 (5.82)	308	0.97 (5.82)	309
7	~ 1 (20)	300	~ 1 (20)	300	~ 1 (20)	300

Table 2.2: Results for the corneal epithelium showing ending values of the decrease fraction for the tear film $h(t_{\text{end}})$, each cell layer $h_i(t_{\text{end}})$ and the osmolarity $c(t_{\text{end}})$. The osmolarity c has units of mOsM; the thickness ratios are dimensionless. The dimensional thickness of each layer is given in μm in parentheses.

The time for the variables to effectively reach their final values appears to be about 100 minutes for the long interblink times, or slightly lower. This value is thus roughly independent of the interblink value. It appears to be limited by the permeability of the cell interfaces based on the results for the conjunctival results discussed below.

2.2.3.3 Permeability Study

The thinning rate calculated from the data collected by the Ohio State College of Optometry determined the permeability value as stated before. So, next we study the effects of varying epithelial membrane permeability of water (\bar{P}_f). Recall that $\bar{P}_f = \frac{P_f v_w \phi_A}{\epsilon U_0}$ and

$P_c = 2\bar{P}_f$. P_c is the permeability between the most anterior layer of the epithelium and the tear film.

In a single blink, \bar{P}_f was varied from 3×10^{-3} to 13×10^{-3} . As shown in Figure 2.7, the most anterior layer (h_1) of the corneal epithelia significantly decreased. This is likely because the permeability between the tear film and most anterior cell is twice that than the permeability between cells. Therefore, more water is able to permeate through that membrane than the others. The response to an increase osmolarity in the tear film occurs faster, resulting in a decrease in thickness with an increase in osmolarity of the most anterior cell layer. That layer is the black line in Figure 2.7. As permeability was increased the thickness change decreased in the most anterior layer. In the posterior layers, the thickness change increased as permeability increased.

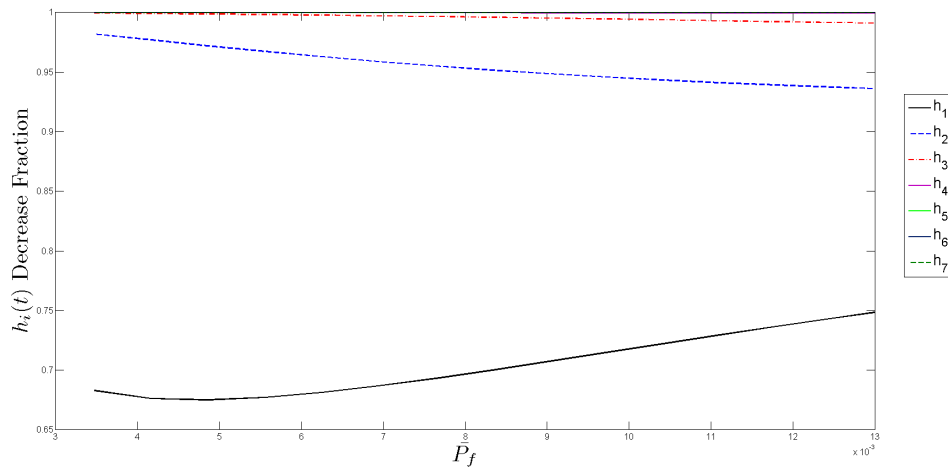


Figure 2.7: This is the final decrease fraction in each corneal epithelia layer (h_1 to h_7) after 90 seconds while varying \bar{P}_f .

The effects of varying \bar{P}_f were also observed for the multiple blink model. The final osmolarity after four hours for each cellular layer is shown in Figure 2.8 for 6 second interblinks and Figure 2.9 for 30 second interblinks.

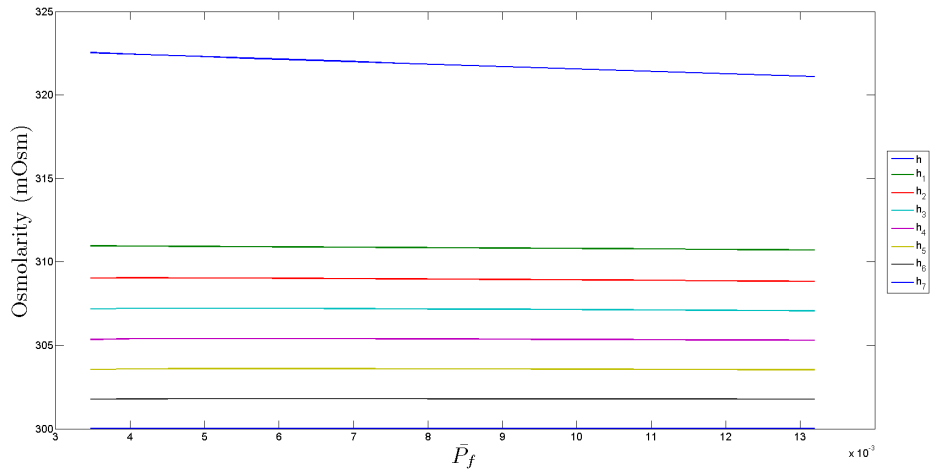


Figure 2.8: While varying \bar{P}_f , this is the final osmolarity in the tear film (h) and layers (h_1 to h_7) after after 4 hours of blink intervals of 6 seconds. The tear film is the top blue line and the epithelium layers from anterior to posterior are under the tear film curve.

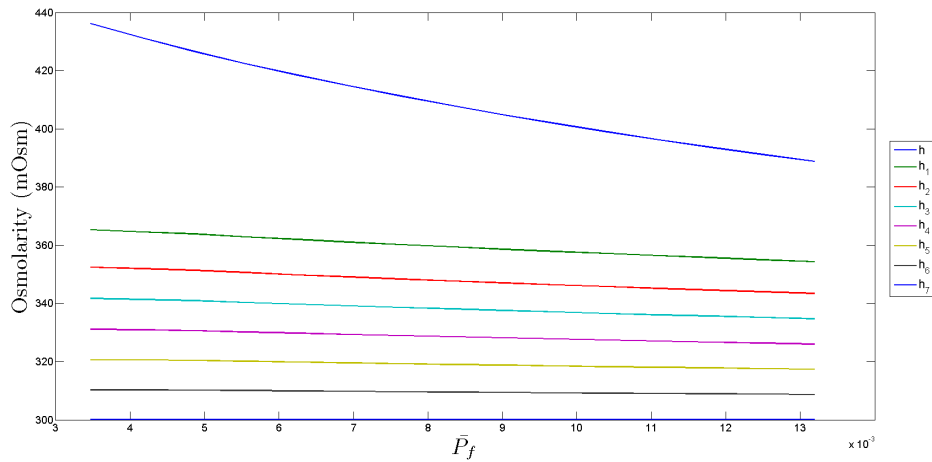


Figure 2.9: While varying \bar{P}_f , this is the final osmolarity in the tear film (h) and layers (h_1 to h_7) after after 4 hours of blink intervals of 30 seconds. The tear film is the top blue line and the epithelium layers from anterior to posterior are under the tear film curve.

In Figure 2.8, the variation in \bar{P}_f did not cause large changes in the tear film or epithelia on the final osmolarity. The lines for each layer are nearly constant for each permeability value. In this case it does not appear that permeability will change the results significantly. Whereas, in Figure 2.9, for a longer interblink, the final osmolarity in the tear film is significantly effected by the varying permeability. However, the final osmolarity in the cellular layers are not effected but varying the permeability. Increased permeability allows water to pass through the anterior layer and into the tear film faster which results in a lower osmolarity in the tear film.

2.2.4 Theory with Conjunctival Epithelium

In this section, we consider the conjunctival model with four cells posterior to the tear film. We study a tear film that is initially isosmolar with thickness $d = 3.5\mu\text{m}$, with two different thinning rates. We do this for a single interblink of 90s duration, and many blink cycles over a four hour period. As in the previous sections, the computed variables all tend to constant values as time increases.

2.2.4.1 Single Interblink

The thinning rates used for the conjunctival model were either the measured rate of $1.4\mu\text{m}/\text{min}$ (obtained from Figure 2.4) or a hypothesized $2.5\mu\text{m}/\text{min}$ to represent a rapid thinning rate. The thinning rate was varied because variation between subjects is expected.

For the thinning rate of $2.5\mu\text{m}/\text{min}$, the tear film concentration increased by 1.25 times to about 376 mOsM at the end of the simulation as shown in Table 2.1. The thickness of the tear film decreased by about 0.8 times which results in the thickness of about $2.79\mu\text{m}$. The epithelial anterior-most layer decreased in thickness by a factor of 0.82 as shown in Table 2.1; the final thickness after 90s for that layer was $4.95\mu\text{m}$. The next layer decreased by a factor of 0.98, resulting in the final thickness of $7.81\mu\text{m}$. The next two layers were not significantly changed. The total decrease in the conjunctiva epithelial thickness was about $1.26\mu\text{m}$ to $40.74\mu\text{m}$ thick.

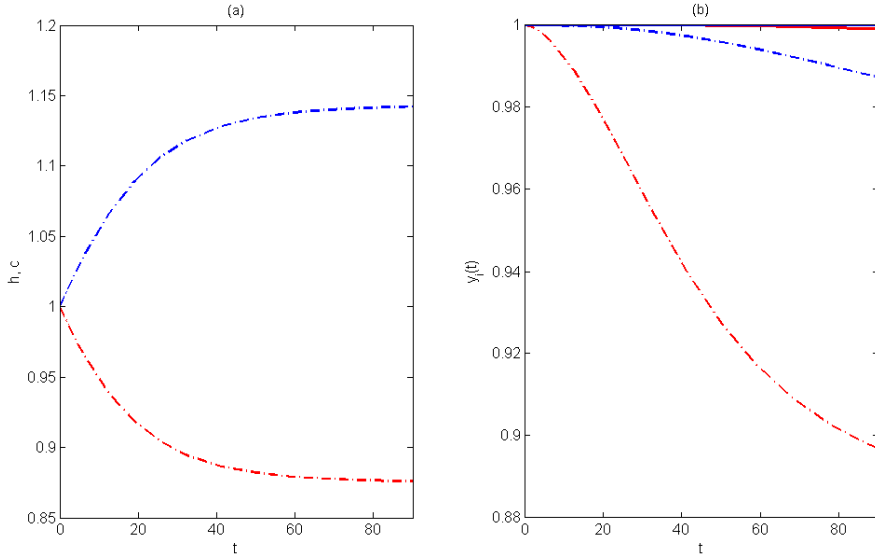


Figure 2.10: This figure models a single interblink over a 90 second interval for the conjunctival model. Plots (a) and (b) are for a thinning rate of $1.4 \mu\text{m}/\text{min}$. Plot (a) shows the tear film concentration and thickness. The curve on top is the concentration increase in the tear film and the curve on the bottom is the tear film thickness decrease. Plot (b) shows the fractional thickness of the epithelium. The curves from bottom to the top represent the anterior to posterior layers of the cornea.

For the thinning rate of $1.4 \mu\text{m}/\text{min}$ in the conjunctiva epithelium, the tear film osmolarity increased by 1.14 times to about 342 mOsM as shown in Figure 2.10(a) and Table 2.3. The thickness of the tear film decreased by about 0.88 times which results in the thickness of about $3.08\mu\text{m}$. The epithelial most anterior layer decreased by 0.9 as shown in Figure 2.10(b). The final thickness after 90 s for that layer is about $5.4\mu\text{m}$. The next layer decreased by 0.99, resulting in the final thickness of $7.92\mu\text{m}$. The next two layers were not significantly changed. The total decrease in the conjunctiva epithelial thickness was about $0.73\mu\text{m}$ to $41.27\mu\text{m}$ thick. Because the permeability of the interface between the conjunctiva and the tear film is larger than for the cornea, the effect on the underlying cells is less than in the cornea and the pre-conjunctival tear film thins less than the pre-corneal tear film.

2.2.4.2 Multiple Interblinks

As in the previous sections, the computed variables all tend to constant values as time increases for the multiple blink cycle results.

In the conjunctival model where the thinning rate was $2.5\mu\text{m}/\text{min}$ and the interblink was 6 s, the tear film osmolarity increases to about 320 mOsM as shown in Table 2.3. The most anterior cells decrease by a factor of 0.97 to $5.8\mu\text{m}$ resulting in 310 mOsM. The next layer decreased by about 0.98 to $7.82\mu\text{m}$ and resulting in a final osmolarity of 307 mOsM. The next layer decreased by 0.99 to $7.9\mu\text{m}$ and giving about 303 mOsM in that layer. The final layer did not significantly change thickness or osmolarity. The final epithelial thickness

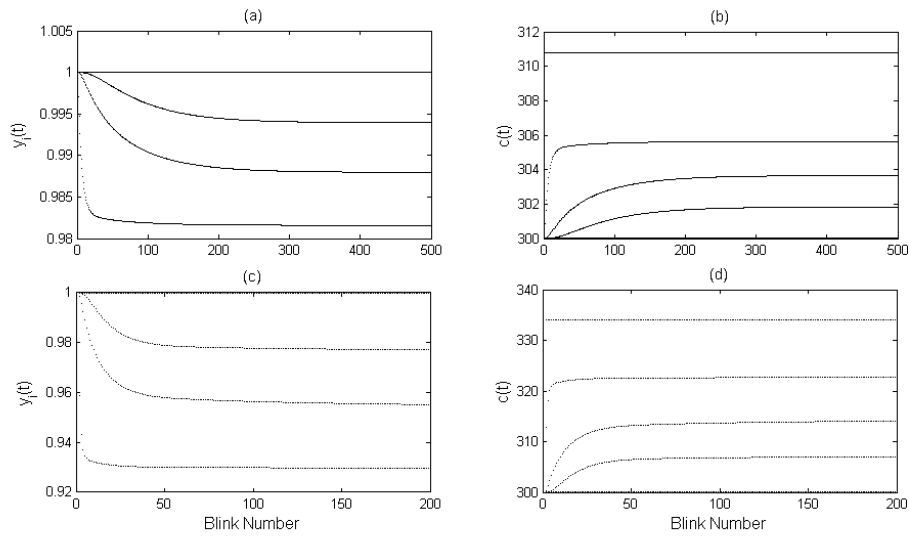


Figure 2.11: Results for the conjunctival multiple blink model are shown. Plots (a) and (b) show the thickness decrease fraction in the epithelium and the osmolarity increase in the tear film and epithelium for repeated interblinks of 6 s and a thinning rate of $1.4\mu\text{m}/\text{min}$ over a period of 4 hours. In plot (b) the top line is the osmolarity of the tear film and the lines below are the osmolarity in the layers. Plots (c) and (d) are the same results but for repeated interblinks of 30 s each.

decreased by $0.46\mu\text{m}$ to about $41.54\mu\text{m}$ over four hours. The layers reach within one percent

	6s interblink						30s interblink			
	1.4 $\mu\text{m}/\text{min}$		2.5 $\mu\text{m}/\text{min}$		10 $\mu\text{m}/\text{min}$		1.4 $\mu\text{m}/\text{min}$		2.5 $\mu\text{m}/\text{min}$	
i	y_i	c	y_i	c	y_i	c	y_i	c	y_i	c
TF	0.97 (3.40)	311	0.93 (3.26)	320	0.88 (3.08)	342	0.90 (3.15)	334	0.83 (2.91)	364
1	0.98 (5.88)	306	0.97 (5.8)	310	0.93 (5.58)	322	0.93 (5.58)	323	0.87 (5.25)	343
2	0.99 (7.92)	304	0.98 (7.82)	307	0.95 (7.60)	314	0.95 (7.60)	314	0.92 (7.33)	327
3	0.99 (7.92)	302	0.99 (7.9)	303	0.98 (7.84)	307	0.98 (7.84)	307	0.96 (7.65)	313
4	~ 1	300	~ 1	300	~ 1	300	~ 1	300	~ 1	300

Table 2.3: Results for the conjunctival epithelium showing ending values of the decrease fraction for the tear film $y(t_{\text{end}})$, each cell layer $y_i(t_{\text{end}})$ and the osmolarity $c(t_{\text{end}})$. The osmolarity c has units of mOsM; the thickness ratios are dimensionless. The dimensional thicknesses are given in parentheses in μm .

of their final osmolarity value very quickly since the change in thickness for the cell layers is small. The most anterior layers reached it in about 8 blinks (48 s). The next layers reached it within 43 blinks (4.3 minutes) and 8 blinks (48 s). The last layer was within one percent of its final osmolarity after the first blink.

For an interblink of 30 s over four hours, the tear film osmolarity increases to about 364 mOsM as shown in Table 2.3. The most anterior cells decrease by 0.87 to 5.25 μm resulting in 343 mOsM. The next layer decreased by about 0.92 to 7.33 μm and about 327 mOsM. The next layer decreased by 0.96 to 7.65 μm and about 313 mOsM. The final layer did not significantly change thickness or osmolarity. The final epithelial thickness decreased by 1.77 μm to about 40.23 μm over four hours. The layers reach within one percent of their final osmolarity value rapidly. The most anterior layers reached it in about 5 blinks (2.5 minutes). The next layers reached it within 28 blinks (14 minutes) and 26 blinks (13 minutes). The most posterior (basal) layer was within one percent of its final osmolarity after the first blink.

In the conjunctival model where the thinning rate was 1.4 $\mu\text{m}/\text{min}$ and the interblink was 6 s, the tear film osmolarity increases to about 311 mOsM as shown in Figure 2.11(b). The most anterior cells decrease by 0.98 to 5.88 μm resulting in 306 mOsM as shown in

Figure 2.11(a). The next layer decreased by about 0.99 to 7.92 μm and about 304 mOsM. The next layer decreased by 0.99 to 7.92 μm and about 302 mOsM. The final layer did not significantly change thickness or osmolarity. The final epithelial thickness decreased by 0.26 μm to about 41.74 μm over four hours. The results were the same for 8 hour duration as the four hour duration; therefore, the equilibrium was reached in both cases within four hours. The layers reach within one percent of their final osmolarity value quickly. The most anterior layers reached it in about 4 blinks (2 min). The next layer reached it within 12 blinks (6 min). The last two layers were within less than one percent of the final osmolarity after the first blink.

For an interblink of 30 s over four hours, the tear film osmolarity increases to about 334 mOsM as shown in Figure 2.11(c). The most anterior cells decrease by 0.93 to 5.58 μm resulting in 323 mOsM as shown in Figure 2.11(c) and (d). The next layer decreased by about 0.95 to 7.60 μm and about 314 mOsM. The next layer decreased by 0.98 to 7.84 μm and about 307 mOsM. The final layer did not significantly change thickness or osmolarity. The final epithelial thickness decreased by 0.98 μm to about 41.02 μm over four hours. The layers reach within one percent of their final osmolarity value quickly. The most anterior layers reached it in about 3 blinks (1.5 minutes). The next layers reached it within 20 blinks (10 minutes) and 18 blinks (9 minutes). The last layer was within one percent of its final osmolarity after the first blink.

In the conjunctival model where the thinning rate was 10 $\mu\text{m}/\text{min}$ and the interblink was 6 s, the tear film osmolarity increases to about 342 mOsM; see Table 2.3. The most anterior cells decrease by 0.93 to 5.58 μm resulting in 322 mOsM. The next layer decreased by about 0.95 to 7.6 μm and about 314 mOsM. The next layer decreased by 0.98 to 7.84 μm and about 302 mOsM. The final layer did not significantly change thickness or osmolarity. The final epithelial thickness decreased by 0.26 μm to about 41.74 μm over four hours. The results were the same for 8 hour duration as the four hour duration; therefore the equilibrium was reached in both case within four hours. The layers reach within one percent of their

final osmolarity value in a short time. The most anterior layers reached it in about 13 blinks (78 s). The next layers reached it within 80 blinks (8 minutes) and 75 blinks (7.5 minutes). The last layer was less than one percent of its final osmolarity after the first blink.

The time to closely approach the final steady state values appeared to be similar to that for the corneal model. Given that the tear film/epithelial interface was twice as permeable for the conjunctival model compared to the corneal model, it appears that the time to reach the steady state is determined by the value of \bar{P}_f representing the permeability between cells inside the epithelium.

Chapter 3

INCLUDING METABOLIC REACTIONS: TEAR FILM AND EPITHELIUM

3.1 Introduction

In this section, metabolic reactions in the cells will be taken into account in the model. Cellular functions involve numerous molecules which undergo many different reactions throughout the cell. However, we will focus on a small number of them in the model. The epithelial cells may function under two conditions; aerobic and anaerobic, meaning they function with or without oxygen, respectively. Therefore, oxygen will be a part of this model to determine if the cell is functioning under aerobic or anaerobic conditions. Cells get most of their energy by breaking down glucose. Glucose can be broken down into pyruvate and other forms of energy through the process called glycolysis. Pyruvate can then enter into the Krebs Cycle and be broken down further carbon dioxide and forms of energy. Hence, glucose and carbon dioxide will be important molecules in the model. If the cell is functioning under anaerobic condition then fermentation occurs and glucose is converted to lactate [20]. Therefore, lactate will also be included in this model. Lactate can be converted to lactic acid when it reacts with a hydronium ion. A cell's pH is also important. Cells use a bicarbonate buffering system so the pH stays within a healthy range in the cell. So, the model will also include bicarbonate and hydronium. Epithelial cells also have sodium potassium pumps and chloride channels which will incorporate sodium and chloride in the model.

The epithelium contains more metabolic activity than the stroma. Therefore, by focusing on the epithelium at a cellular level, the changes in certain metabolic species could help understand the causes for corneal swelling or stages that the cells are in. Simulating the epithelial at a cellular level with metabolic reaction has not been studied before to our

knowledge. Looking at the results could help understand why corneal swelling occurs due to hydration [8]. When the stroma is over-hydrated the tissue may swell leading to loss of transparency. Water is produced by both anaerobic and aerobic processes. By simulating the metabolic reactions products, one can observe the amount of water contributed by the epithelial cells. In addition, the stroma is rich in sodium ions compared to the epithelium [18]. The cornea epithelium plays an important role in maintaining normal vision by the dehydration and balance of ions in the stroma. Also, the simulations will model the aerobic or anaerobic processes that occur in the cells. This could help interpret if the cells are entering apoptosis under different conditions.

We propose a model that combines the metabolic reactions used in the epithelium from Leung *et al* [3] and the cell-level model from Levin and Verkman [6]. The model will account for thickness change and the concentration of various metabolic species and ions that are common within each epithelial layer. It will also incorporate intercellular transport through membrane fluxes of some of these species including water.

3.2 Proposed Model

The proposed model focuses on the metabolism in the epithelial layer of the cornea. The epithelial layer is one of the most metabolic layers of the cornea. In comparison to the stroma which makes up a significant thickness in the cornea, the consumption rate of O_2 represented as QO_2 in the epithelium is 5 to 6 whereas in the stroma it is 0.23 [18]. Therefore, we will focus on the metabolism in the epithelium because it is significantly higher.

The schematic drawing for the proposed model is shown in Figure 3.1. The epithelium in the cornea is seven cells thick. The cells are numbered from anterior to posterior as $j = 1$ to $j = 7$. The equations for the cells are described in Section 3.2.2. In Section 3.2.3, the equations that represent the tear film at the $j = 0$ position are shown. The stroma is at the $j = 8$ position and the initial conditions are described in Section 3.2.1. The tear film/ air interface is at the $j = 0$ boundary and the conditions are described in Section 3.2.4.1. The cell layer that is located behind the tear film is numbered as $j = 1$ and the boundary conditions are

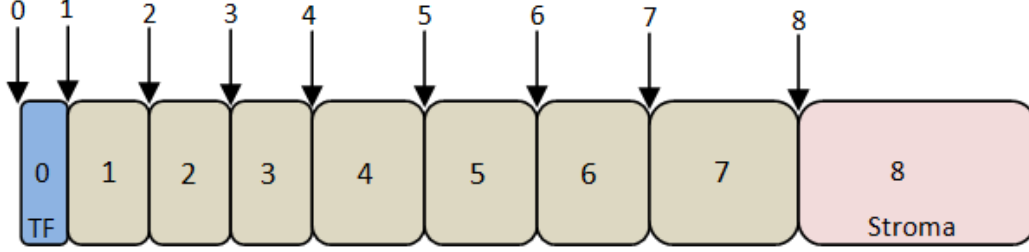


Figure 3.1: This is the schematic drawing of the proposed model. There is a tear film layer ($j = 0$), with seven epithelial layers ($j = 1$ to $j = 7$) and the stroma. The cells will be referred to as the j^{th} cell with the j^{th} membrane located anteriorly and the $(j + 1)^{\text{st}}$ membrane located posteriorly in regards to the j^{th} cell.

described in Section 3.2.4.2. The j^{th} membrane for the cells in the epithelium are represented by the more anterior membrane of the cell layers. For instance, the j^{th} membrane is between the anterior side of the j^{th} cell. The boundary conditions for the inner cells are shown in Section 3.2.4.3. The $j = 8$ membrane is between the most posterior cell of the epithelium, the basal cell ($j = 7$) and the stroma ($j = 8$).

3.2.1 Initial Conditions

First, we will describe the initial conditions in the tear film and the epithelial cells. In the tear film, the initial thickness is $h_0(0) = 3.5 \mu\text{m}$ [28]. The initial concentration of the tear film is 300 mOsm. The osmolality is determined by the sum of the products of the ion species valence (z_i) and concentration (C_i). The valence for the solutes are shown in Table C.2. The equation used to calculate osmolality (C) is

$$C = \sum_i |z_i| C_i. \quad (3.1)$$

The initial concentrations of the solutes sodium, chloride and bicarbonate in the tear film are shown in Table C.1. There is no glucose or lactate present in the tear film. The initial

concentrations were taken from [3]. The initial pH of the tear film is assumed to be 7.6. The initial concentration of hydronium was calculated from this value using

$$\text{pH} = -\log(C_H). \quad (3.2)$$

The initial concentrations of oxygen and carbon dioxide in the tear film were determined using Henry's Law since the partial pressures of oxygen and carbon dioxide are known from [3]. Henry's law describes the partial pressures of oxygen (P_O) and carbon dioxide (P_C) are shown in Equations 3.3 and 3.4.

$$P_O = k_{H,O}C_O \quad (3.3)$$

$$P_C = k_{H,C}C_C \quad (3.4)$$

In Equations 3.3 and 3.4, Henry's constants k_H are shown in Table C.2.

In the cells in the epithelium ($j = 1$ to $j = 7$), the initial concentrations of the solutes sodium, chloride, glucose, lactate, and bicarbonate are shown in Table C.3. The initial partial pressure of oxygen and carbon dioxide are shown in Table C.3. It was assumed that all of the cells' initial conditions for all solutes but hydronium were estimated using the steady state results from [3]. The initial value was chosen from their graphs of the steady states of the solutes in the results section roughly in the middle of the epithelium. The initial concentrations of hydronium was chosen so the cell was in a neutral state at a pH of 7.6. The initial conditions for the thickness of the seven epithelial cells is the same as the model in Chapter 2. The initial conditions are

$$h_1(0) = h_2(0) = h_3(0) = 4\mu\text{m}, \quad h_4(0) = h_5(0) = h_6(0) = 6\mu\text{m}, \quad h_7(0) = 20\mu\text{m}. \quad (3.5)$$

3.2.2 Inner Cell Equations

Next, we will discuss the equations used to represent the solute concentrations within a single cell. Here we will look at an inner epithelial cell j . A schematic drawing for this case is shown in Figure 3.2.

j+1

j

j-1

$$\begin{aligned} \frac{dh_j}{dt} &= -(J_{V,j} - J_{V,j+1}) + \frac{\rho_f Q_W h_j}{M_W} \\ \frac{dC_{Na,j}}{dt} &= -\frac{J_{Na,j} - J_{Na,j+1}}{h_j} \\ \frac{dC_{Cl,j}}{dt} &= -\frac{J_{Cl,j} - J_{Cl,j+1}}{h_j} \\ \frac{dC_{O,j}}{dt} &= -\frac{J_{O,j} - J_{O,j+1}}{h_j} + \\ &\quad Q_O^{max} \left[1 + 0.8 \frac{7.6 - pH}{K_{pH} + 7.6 - pH} \right] \left[1 + \frac{C_G}{K_O^G + C_G} \right] \left[\frac{P_O}{K_O^O + P_O} \right] \\ \frac{dC_{G,j}}{dt} &= -\frac{J_{G,j} - J_{G,j+1}}{h_j} - \frac{Q_L^{min}}{2} \left[1 + \frac{K_O^L}{K_O^L + P_O} \right] \left[\frac{C_G}{K_G^L + C_G} \right] \\ &\quad - \frac{Q_O^{max}}{6} \left[1 + 0.8 \frac{7.6 - pH}{K_{pH} + 7.6 - pH} \right] \left[1 + \frac{C_G}{K_O^G + C_G} \right] \left[\frac{P_O}{K_O^O + P_O} \right] \\ \frac{dC_{L,j}}{dt} &= -\frac{J_{L,j} - J_{L,j+1}}{h_j} + Q_L^{min} \left[1 + \frac{K_O^L}{K_O^L + P_O} \right] \left[\frac{C_G}{K_G^L + C_G} \right] \\ 0 &= -\frac{J_{H,j} - J_{H,j+1}}{h_j} + \frac{J_{B,j} - J_{B,j+1}}{h_j} + Q_L^{min} \left[1 + \frac{K_O^L}{K_O^L + P_O} \right] \left[\frac{C_G}{K_G^L + C_G} \right] \\ 0 &= -\frac{J_{C,j} - J_{C,j+1}}{h_j} - \frac{J_{B,j} + J_{B,j+1}}{h_j} \\ &\quad + Q_O^{max} \left[1 + 0.8 \frac{7.6 - pH}{K_{pH} + 7.6 - pH} \right] \left[1 + \frac{C_G}{K_O^G + C_G} \right] \left[\frac{P_O}{K_O^O + P_O} \right] \\ K_B &= \frac{C_B C_H}{s_C P_C} \\ pH &= pK_a + \log \left(\frac{C_B}{C_C} \right) \\ \sum_i z_i C_i &= C_{Na} + C_L - C_{Cl} - C_B = 0 \end{aligned}$$

Figure 3.2: Inside Cell j

Within the cells we will assume that the positive flux pointing toward the tear film, or pointing from the $(j + 1)^{\text{st}}$ boundary toward the j^{th} direction. Assuming conservation of mass, Equation 3.6 can be written to determine the thickness of cell j (h_j).

$$\frac{\rho_f}{M_W} \frac{dh_j}{dt} = -(J_{V,j} - J_{V,j+1}) \frac{S\rho_f}{M_W} + Q_W S h_j \quad (3.6)$$

Equation 3.6 simplifies to

$$\frac{dh_j}{dt} = -(J_{V,j} - J_{V,j+1}) + \frac{Q_W M_W h_j}{\rho_f}. \quad (3.7)$$

In Equation 3.6, M_W is the molecular weight of water. S is the cross sectional area of the cell which was assumed to be constant. $J_{V,j}$ is the volumetric flux of water. Q_W is the source term for water. There are two sources of water; water production from the aerobic reactions involving the Krebs cycle and water production from the bicarbonate buffering reaction which will be described later on in this section. The parameter ρ_f is represented by Equation 3.8. This scaled the fluid density of water in the cell by a factor of the sum of the moles of solute in the cell divided by the moles of water, after Leung et al [3].

$$\rho_f = \rho_w \left(1 + \frac{\sum_{i \neq W} C_i M_i}{C_W M_W} \right) \quad (3.8)$$

We also assume conservations of mass for all solutes present within the cell. Letting i designate the solute for the j^{th} cell, the equation for the conservation is

$$S h_j \frac{dC_{i,j}}{dt} = -(J_{i,j} - J_{i,j+1}) S + Q_{i,j} S h_j. \quad (3.9)$$

This can be simplified to

$$\frac{dC_{i,j}}{dt} = -\frac{(J_{i,j} - J_{i,j+1})}{h_j} + Q_{i,j}. \quad (3.10)$$

In Equation 3.10, $C_{i,j}$ is the concentration of solute i in cell j . $J_{i,j}$ is the molar flux of solute i across the j^{th} membrane. $Q_{i,j}$ is the source or sink term for solute i in the j^{th} cell.

The solutes that are present in the epithelial cells are sodium (Na), chloride (Cl), oxygen (O), lactate (L), glucose (G), bicarbonate (B), carbon dioxide (C), and hydronium

(H). The differential and algebraic equations in this model will now be described for each solute. Thus i can take on these values in our model.

Sodium and chloride ions in the cells do not have a source or sink term because they are not involved in metabolic reactions. Using Equation 3.10, the equations used to represent these solutes are shown in Equation 3.11 and 3.12.

$$\frac{dC_{Na,j}}{dt} = -\frac{J_{Na,j} - J_{Na,j+1}}{h_j} \quad (3.11)$$

$$\frac{dC_{Cl,j}}{dt} = -\frac{J_{Cl,j} - J_{Cl,j+1}}{h_j} \quad (3.12)$$

Oxygen, lactate and glucose are solutes involved in aerobic and anaerobic reactions. The source and sink terms were taken from [3]. Glucose is broken down to smaller molecules to make energy in cells. The processes are shown in Figure 1.3. First glucose is broken down to pyruvate during glycolysis. Pyruvate can then be broken down aerobically to water and carbon dioxide or anaerobically to lactate. Therefore, glucose is consumed in both conditions. The consumption terms are dependent on the production of lactate and oxygen. The equations for glucose is shown as Equation 3.13.

$$\begin{aligned} \frac{dC_{G,j}}{dt} = & -\frac{J_{G,j} - J_{G,j+1}}{h_j} - \frac{Q_L^{min}}{2} \left[1 + \frac{K_O^L}{K_O^L + P_O} \right] \left[\frac{C_G}{K_G^L + C_G} \right] \\ & - \frac{Q_O^{max}}{6} \left[1 + 0.8 \frac{7.6 - \text{pH}}{K_{\text{pH}} + 7.6 - \text{pH}} \right] \left[1 + \frac{C_G}{K_O^G + C_G} \right] \left[\frac{P_O}{K_O^O + P_O} \right] \end{aligned} \quad (3.13)$$

Next, oxygen consumption is dependent on the pH, glucose and rate expression. During the Krebs cycle, oxygen is consumed to produce water and energy. Equation 3.14 is used to represent the concentration change in oxygen.

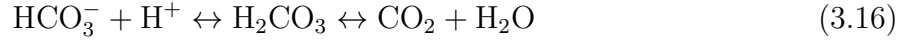
$$\begin{aligned} \frac{dC_{O,j}}{dt} = & -\frac{J_{O,j} - J_{O,j+1}}{h_j} + \\ & Q_O^{max} \left[1 + 0.8 \frac{7.6 - \text{pH}}{K_{\text{pH}} + 7.6 - \text{pH}} \right] \left[1 + \frac{C_G}{K_O^G + C_G} \right] \left[\frac{P_O}{K_O^O + P_O} \right] \end{aligned} \quad (3.14)$$

Lactate is produced when the cell is functions under anaerobic conditions. The production of lactate is dependent on oxygen tension and glucose concentration. The differential equation used to represent lactate concentration is Equation 3.15.

$$\frac{dC_{L,j}}{dt} = -\frac{J_{L,j} - J_{L,j+1}}{h_j} + Q_L^{min} \left[1 + \frac{K_O^L}{K_O^L + P_O} \right] \left[\frac{C_G}{K_G^L + C_G} \right] \quad (3.15)$$

In Equations 3.14 to 3.15, P_O is the partial pressure of oxygen and the parameter values are shown in Table C.4. Note that the partial pressure equation for oxygen is described using Henry's Law as shown in Equation 3.3.

Next, we will look at the equations that describe the solutes bicarbonate (B), hydronium (H), and carbon dioxide (C) are present. These solutes are important for maintaining a neutral pH in the cells. Cells have a natural bicarbonate buffering system used to keep a neutral pH. The reaction for this system is shown in Reaction 3.16.



The differential equations to represent the change in concentrations of bicarbonate, hydronium, and carbon dioxide are Equations 3.17 to 3.19.

$$\frac{dC_{B,j}}{dt} = -\frac{(J_{B,j} - J_{B,j+1})}{h_j} + Q_{B,j} \quad (3.17)$$

$$\frac{dC_{H,j}}{dt} = -\frac{(J_{H,j} - J_{H,j+1})}{h_j} + Q_{H,j} \quad (3.18)$$

$$\frac{dC_{C,j}}{dt} = -\frac{(J_{C,j} - J_{C,j+1})}{h_j} + Q_{C,j} \quad (3.19)$$

The source term for hydronium is dependent on the consumption of bicarbonate and production of lactate. The source term for carbon dioxide is dependent on the production of bicarbonate and consumption of oxygen. However, the source term for bicarbonate is unknown. Therefore, we can to eliminate the source term for bicarbonate. This was done by subtracting Equation 3.17 from Equation 3.18 and adding Equation 3.17 to Equation 3.19 to eliminate the consumption or production term for bicarbonate. We assume that this reaction system preceeds very rapidly and is thus assumed to be at equilibrium. Therefore, the

changes in concentrations will be set to zero. This is shown in 3.20 and 3.21 which represent a relationship between the fluxes of hydronium ($J_{H,j}$), bicarbonate ($J_{B,j}$) and carbon dioxide ($J_{C,j}$).

$$0 = -\frac{J_{H,j} - J_{H,j+1}}{h_j} + \frac{J_{B,j} - J_{B,j+1}}{h_j} + Q_L^{min} \left[1 + \frac{K_O^L}{K_O^L + P_O} \right] \left[\frac{C_G}{K_G^L + C_G} \right] \quad (3.20)$$

$$0 = -\frac{J_{C,j} - J_{C,j+1}}{h_j} - \frac{J_{B,j} + J_{B,j+1}}{h_j} + Q_O^{max} \left[1 + 0.8 \frac{7.6 - pH}{K_{pH} + 7.6 - pH} \right] \left[1 + \frac{C_G}{K_O^G + C_G} \right] \left[\frac{P_O}{K_O^O + P_O} \right] \quad (3.21)$$

Equations 3.20 to 3.21 create an algebraic system that will need to be solved along with the differential system. There are an additional three algebraic equations that need to be satisfied in the system as well. The cell maintain an electronuetral environment because a charge can not build up in a cell. This is imposed with Equation 3.22.

$$\sum_i z_i C_i = C_{Na} + C_L - C_{Cl} - C_B = 0 \quad (3.22)$$

In Equation 3.22, the concentrations of sodium, lactate and chloride can be found using the differential Equations 3.11, 3.15, and 3.12. Therefore, Equation 3.22 can be used to solve for the concentration of bicarbonate (C_B).

The next equation involves the bicarbonate buffering equilibrium constant K_B and is shown in Equation 3.23.

$$K_B = \frac{C_B C_H}{s_C P_C} \quad (3.23)$$

In Equation 3.23, K_B and the solubility constant for carbon dioxide in water are constants in Table C.4. The third equation involves pH. The pH can be calculated by Equation 3.24.

$$pH = pK_a + \log \left(\frac{C_B}{C_C} \right) \quad (3.24)$$

Note that the definition of pH is Equation 3.2. Equations 3.23 and 3.24 can be used to calculate concentrations of hydronium (C_H) and carbon dioxide (C_C).

A summary of this section's equations that represent inside the cells are shown in Figure 3.2.

3.2.3 Tear Film Equations

Next we will describe the equations represented in the tear film. A schematic drawing of this is shown in Figure 3.3.

Equation 3.25 specifies the dynamics of the tear film thickness. The first term represents the water flux between the tear film and the most anterior epithelial layer. The second term represents the water lost from evaporation into the air. The flux term for water represented as Equation 3.26 and is the same evaporative flux ($J_{v,0}$) used in Chapter 2.

$$\frac{dh_0}{dt} = -(EJ_{v,0} - J_{v,1}) \quad (3.25)$$

$$J_{v,0} = \frac{1}{\bar{K} + h_0}(1 - A\delta h_0^{-3}) \quad (3.26)$$

Within the tear film we will assume that the positive flux pointing toward the air. Assuming conservation of mass, Equation 3.27 can be written to determine the concentration of a general species i in the tear film at $j=0$.

$$\frac{d(h_0 C_{i,0})}{dt} = -(J_{i,0} - J_{i,1}) \quad (3.27)$$

Equation 3.27 can simplify to Equation 3.28 using the chain rule.

$$C_{i,0} \frac{dh_0}{dt} + h_0 \frac{dC_{i,0}}{dt} = -(J_{i,0} - J_{i,1}) \quad (3.28)$$

We want to solve Equation 3.28 for $\frac{dC_i}{dt}$. We can substitute Equation 3.25 and divide through by h_0 to obtain Equation 3.29.

$$\frac{dC_{i,0}}{dt} = \frac{-(J_{i,0} - J_{i,1}) + C_{i,0}(EJ_{v,0} - J_{v,1})}{h_0}. \quad (3.29)$$

The solutes present in the tear film are sodium (Na), chloride (Cl), oxygen (O), carbon dioxide (C), bicarbonate (B) and hydronium (H). There is no concentration of glucose or lactate in the tear film. Therefore Equation 3.29 will be written for these solutes.

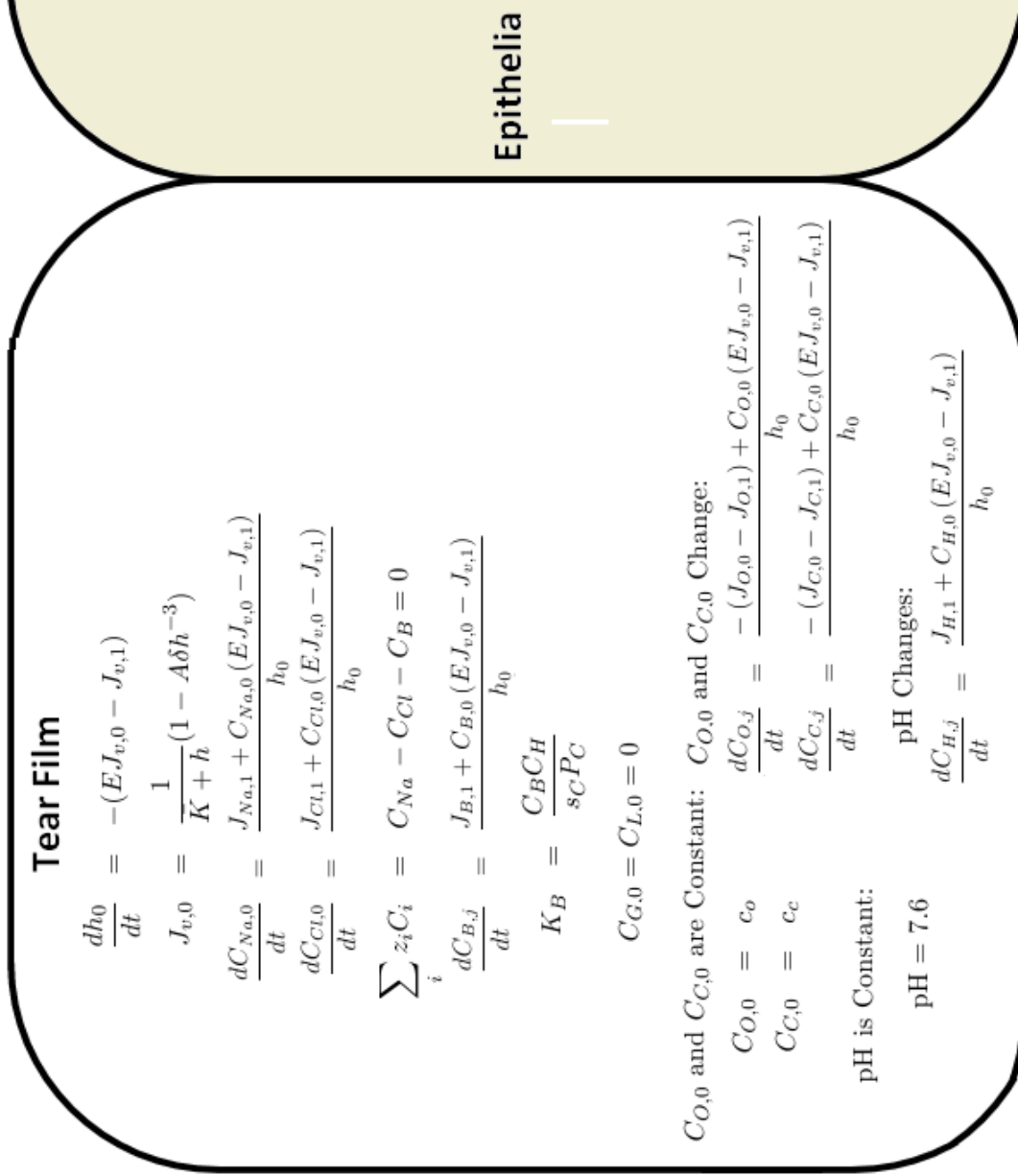


Figure 3.3: A schematic drawing of the tear film. This includes the equations that are applied in the tear film. There are two cases each for oxygen and carbon dioxide concentrations and the pH. If one choose to keep the variable constant (C_O , C_C or C_H) constant then the equations that are used for that conditions are under that constant choice. If one choose to allow the variable to change (C_O , C_C or C_H) then the equations that are used for that condition are under that change choice.

In the tear film sodium and chloride are driven by the change in flux between the tear film and epithelium. Sodium and chloride are unable to permeate through the tear film/air interface creating no flux across that boundary ($J_{Na,0} = 0$ and $J_{Cl,0} = 0$). There is no production or consumption of these species because there are no metabolic reactions in the tear film. The equations for sodium and chloride are shown as Equations 3.30 and 3.31.

$$\frac{dC_{Na,0}}{dt} = \frac{J_{Na,1} + C_{Na,0}(EJ_{v,0} - J_{v,1})}{h_0} \quad (3.30)$$

$$\frac{dC_{Cl,0}}{dt} = \frac{J_{Cl,1} + C_{Cl,0}(EJ_{v,0} - J_{v,1})}{h_0} \quad (3.31)$$

There are two cases to consider for oxygen and carbon dioxide. One case would be to set the concentrations of oxygen and carbon dioxide to constant (c_o and c_c). The second case would be to allow the concentrations to vary by allowing a flux between the tear film/air interface, which will be discussed in Section 3.2.4.1. This case would be to allow a flux of oxygen ($J_{O,0}$) and carbon dioxide ($J_{C,0}$) across the tear film/air boundary. Equations 3.32 and 3.33 represent the equations that would be used if there was change in the concentrations of oxygen and carbon dioxide in the tear film. However, the equations for $J_{O,0}$ and $J_{C,0}$ at the boundary have not been determined at this time. Therefore, for simplicity we will assume that the concentrations of oxygen and carbon dioxide is constant in the tear film.

$$\frac{dC_{O,j}}{dt} = \frac{-(J_{O,0} - J_{O,1}) + C_{O,0}(EJ_{v,0} - J_{v,1})}{h_0} \quad (3.32)$$

$$\frac{dC_{C,j}}{dt} = \frac{-(J_{C,0} - J_{C,1}) + C_{C,0}(EJ_{v,0} - J_{v,1})}{h_0} \quad (3.33)$$

Next, we will look at the equations that describe the solutes bicarbonate (B) and hydronium (H). The differential equations to represent the change in concentrations of bicarbonate and hydronium are Equations 3.34 and 3.35. However, each source or sink term will be zero since there are no metabolic reactions in the tear film. We also assume that there is zero flux of bicarbonate and hydronium at the tear film/air interface. Therefore the

equations will simplify to Equations 3.34 and 3.35.

$$\frac{dC_{B,j}}{dt} = \frac{J_{B,1} + C_{B,0}(EJ_{v,0} - J_{v,1})}{h_0} \quad (3.34)$$

$$\frac{dC_{H,j}}{dt} = \frac{J_{H,1} + C_{H,0}(EJ_{v,0} - J_{v,1})}{h_0} \quad (3.35)$$

Using Equations 3.34 and 3.35, we can determine the concentration of bicarbonate and hydronium in the tear film. The concentration of bicarbonate will contribute to calculating the osmolarity in the tear film.

However there are two cases to consider for pH in the model. The first case would be to set the pH to a constant of 7.6. This would force the tear film to stay at neutral conditions. The second case would be to let the initial pH be 7.6 and observe how the pH changes over time which would imply that Equation 3.35 would be used. Since bicarbonate is present in the tear film, variation in pH could cause the bicarbonate reactions to occur which would cause changes in the pH. If the pH reaches an acidic or basic value, there could be potential damage to the underlying cells.

The equations that will be applied in the tear film are also shown in Figure 3.3. There are two cases to choose for both the oxygen and carbon dioxide concentrations and the pH.

3.2.4 Boundary Fluxes

Next we will look at the boundary conditions for the proposed model. There are four separate cases to consider; the tear film/air interface ($j = 0$), the tear film/epithelial interface ($j = 1$), the cell/cell interface ($j = 2$ to $j = 7$) and the epithelial/stroma interface ($j = 8$). In general, the Kedem and Katchalsky (KK) equations [[29], [3]] are used to represent water transport across the epithelial membrane. This is shown as Equation 3.36. KK equations are also used to represent solute fluxes. Equation 3.37 is the general equation used for solutes glucose, lactate, bicarbonate, hydronium, sodium and chloride. Oxygen and carbon dioxide

diffuse through the cells. The boundary condition shown as Equation 3.38 is used for oxygen and carbon dioxide [3, 29].

$$J_{v,j} = -L_p \left[- \sum \sigma_{i,j} (RT \Delta C_{i,j} + z_{i,j} < C_{i,j} > F \Delta \psi_j) \right] \quad (3.36)$$

$$J_{i,j} = (1 - \sigma_{i,j}) J_{v,j} < C_{i,j} > - \omega_{i,j} (RT \Delta C_{i,j} + z_{i,j} < C_{i,j} > F \Delta \psi_j) + J_{ai,j} \quad (3.37)$$

$$J_{i,j} = (1 - \sigma_{i,j}) J_{v,j} < C_{i,j} > - \omega_{i,j} RT \Delta C_{i,j} \quad (3.38)$$

Note that the conditions vary for the four cases. Equations 3.36 to 3.38 are the general boundary conditions for water and solute fluxes.

In addition, there is zero net current through the cell and tear film interface. Nonzero net current into a cell could lead to charge build up that would damage the cells. Therefore, Equation 3.39 will be imposed at each boundary. This equation is relative to the tear film, so the electric potential in the tear film is always zero. Equation 3.39 is used to calculate the value for $\Delta \psi_j$, the change in electric potential.

$$\sum_j z_i J_{i,j} = 0 \quad (3.39)$$

$$z_{Na} J_{Na,j} + z_L J_{L,j} - z_{Cl} J_{Cl,j} - z_B J_{B,j} = 0 \quad (3.40)$$

All parameter values are found in Table C.5.

3.2.4.1 Tear Film/Air Interface

The schematic drawing for the tear film/ air interface at $j = 0$ is shown in Figure 3.4. As shown in this figure water, oxygen and carbon dioxide are the only molecules that can cross this boundary. The flux of water due to evaporation is shown as Equation 3.26. The fluxes of sodium, chloride, lactate, glucose, bicarbonate and hydronium are zero.

The tear film is one of the main sources of oxygen for the epithelium. Therefore, by allowing the concentration to change one can study how oxygen will diffuse throughout the epithelium. It would also be important to include a flux of oxygen and carbon dioxide

between the tear film and air. This will allow the air to constantly supply oxygen to the tear film so the epithelial cells can be supplied with oxygen. If oxygen is able to diffuse through the air/tear film boundary easily, then epithelial cells will have a steady supply of oxygen which will be used in the Krebs cycle to produce energy. However, if the tear film is unable to provide enough oxygen to the epithelial cells, then the cells will have to enter anaerobic processes and produce less energy. This lack of energy and supply of oxygen can hinder the cells ability to function. However for simplicity, the concentrations of oxygen and carbon dioxide could be set to constants creating a boundary condition.

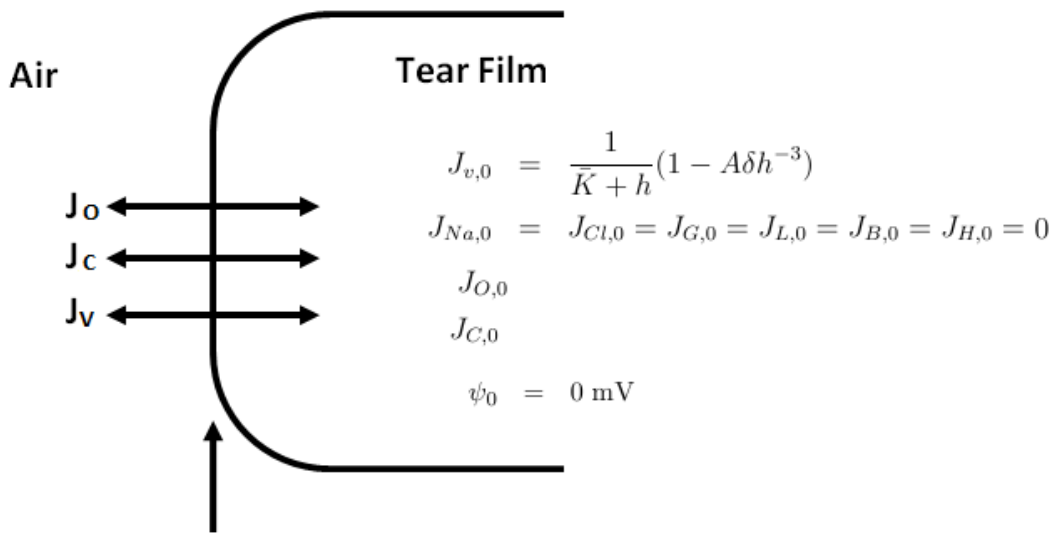


Figure 3.4: Tear Film/ Air Interface $j = 0$. There is a flux of water (J_V) out of the tear film due to evaporation. Solutes and metabolites have no flux between the tear film/air interface. The equation for the flux of oxygen and carbon dioxide at this boundary are still to be determined. The $\Delta\psi$ value was taken from [3].

3.2.4.2 Tear Film/Epithelial Cell Interface

A schematic for the tear film/epithelial interface ($j = 1$) is shown in Figure 3.5. At this interface the solutes sodium, chloride, bicarbonate, and hydronium are able to cross the anterior membrane of the cell. The flux boundary condition used Equation 3.37 at the $j = 1$ position. Water is also able to permeate through the membrane. The water flux boundary condition at the $j = 1$ position is Equation 3.36. In addition, oxygen and carbon dioxide can diffuse through the membrane. Equation 3.38 is used to represent these fluxes. Glucose and lactate are not able to permeate through the $j = 1$ interface which results in a zero flux. The schematic drawing in Figure 3.5, shows the equations at this interface.

We solve for the electric potential by imposing zero current at this boundary with Equation 3.39. The solutes that contribute to this are sodium ions, lactate, chloride ions, and bicarbonate. After inputting the fluxes for each of the solutes at this bound ($j = 1$) into Equation 3.39, Equation 3.41 is obtained.

$$\begin{aligned} \Delta\psi_1 = \frac{1}{D_1} & [(1 - \sigma_{Na,1})J_{v,1} \langle C_{Na,1} \rangle - \omega_{Na,1}RT\Delta C_{Na,1} + (1 - \sigma_{L,1})J_{v,1} \langle C_{L,1} \rangle \\ & - \omega_{L,1}RT\Delta C_{L,1} - (1 - \sigma_{Cl,1})J_{v,1} \langle C_{Cl,1} \rangle + \omega_{Cl,1}RT\Delta C_{Cl,1} - J_{aCl,1} \\ & - (1 - \sigma_{B,1})J_{v,1} \langle C_{B,1} \rangle + \omega_{B,1}RT\Delta C_{B,1}] \end{aligned} \quad (3.41)$$

$$D_1 = F(\omega_{Na,1} \langle C_{Na,1} \rangle + \omega_{L,1} \langle C_{L,1} \rangle + \omega_{Cl,1} \langle C_{Cl,1} \rangle + \omega_{B,1} \langle C_{B,1} \rangle)$$

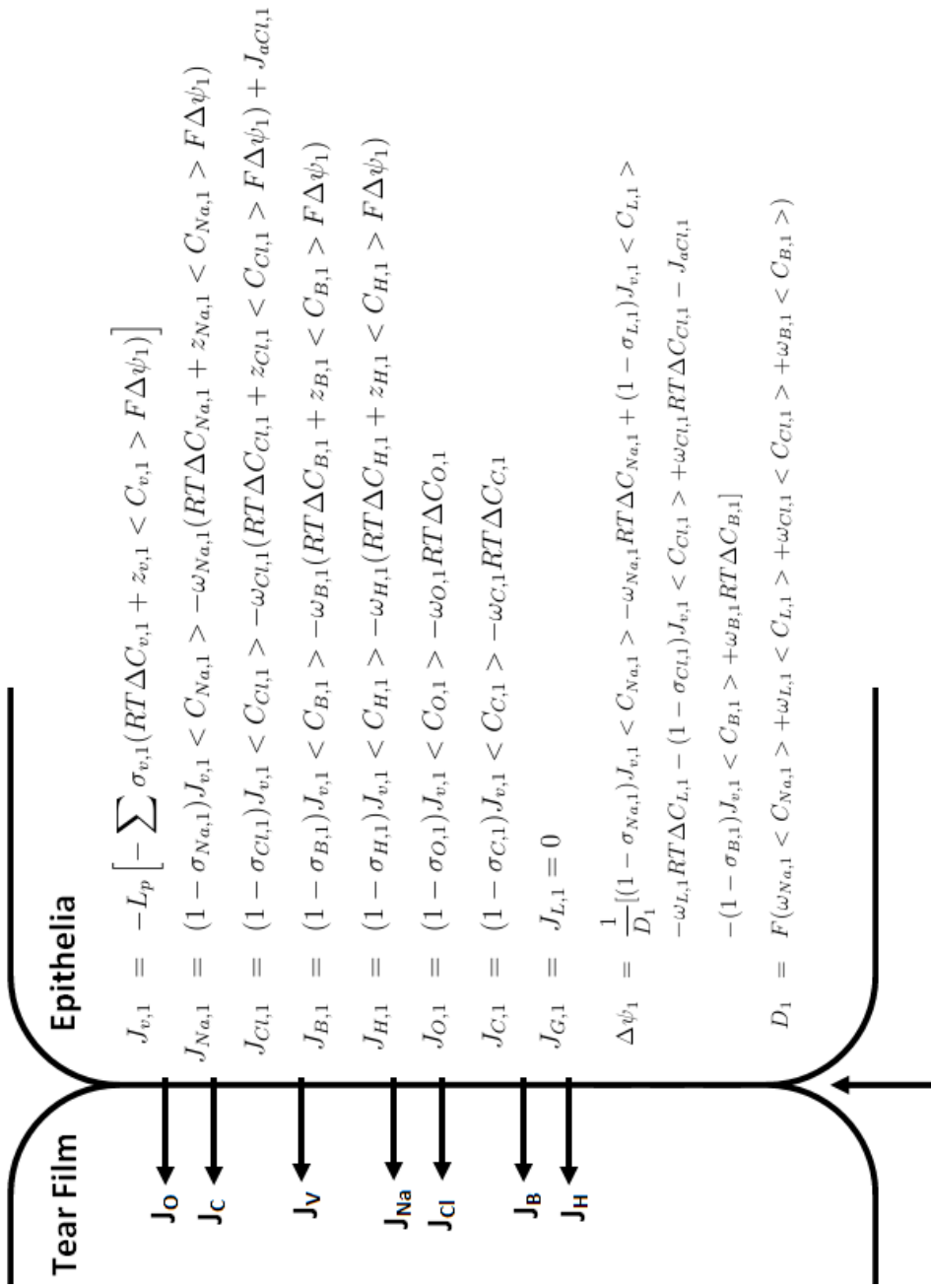


Figure 3.5: Tear Film/ Epithelial Cell Boundary $j = 1$

3.2.4.3 Epithelial Cell/Epithelial Cell Interface

Figure 3.6 is a schematic drawing for cell to cell boundary conditions. These conditions shown in the figure are for boundaries $j = 2, 3, 4, 5, 6,$ and 7 ; these boundaries are permeable to water and all solutes.

We solve for the electric potential by imposing zero current at these boundaries with Equation 3.39. After inputting the fluxes for each of the solutes at this boundary ($j = 1$) into Equation 3.39, Equation 3.42 is obtained.

$$\begin{aligned} \Delta\psi_j &= \frac{1}{D_j} [(1 - \sigma_{Na,j})J_{v,j} < C_{Na,j} > - \omega_{Na,j}RT\Delta C_{Na,j} + (1 - \sigma_{L,j})J_{v,j} < C_{L,j} > \\ &\quad - \omega_{L,j}(RT\Delta C_{L,j} - (1 - \sigma_{Cl,j})J_{v,j} < C_{Cl,j} > + \omega_{Cl,j}RT\Delta C_{Cl,j} - J_{aCl,j} \\ &\quad - (1 - \sigma_{B,j})J_{v,j} < C_{B,j} > + \omega_{B,j}RT\Delta C_{B,j}] \end{aligned} \quad (3.42)$$

$$D_j = F (\omega_{Na,j} < C_{Na,j} > + \omega_{L,j} < C_{L,j} > + \omega_{Cl,j} < C_{Cl,j} > + \omega_{B,j} < C_{B,j} >)$$

The equations are shown in Figure 3.6.

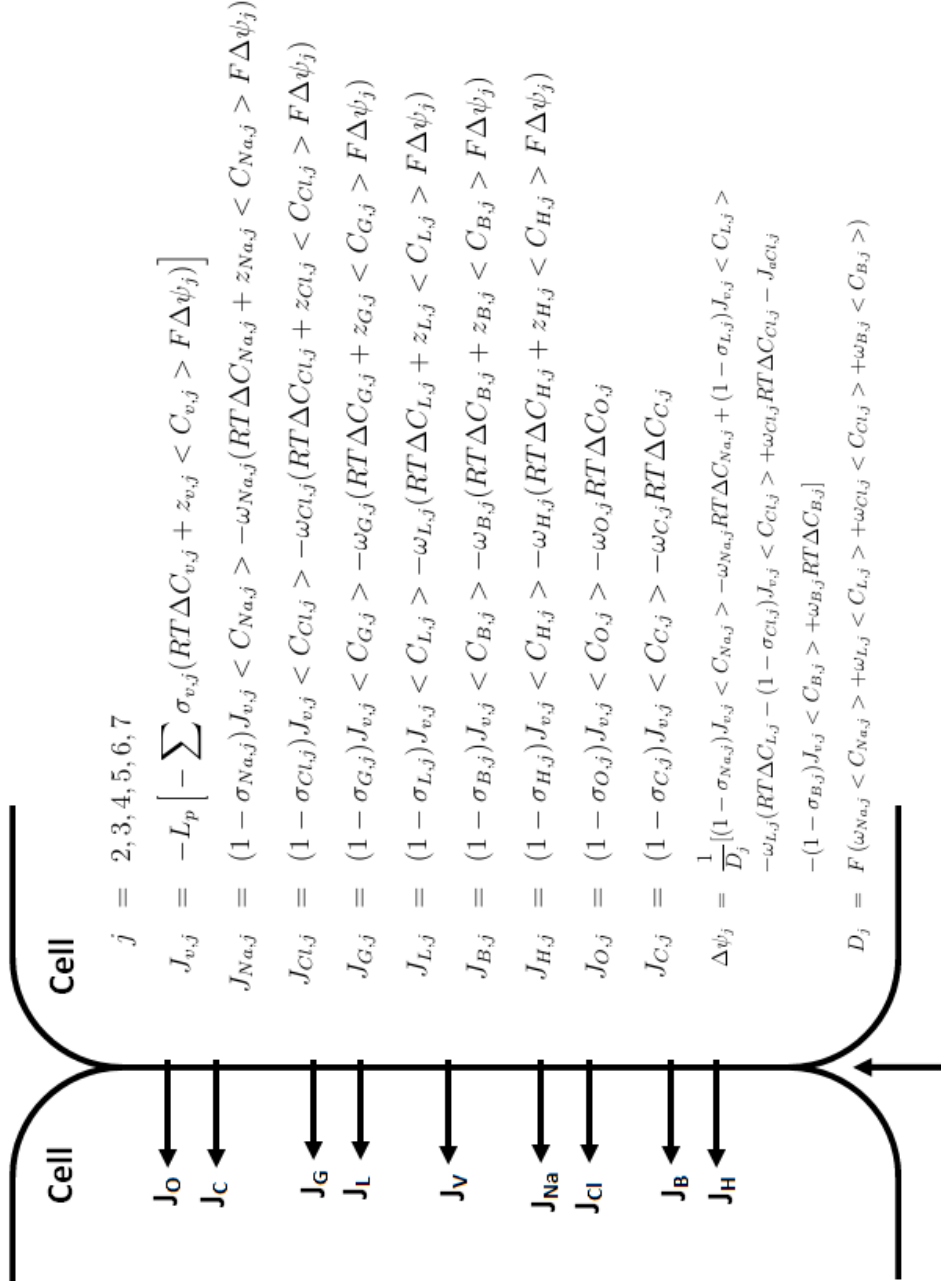


Figure 3.6: Epithelial Cell/Epithelial Cell Interface ($j = 2, 3, 4, 5, 6, 7$)

3.2.4.4 Epithelial Cell/Stroma Interface

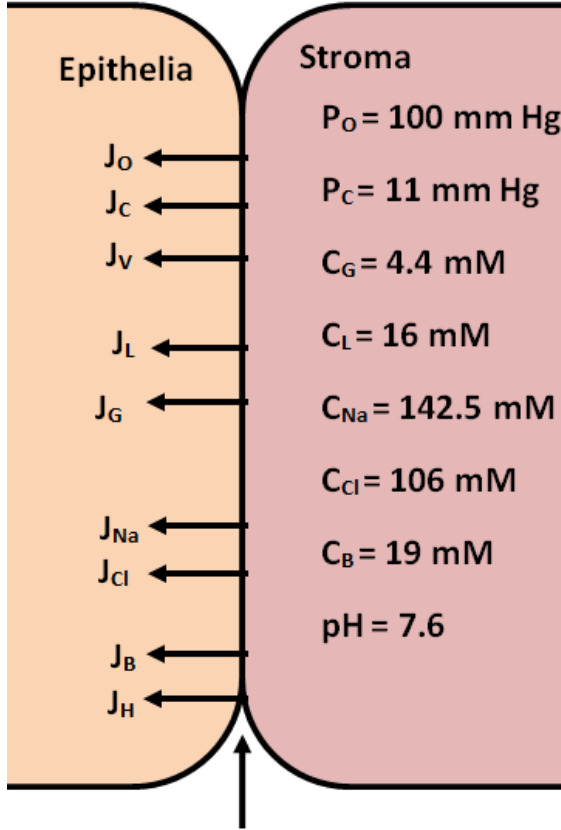
The epithelial/stroma boundary schematic is shown in Figure 3.7 at $j = 8$. There are constant conditions in the stroma. These values are the same as the constant conditions are the steady state results in the stroma from the Leung *et al* [3] and the values are shown in Table C.4. This boundary is permeable to water and all solutes.

We solve for the electric potential by imposing zero current at these boundaries with Equation 3.39. After inputting the fluxes for each of the solutes at this bound ($j = 1$) into Equation 3.39, Equation 3.43 is obtained.

$$\begin{aligned} \Delta\psi_8 = & \frac{1}{D_8} [(1 - \sigma_{Na,8})J_{v,8} \langle C_{Na,8} \rangle - \omega_{Na,8}RT\Delta C_{Na,8} + (1 - \sigma_{L,8})J_{v,8} \langle C_{L,8} \rangle \\ & - \omega_{L,8}(RT\Delta C_{L,8} - (1 - \sigma_{Cl,8})J_{v,8} \langle C_{Cl,8} \rangle + \omega_{Cl,8}RT\Delta C_{Cl,8} - J_{aCl,8} \\ & - (1 - \sigma_{B,8})J_{v,8} \langle C_{B,8} \rangle + \omega_{B,8}RT\Delta C_{B,8}] \end{aligned} \quad (3.43)$$

$$D_8 = F (\omega_{Na,8} \langle C_{Na,8} \rangle + \omega_{L,8} \langle C_{L,8} \rangle + \omega_{Cl,8} \langle C_{Cl,8} \rangle + \omega_{B,8} \langle C_{B,8} \rangle)$$

The equations are shown in the schematic drawing in in Figure 3.7.



$$\begin{aligned}
 J_{v,8} &= -L_p \left[\Delta P - \sum \sigma_{v,8} (RT \Delta C_{v,8} + z_{v,8} \langle C_{v,8} \rangle F \Delta \psi_8) \right] \\
 J_{Na,8} &= (1 - \sigma_{Na,8}) J_{v,8} \langle C_{Na,8} \rangle - \omega_{Na,8} (RT \Delta C_{Na,8} + z_{Na,8} \langle C_{Na,8} \rangle F \Delta \psi_8) \\
 J_{Cl,8} &= (1 - \sigma_{Cl,8}) J_{v,8} \langle C_{Cl,8} \rangle - \omega_{Cl,8} (RT \Delta C_{Cl,8} + z_{Cl,8} \langle C_{Cl,8} \rangle F \Delta \psi_8) \\
 J_{G,8} &= (1 - \sigma_{G,8}) J_{v,8} \langle C_{G,8} \rangle - \omega_{G,8} (RT \Delta C_{G,8} + z_{G,8} \langle C_{G,8} \rangle F \Delta \psi_8) \\
 J_{L,8} &= (1 - \sigma_{L,8}) J_{v,8} \langle C_{L,8} \rangle - \omega_{L,8} (RT \Delta C_{L,8} + z_{L,8} \langle C_{L,8} \rangle F \Delta \psi_8) \\
 J_{B,8} &= (1 - \sigma_{B,8}) J_{v,8} \langle C_{B,8} \rangle - \omega_{B,8} (RT \Delta C_{B,8} + z_{B,8} \langle C_{B,8} \rangle F \Delta \psi_8) \\
 J_{H,8} &= (1 - \sigma_{H,8}) J_{v,8} \langle C_{H,8} \rangle - \omega_{H,8} (RT \Delta C_{H,8} + z_{H,8} \langle C_{H,8} \rangle F \Delta \psi_8) \\
 J_{O,8} &= (1 - \sigma_{O,8}) J_{v,8} \langle C_{O,8} \rangle - \omega_{O,8} RT \Delta C_{O,8} \\
 J_{C,8} &= (1 - \sigma_{C,8}) J_{v,8} \langle C_{C,8} \rangle - \omega_{C,8} RT \Delta C_{C,8} \\
 \Delta \psi_8 &= \frac{1}{D_8} [(1 - \sigma_{Na,8}) J_{v,8} \langle C_{Na,8} \rangle - \omega_{Na,8} RT \Delta C_{Na,8} + (1 - \sigma_{L,8}) J_{v,8} \langle C_{L,8} \rangle \\
 &\quad - \omega_{L,8} (RT \Delta C_{L,8} - (1 - \sigma_{Cl,8}) J_{v,8} \langle C_{Cl,8} \rangle + \omega_{Cl,8} RT \Delta C_{Cl,8} - J_{aCl,8} \\
 &\quad - (1 - \sigma_{B,8}) J_{v,8} \langle C_{B,8} \rangle + \omega_{B,8} RT \Delta C_{B,8}] \\
 D_8 &= F (\omega_{Na,8} \langle C_{Na,8} \rangle + \omega_{L,8} \langle C_{L,8} \rangle + \omega_{Cl,8} \langle C_{Cl,8} \rangle + \omega_{B,8} \langle C_{B,8} \rangle)
 \end{aligned}$$

Figure 3.7: Epithelial Cell/Stroma Interface ($j = 8$)

Chapter 4

DISCUSSION

4.1 Cornea and Conjunctiva

Using a perfect semipermeable barrier to model the cornea and a constant evaporation term allows a single equation model for the tear film to estimate the permeability for the cornea. The estimated values can fit thinning data for some subjects quite well. This information is valuable for estimating the osmolarity that occurs over the cornea and conjunctiva during thinning. We view the values for the permeability found in this work may near the upper end of the range in humans, and there may certainly be subjects with less permeable ocular surfaces, and there may be heterogeneity in the ocular surface that is neglected here. Nevertheless, we believe that our results give useful insight into the values of the osmolarity around the ocular surface.

Using our models with epithelial cells, after many 30s interblinks over a four-hour period, the osmolarity in the pre-conjunctival tear film is 334 mOsM with a thinning rate of 1.4 $\mu\text{m}/\text{min}$. Using a thinning rate of 2.5 $\mu\text{m}/\text{min}$ with 30s interblinks, the osmolarity is 364 mOsM at that location. The osmolarity in the pre-corneal tear film with 30s interblinks was 394 mOsM, a high value. This leads to an elevated osmolarity of 356 mOsM in the squamous cell layer directly beneath the tear film because the osmotic gradient induces water transport from the cells to the tear film. This osmotic stress will lead to cellular responses such as protein production or depolarization, which will cause cells to enter into and accelerate apoptosis, as well as increased cornification (discussed further below).

The osmolarity of the pre-corneal tear film increases more than for the pre-conjunctival tear film, and similarly for the corresponding anterior cell layers. The increased permeability

of the conjunctival surface contributes to this result. We believe that this result shows that the osmolarity over the cornea is higher than over the surrounding conjunctiva. The black line is thought to be a barrier between the meniscus and the rest of the tear film and that it may seal off fresh tear fluid that could enter the tear film between blinks [30]. We find that the tear film near the meniscus may already have lower osmolarity than in the precorneal tear film because of the increased permeability of the conjunctiva, in agreement with previous evidence [24].

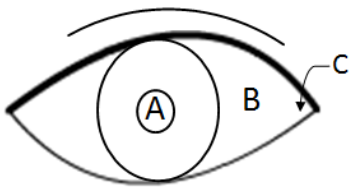


Figure 4.1: A sketch of the locations described by the theoretical models and the experimental measurements. The central cornea (A) and the conjunctiva not far from the limbus (B) are locations considered. C denotes the meniscus in the temporal canthus and represents the location used for TearLab or similar measurements.

The TearLab device is used to diagnose dry eye by obtaining a 50 nL sample near the corner of the eye at point C in Figure 4.1. Using this technology, an osmolarity measured between 308 and 316 mOsM is elevated from normal conditions according to the study performed by Lemp et al [31]. Therefore, a TearLab measurement of this value or higher diagnoses dry eye. Average osmolarity values for normal, moderate and severe dry eye are about 302 mOsM, 315 mOsM and 336 mOsM according to Sullivan et al [32]. Our model shows that the highest osmolarity occurs over the cornea and a lower value occurs over the conjunctiva in all cases. The conjunctival values are much closer to the values measured via TearLab than for the cornea. The lower osmolarity together over the conjunctiva with the black line acting as a barrier [30, 33] are consistent with meniscus osmolarity values.

Cultured human corneal epithelial cells have been used to measure the cellular response in increased osmolarities. In Chen *et al* [19], primary cultured human corneal epithelial (PCHCE) cells were plated and exposed to medium with various osmolarity. They used electrophoresis to run proteins expressed during apoptosis on the gel. Their results

concluded that the PCHCE cells in a 400 mOsM solution over 24 hours increased expression of SPRR2, involucrin and Transglutaminase-1 (TG1) compared to the the corneal epithelial cells in an isotonic 300 mOsM solution. SPRR2 and involucrin are precursors proteins in the corneal epithelium and promote cell death by cornification in an epidermal cell line. TGs are Ca^{2+} -dependent enzymes that catalyze bonds between proteins that function as bridges and they cause cross-linking of cornification envelope precursors in epidermal keratinocytes. Since our multiple blink model of the cornea reached a tear film osmolarity of 394 mOsM, it appears that long periods of long interblinks, such as during intense concentration like studying or computer games, may produce osmolarity levels that will cause an increase in the expression of the proteins involved in apoptosis. Thus, we conclude that apoptosis is accelerated under these conditions.

The simplified models that we studied for the combined dynamics of the tear film and the epithelia of the cornea and conjunctiva appear to give reasonable results. For a single interblink and for observed thinning rates, we find that there is little increase in osmolarity in the tear film and little effect on the epithelium in either region of the ocular surface. For many blink cycles with short interblink times, there is a small cumulative effect on the epithelial cells for either the conjunctiva or cornea. However, when there are many blink cycles with relatively long interblinks, there is a cumulative effect on the epithelial cells as they supply water to the tear film from repeated hyperosmolar states in the tear film. The effect observed in the model is enough to accelerate apoptosis in the squamous cells of the epithelium assuming that the osmolarity in the cells is not strongly affect by other cellular processes which have been neglected in the model.

4.2 Corneal Metabolism

The proposed model couples differential equations and algebraic equations. Water flux in this model is driven by evaporation of water between the tear film and air. This will drive water to from the epithelial cells to the tear film. In addition, this model also takes into account metabolic reactions that occur within each epithelial cell layer. Sodium and chloride

are ions present in cells that contribute to keeping cells more negatively charged than their surrounding extracellular space. This is very important for cellular function. Modeling the transport of these ions would be important to understand the states of these cells. This model also predicts the cellular concentrations of glucose, lactate, oxygen and carbon dioxide. When oxygen is readily available then the cell is able to undergo aerobic processes which produces a large amount of cellular energy in the form of adenosine triphosphate (ATP). When modeling the cellular concentrations of these metabolic species, the cellular state can be determine. If a cell is synthesizing much more lactate than carbon dioxide, then the cell is undergoing fermentation and producing very little energy. Producing little energy, the cell will not fully be able to functions properly if this state is continued for an extended time. This can possible contribute to cells entering apoptosis or cell death. Therefore, continuous exposure to low oxygen might contribute to decrease in corneal health because cells are entering apoptosis more readily.

An improvement to this model would be to include an oxygen and carbon dioxide flux across the tear film/air boundary. This will enable one to use an ordinary differential equations to solve for the concentration of oxygen and carbon dioxide in the tear film. This will allow the air to constantly supply oxygen and consume carbon dioxide from the tear film. If the tear film is rich in oxygen, the epithelial cells can be supplied with enough oxygen to function aerobically. If oxygen is able to diffuse through the air/tear film boundary easily, then epithelial cells will have a steady supply of oxygen which will be used in the Krebs cycle to produce energy. However, if the tear film is unable to provide enough oxygen to the epithelial cells, then the cells will have to enter anaerobic processes and produce less energy.

In addition, the osmolarity in each cell can be measured in each cell because the solutes that contribute to osmolarity are simulated. The results can be compared to the model in Chapter 1. If the results are similar, then it would be interesting to see the relationship between the metabolism that occurs in the cell and the osmolarity changes. This can be further compared to literature. It would be interesting to look at enzymes

expressed under the osmotic states and see if they match the metabolic enzymes that are used in the conditions that were modeled. For instance, if the cells had low oxygen, would the enzyme be able to be synthesized and expressed at that cellular state. If the results are not similar, then further comparison of the models would be needed. Looking deeper into literature to see what kind of states the cells undergo through the osmotic changes would be necessary.

Moreover, it would be interesting to vary the parameters in the model to observed the effects. Also, to change the initial conditions. For instance, if we assume that the squamous layer of cells is further along in apoptosis, their cell conditions can be slightly different than the basal cell layer which is still able to undergo mitosis. The aqueous humor provides a large amount of glucose to the cells. So it is possible that the basal cells will have a higher initial concentration of glucose than the squamous cells. Also, basal cells undergo mitosis, so they differentiate. This might be a condition where the cells need and undergo certain reactions to function properly. In addition, since the tear film is rich in oxygen, the initial concentration of oxygen could be higher in the squamous cells than the basal cells. By varying the initial conditions and figuring out what kind of states the cells are in to function properly might be essential to the model.

Appendix A
PARAMETERS FOR CHAPTER 1

Table A.1: Parameter definitions and values. Unless otherwise noted, these values were used to generate the computational results. K and \bar{K} are chosen to satisfy the experimentally measured thinning rate. α and A^* are recovered from the nondimensional parameters in Winter *et al* [1]. Ajaev and Homsy [2] discuss α and K .

Dimensional parameters		
Parameter	Description	Value
μ	Viscosity [34]	1.3×10^{-3} Pa·s
σ	Surface tension [35]	0.045 N·m ⁻¹
k	Tear film thermal conductivity (Water)	0.68 W·m ⁻¹ ·K ⁻¹
k_c	Corneal thermal conductivity [36]	0.58 W·m ⁻¹ ·K ⁻¹
ρ	Density (Water)	10^3 kg·m ⁻³
L_m	Latent heat of vaporization (Water)	2.3×10^6 J·kg ⁻¹
T'_s	Saturation temperature (Estimated)	27°C
T'_B	Body temperature (Estimated)	37°C
d	Characteristic tear film thickness [28]	3.5×10^{-6} m
L	Half width of an open eye (Estimated)	5×10^{-3} m
A^*	Hamaker constant [1]	3.5×10^{-19} Pa·m ³
α	Pressure coefficient for evaporation [1]	3.6×10^{-2} K·Pa ⁻¹
K	Non-equilibrium coefficient (Estimated)	2.4×10^5 K·m ² ·s·kg ⁻¹
v_w	Molar volume of water	1.8×10^{-4} m ³ ·mol ⁻¹
c_0	Isosmolar concentration	300 mOsM
P_f	tissue permeability	7.56×10^{-4} cm/s
Dimensionless parameters		
ϵ	$\frac{d'}{L}$	7×10^{-4}
E	$\frac{k(T'_B - T'_s)}{dL_m \epsilon \rho U_0}$	241.3
\bar{K}	$\frac{dL_m \epsilon \rho U_0}{kK}$	2.03×10^4
δ	$\frac{dL_m \epsilon \rho U_0}{\alpha \mu U_0}$	0.95
A	$\frac{L d \mu U_0}{A^*}$	3.06×10^{-6}
\bar{P}_f	$\frac{P_f v_w c_0}{\epsilon U_0}$	0.0117
P_c	$2\bar{P}_f$ (corn.) or $4\bar{P}_f$ (conj.)	0.0233 or 0.0466
λ	$\frac{d\bar{P}_f}{y_1(0)}$	0.0102

Appendix B

CODES FOR CHAPTER 1

B.1 Equations for Cornea

```
%% Function for tear film and epithelial layers
% Function outputs concentration and thickness for TF and epi layers
%%
function f =tearlayers7(t, y, Pc, E, Kbar, delta, A, lambda, h10, h20, h30,
h40, h50, h60, h70)

h = y(1);
c = y(2) ;
H1 = y(3) ;
H2 = y(4);
H3 = y(5);
H4 = y(6);
H5 = y(7);
H6 = y(8);
H7 = y(9);

f(1, 1) = Pc*(c-1) -E/(Kbar + h)*(1-delta*A*h^(-3));
f(2, 1) = (E/(Kbar + h)*(1-delta*A*h^(-3)) -Pc*(c-1))*c/h ;
f(3, 1) = lambda*(2/H1 - 2*c - 0.5/H2 + 0.5/H1);
f(4, 1) = lambda*(.5*h10/h20)*((1/H2) - 1/(H1) - (1/(H3)) + (1/(H2)));
f(5, 1) = lambda*(.5*h10/h30)*((1/(H3)) - 1/(H2) - (1/(H4)) + (1/(H3)));
f(6, 1) = lambda*(.5*h10/h40)*((1/(H4)) - 1/(H3) - (1/(H5)) + (1/(H4)));
f(7, 1) = lambda*(.5*h10/h50)*((1/(H5)) - 1/(H4) - (1/(H6)) + (1/(H5)));
```

```
f(8, 1) = lambda*(.5*h10/h60)*((1/(H6)) - 1/(H5) - (1/(H7)) + (1/(H6)));
f(9, 1) = lambda*(.5*h10/h70)*((1/H7) - (1/H6)) - (h10/h70)*(1 - (1/H7));
```

B.2 Permeability Studies Single Blink

```
%% Permeability values for a single blink
% shows the decrease in layers of the corneal epithelial layers
% as well as the cumulative decrease over the layers. Plots
% 2 graphs. Fig 1- Pfbars Values verses the Decrease over ind layers.
% Fig2- Pfbars Values verses the Cumulative Decrease over all the layers.
%%
clear all
close all

tstart = 0; tend = 90; %time start and end

h0 = 1; % initial value for TF thickness(h)
c0 = 1; % and concentration (c)
h10 = 4e-6; % initial h value (cm)
h20 = 4e-6;
h30 = 4e-6;
h40 = 6e-6;
h50 = 6e-6;
h60 = 6e-6;
h70 = 2e-5;

R = 8.314e7; %ideal gas constant
Teye = 308; %corneal surface temperature
PhiA = 3e-4; %osmolarity
Sc = 1.47; %surface area cornea

%Rt= 2.15*10^11 to get Pc=0.0694
%Rt= 7.24*10^11 to get Pc=0.0206
```

```

Rt = 2.15*10^11; %resistance to flow through material
                    %below film

epsilon = 7e-4; % ratio of length (d/L) => (cm/cm)
U = 0.5; % film (cm/ s)
k = 0.68; %thermal conductivity befor 0.68(W/m/K)
Teye_Ts = 10; %corneal surface temp-saturation temp
p = 1000; % (kg/m^3)
d = 3.5*10^-6; % thickness (m)
Lm = 2.3*10^6; %latent heat of vaporization (J/kg)

%gives A=0.0616
K= 2.4*10^5; %length evaporation rate from thermal
sigma = 45e-3; %surface tension (N/m)
mu = 1.3e-3;
%mu = 1.3; % Pa s
U0 = 0.005; % (m/s)
a = 3.484*10^-19;
l = 5*10^-3; % m
alpha = 3.59*10^(-3); %relates evaporative mass flux to
                    %pressure difference

Pf = 0.045; % (cm/s)
Vw = 18; % molar mass water
Phii = 0.0003; %concentration

J0 = (k*Teye_Ts)/(d*Lm);

%Braun and Smith
%Kbar over 2, 4, 8
Kbar = (k*K)/(d*Lm); %constitutive equ for evapoatuve rate
E = (k*Teye_Ts)/(epsilon*p*U0*d*Lm); %energy balance
S = (sigma*(epsilon^3))/(mu*U0); %Normal stress & Kinematic Condition

```

```

A = a/(mu*U0*d*1) ; %tangential immobility
delta = (alpha*mu*U0)/((epsilon^2)*1*Teye_Ts); %conservation of solute

lambda1 = zeros(15, 1);

x1=[0.005:0.001:0.020]; %used to vary Pfbars Values

hmin = zeros(15, 1);
H1max = zeros(15, 1);
H2max = zeros(15, 1);
H3max = zeros(15, 1);
H4max = zeros(15, 1);
H5max = zeros(15, 1);
H6max = zeros(15, 1);
H7max = zeros(15, 1);
cmax = zeros(15, 1);
Pfbar1= zeros(15, 1);
Pc1 = zeros(15, 1);
cumdec = zeros(15, 1);
cumdec2 = zeros(15, 1);

%y0 = [h c H1 H2 H3 H4 H5] inital values
y0 = [h0; c0; 1; 1; 1; 1; 1; 1; 1; 1];

for i=1:15
    Pfbar1(i)=(x1(i)*Pf*Vw*PhiA)/(epsilon*U0*100);
    Pc1(i) = 2*Pfbar1(i);
    lambda1(i) = (d/h10)*Pfbar1(i);
    %ode45, ode23s, odel5s
    Mytols = odeset('RelTol', 1e-6, 'AbsTol', 1e-7);
    [t, y] = odel5s(@(t, y) tearlayers7(t, y, Pc1(i), E, Kbar, delta, A,
    lambda1(i), h10, h20, h30, h40, h50, h60, h70), [tstart tend], y0);

```

```

Mytols;
h = y(:, 1);
c = y(:, 2) ;
H1 = y(:, 3) ;
H2 = y(:, 4);
H3 = y(:, 5);
H4 = y(:, 6);
H5 = y(:, 7);
H6 = y(:, 8);
H7 = y(:, 9);

hmin(i) = min(h);      %Find max values in plots on the y-axis
cmax(i) = max(c);
H1max(i) = min(H1);
H2max(i) = min(H2);
H3max(i) = min(H3);
H4max(i) = min(H4);
H5max(i) = min(H5);
H6max(i) = min(H6);
H7max(i) = min(H7);

end

endpts = [H1max, H2max, H3max, H4max, H5max, H6max, H7max];
endptst = endpts';

for j=1:15
    cumdec(j) = [(H1max(j)*h10+ H2max(j)*h20+ H3max(j)*h30+ H4max(j)*h40+
H5max(j)*h50+ H6max(j)*h60+ H7max(j)*h70)/(h10 + h20 + h30 + h40 + h50
+ h60 + h70)];
    cumdec2(j) = [(hmin(j)*d +H1max(j)*h10+ H2max(j)*h20+ H3max(j)*h30+

```

```

H4max(j)*h40+ H5max(j)*h50+ H6max(j)*h60+ H7max(j)*h70)/(d + h10 + h20
+ h30 + h40 + h50+ h60 + h70)];
end

[hrows, hcols] = size(endptst);
psym = ['ko', 'ro', 'go', 'b*' , 'r*', 'bo' , 'k*' ];

figure
for k=1:7
    plot(Pfbar1, endpts(:, k), psym(k))
    hold on;
end
xlabel('Pfbar Value ', 'FontSize', 15)    %Label the horizontal axis
ylabel('%h_i(t) Decrease Fracion', 'FontSize', 15)
hold off;

figure
plot(Pfbar1, endpts(:, 1), Pfbar1, endpts(:, 2), Pfbar1, endpts(:, 3),
Pfbar1, endpts(:, 4), Pfbar1, endpts(:, 5), Pfbar1, endpts(:, 6), Pfbar1,
endpts(:, 7))
title('Corneal Epithelial Cell Thickness Verses Pfbar Value', 'FontSize',
16) %Title for the plot
xlabel('Pfbar Value ', 'FontSize', 15)    %Label the horizontal axis
ylabel('%h_i(t) Decrease Fraction', 'FontSize', 1) %Label the vertical axis

figure
plot(Pfbar1, cumdec)
title('Cumulative Decrease in Corneal Epithelial Thickness Verses Pfbar
Value', 'FontSize', 16) %Title for the plot
xlabel('Pfbar Value ', 'FontSize', 15)    %Label the horizontal axis
ylabel('Cumulative Decrease Fraction', 'FontSize', 15)%Label the vertical
%axis

```

```
figure
plot(Pfbar1, cumdec2)
```

B.3 Permeability Studies Multiple Blink

```
%Pfvalues
%shows the decrease in layers of the corneal epithelial layers
% as well as the cumulative decrease over the layers. Plots
% 5 graphs. Fig 1- Pfbar Values verses the Decrease over ind layers.
% Fig2- Pfbar Values verses the Cumulative Decrease epi layers.
% Fig3- Pfbar Values verses the Cumulative Decrease over all the layers.
% Fig4- Pfbar Values verses the Cumulative Decrease over ind h1 layers.
% Fig5- Pfbar Values verses the Cumulative Decrease over all h1 the layers.

% clear all
% close all

tstart = 0; tend = 30;           %time start and end

n= 960;

%30 sec blinks [1 hr 4hrs 8 hrs]
%n=[120 480 960]

%6 sec blinks [1 hr 4hrs 8 hrs]
%n=[600 2400 4800]

h0 = 1;                          % initial value
c0 = 1;
h10 = 4e-6;                       % initial h value (cm)
h20 = 4e-6;
h30 = 4e-6;
h40 = 6e-6;
```

```

h50 = 6e-6;
h60 = 6e-6;
h70 = 2e-5;

R = 8.314e7;           %ideal gas constant
Teye = 308;           %corneal surface temperature
PhiA = 3e-4;          %osmolarity
Sc = 1.47;            %surface area cornea

%Rt= 2.15*10^11 to get Pc=0.0694
%Rt= 7.24*10^11 to get Pc=0.0206
Rt = 2.15*10^11;     %resistance to flow through material
                        %below film

epsilon = 7e-4;       % ratio of length (d/L) => (cm/cm)
%epsillon = 7e8;     % m/m
U = 0.5;              % film (cm/ s)
%U = 0.005;          % (m/s)
k = 0.68;             %thermal conductivity befor 0.68 (W/m/K)
Teye-Ts = 10;         %corneal surface temp-saturation temp
p = 1000;             % (kg/m^3)
d = 3.5*10^-6;        % thickness (m)
Lm = 2.3*10^6;        %latent heat of vaporization (J/kg)

%gives A=0.0616
K= 2.4*10^5;          %length evaporation rate from thermal
sigma = 45e-3;        %surface tension (N/m)
mu = 1.3e-3;          % Pa s
%mu = 1.3;           % (m/s)
U0 = 0.005;           % (m/s)
a = 3.484*10^-19;
l = 5*10^-3;          % m

```

```

alpha = 3.59*10^(-3);           %relates evaporative mass flux to
                                %pressure difference

Pf = 0.045;                     %(cm/s)
Vw = 18;
Phii = 0.0003;

J0 = (k*Teye-Ts)/(d*Lm);

%Braun and Smith
%Kbar over 2, 4, 8
Kbar = (k*K)/(d*Lm);           %constitutive equ for evapoatue rate
E = (k*Teye-Ts)/(epsilon*p*U0*d*Lm);           %energy balance
S = (sigma*(epsilon^3))/(mu*U0);           %Normal stress & Kinematic Condition
A = a/(mu*U0*d*1) ;           %tangential immobility
delta = (alpha*mu*U0)/((epsilon^2)*l*Teye-Ts); %conservation of solute

lambda1 = zeros(15, 1);

x1=[0.005:0.001:0.020]; %used to vary Pfbar Values

% cmax = zeros(n, 1);
Pfbar1= zeros(15, 1);
Pc1 = zeros(15, 1);
cumfracepi = zeros(15, 1);
cumfractot = zeros(15, 1);
ltt = zeros(15, 1);

y0 = zeros(n+1, 7);
et = zeros(n+1, 7);
cumdecepi = zeros (n, 15);
cumdectot = zeros (n, 15);
lt = zeros(n, 15);

```

```

tft = zeros (n, 1);
y0(1:9, 1) = [h0; c0; 1; 1; 1; 1; 1; 1; 1];
et(1, 1:7) = [1 1 1 1 1 1 1];

ha = zeros (n+1, 15);           %Find max values in plots on the y-axis
H1a = zeros (n+1, 15);
H1a(1, 1:15) = ones(1, 15);
ha(1, 1:15) = ones(1, 15);

hmin = zeros(n+1, 15);
cmax = zeros(n+1, 15);
H1max = zeros(n+1, 15);
H2max = zeros(n+1, 15);
H3max = zeros(n+1, 15);
H4max = zeros(n+1, 15);
H5max = zeros(n+1, 15);
H6max = zeros(n+1, 15);
H7max = zeros(n+1, 15);
hmin(1, 1:15) = ones(1, 15);
cmax(1, 1:15) = ones(1, 15);
H1max(1, 1:15) = ones(1, 15);
H2max(1, 1:15) = ones(1, 15);
H3max(1, 1:15) = ones(1, 15);
H4max(1, 1:15) = ones(1, 15);
H5max(1, 1:15) = ones(1, 15);
H6max(1, 1:15) = ones(1, 15);
H7max(1, 1:15) = ones(1, 15);
finalosmo=zeros(8, 15);

for k=1:15
    Pfbar1(k)=(x1(k)*Pf*Vw*PhiA)/(epsilon*U0*100);
    Pcl(k) = 2*Pfbar1(k);

```

```

lambda1(k) = (d/h10)*Pfbars(k);

end

for j=1:15
    for i=1:n
        Mytols = odeset('RelTol', 1e-6, 'AbsTol', 1e-7);
        [t, y] = ode15s(@(t, y) tearlayers7(t, y, Pcl(j), E, Kbar, delta, A,
        lambda1(j), h10, h20, h30, h40, h50, h60, h70), [tstart tend],
        y0(1:9, i)); Mytols;
        h = y(:, 1);
        c = y(:, 2) ;
        H1 = y(:, 3) ;
        H2 = y(:, 4);
        H3 = y(:, 5);
        H4 = y(:, 6);
        H5 = y(:, 7);
        H6 = y(:, 8);
        H7 = y(:, 9);

        hmin(i+1, j) = min(h);      %Find max values in plots on the y-axis
        cmax(i+1, j) = max(c);
        H1max(i+1, j) = min(H1);
        H2max(i+1, j) = min(H2);
        H3max(i+1, j) = min(H3);
        H4max(i+1, j) = min(H4);
        H5max(i+1, j) = min(H5);
        H6max(i+1, j) = min(H6);
        H7max(i+1, j) = min(H7);

        ha(i+1, j) = min(h);      %Find max values in plots on the y-axis
        H1a(i+1, j) = min(H1);
    end
end

```

```

y0(1:9, i+1) = [h0; c0; H1max(i+1, j); H2max(i+1, j); H3max(i+1, j);
    H4max(i+1, j); H5max(i+1, j); H6max(i+1, j); H7max(i+1, j)];
tft(i) = [hmin(i+1, j)];
et(i+1, 1:7) = [H1max(i+1, j); H2max(i+1, j); H3max(i+1, j);
    H4max(i+1, j); H5max(i+1, j); H6max(i+1, j); H7max(i+1, j)];
cumdecepi(i, j) = [(H1max(i+1, j)*h10+ H2max(i+1, j)*h20+
    H3max(i+1, j)*h30+ H4max(i+1, j)*h40+ H5max(i+1, j)*h50 +
    H6max(i+1, j)*h60 +H7max(i+1, j)*h70)/(h10 + h20 + h30 + h40 + h50+
    h60 + h70)];
cumdectot(i, j) = [(hmin(i+1, j)*d + H1max(i+1, j)*h10+
    H2max(i+1, j)*h20+ H3max(i+1, j)*h30+ H4max(i+1, j)*h40+
    H5max(i+1, j)*h50 + H6max(i+1, j)*h60 +H7max(i+1, j)*h70)/(d + h10
    + h20 + h30 + h40 + h50 + h60 + h70)];
k = H1max(i+1, j)*h10+ H2max(i+1, j)*h20+ H3max(i+1, j)*h30+
    H4max(i+1, j)*h40+ H5max(i+1, j)*h50 + H6max(i+1, j)*h60
    + H7max(i+1, j)*h70;
lt (i, j) = [k];

```

end

```

cumfracepi(j) = [cumdecepi(n, j)];
cumfractot(j) = [cumdectot(n, j)];
ltt(j) = [lt(n, j)];

```

end

```
p = [0:n]';
```

```

OsmoH1= zeros(n+1, 15);
OsmoH2 = zeros(n+1, 15);
OsmoH3= zeros(n+1, 15);
OsmoH4 = zeros(n+1, 15);
OsmoH5 = zeros(n+1, 15);
OsmoH6 =zeros(n+1, 15);

```

```

OsmoH7 = zeros(n+1, 15);
OsmoTF = zeros(n+1, 15);

%calculates osmolarity for each layer after every blink for all 15 Pfbars
for k=1:n+1
    for f=1:15
        OsmoH1(k, f) = 300/H1max(k, f);
        OsmoH2(k, f) = 300/H2max(k, f);
        OsmoH3(k, f) = 300/H3max(k, f);
        OsmoH4(k, f) = 300/H4max(k, f);
        OsmoH5(k, f) = 300/H5max(k, f);
        OsmoH6(k, f) = 300/H6max(k, f);
        OsmoH7(k, f) = 300/H7max(k, f);
        OsmoTF(k, f) = 300/hmin(k, f);
    end
end

%Calc final osmolarity for each layer for each Pfbar (tf then layers down,
%Pfbar across)
for l=1:15
    finalosmo(1, l) = OsmoTF(n, l);
    finalosmo(2, l) = OsmoH1(n, l);
    finalosmo(3, l) = OsmoH2(n, l);
    finalosmo(4, l) = OsmoH3(n, l);
    finalosmo(5, l) = OsmoH4(n, l);
    finalosmo(6, l) = OsmoH5(n, l);
    finalosmo(7, l) = OsmoH6(n, l);
    finalosmo(8, l) = OsmoH7(n, l);
end

%plot final osmolarities of all layers

```

```

figure
plot( Pfbar1, finalosmo)
xlabel('Blink Number (30 sec intervals)', 'FontSize', 15)
ylabel('Osmolarity', 'FontSize', 15)

```

```

% figure
%   plot(p, H1a(:, 1), 'k-')
% hold on;
%   plot(p, H1a(:, 4), 'b-')
%   plot(p, H1a(:, 9), 'r-')
%   plot(p, H1a(:, 15), 'g-')
% hold off;
%

```

```

% plots cum on subplots if want
%figure
%subplot(2, 3, 2)
%plot(Pfbar1, cumfracepi)
%

```

```

% figure
% plot(Pfbar1, cumfractot)
%

```

```

% figure
% plot(p, H1a)
%

```

```

% figure
% plot(p, ha)

```

```

%plot change in thickness and final dec fraction

```

```

%chnngthickness = (h10+h20+h30+h40+h50+h60+h70)-ltt;

%figure
%[AX,H1,H2] = plotyy(Pfbar1,cumfracepi,Pfbar1,chnngthickness,'plot');
xlabel('Pfbar')
% set(H1,'LineStyle','--')
% set(H2,'LineStyle',':')

```

B.4 Single Blink Cornea

```

% model problem: Osmolarity for tear film
% uses ode solver to compute
% uses tearlayers3.m as a function

clear all
close all

tstart = 0; tend =10000;           %time start and end

h0 = 1;                            % initial value
c0 = 1;
h10 = 4e-6;                         % initial h value (cm)
h20 = 4e-6;
h30 = 4e-6;
h40 = 6e-6;
h50 = 6e-6;
h60 = 6e-6;
h70 = 2e-5;

R = 8.314e7;                       %ideal gas constant

```

```

Teye = 308; %corneal surface temperature
PhiA = 3e-4; %osmolarity
Sc = 1.47; %surface area cornea (cm^2)

%Rt= 2.15*10^11 to get Pc=0.0694
%Rt= 7.24*10^11 to get Pc=0.0206
Rt = 2.15*10^11; %resistance to flow through material
%below film: table 6.2 of F&W

epsilon = 7e-4; % ratio of length (d/L) => (cm/cm)
%epsilon = 7e8; % m/m
U = 0.5; % film (cm/ s)
%U = 0.005; % (m/s)
k = 0.68; %thermal conductivity befor 0.68 (W/m/K)
Teye-Ts = 10; %corneal surface temp-saturation temp
p = 1000; % (kg/m^3)
d = 3.5*10^-6; % thickness (m)
Lm = 2.3*10^6; %latent heat of vaporization (J/kg)

%gives A=0.0616
K= 2.4*10^5; %length evaporation rate from thermal
%adjusting Kbar, gives 2.5e-5
sigma = 45e-3; %surface tension (N/m)
mu = 1.3e-3;
%mu = 1.3; % Pa s
U0 = 0.005; % (m/s)
a = 3.484*10^-19;
l = 5*10^-3; % m
alpha = 3.59*10^(-3); %relates evaporative mass flux to
%pressure difference

```

```

Pf = 0.045; % (cm/s)
Vw = 18; % (cm^3/mol)
Phii = 0.0003;

%Kbar = 1.5*10^4; %Longfei's numbers
%S = 1.5*10^-6;
%E = 328.5;
%A = 6.51*10^-5;
%delta = 153.61; %or 15.36

J0 = (k*Teye-Ts)/(d*Lm);

%Braun and Smith
%Kbar over 2, 4, 8
Kbar = (k*K)/(d*Lm); %constitutive equ for evapoative rate
x = 0.0168;
%Pfbare = 0.009025714285714;
Pfbare = (x*Pf*Vw*PhiA)/(epsilon*U0*100); %cgs units
Pc = 2*Pfbare; %Nondim permeability of the
E = (k*Teye-Ts)/(epsilon*p*U0*d*Lm); %energy balance
S = (sigma*(epsilon^3))/(mu*U0); %Normal stress & Kinematic Condition
A = a/(mu*U0*d*1) ; %tangential immobility
delta = (alpha*mu*U0)/((epsilon^2)*l*Teye-Ts); %conservation of solute
%adelta = (A*delta)^(1/3);

lambda = (d/h10)*Pfbare;
%lambda = (d/h10)*Pf;

%Rt2=(R*Teye)/(2*Vw*Sc*x*Pf);

%y0 = [h c H1 H2 H3 H4 H5 H6 H7] inital values
y0 = [h0; c0; 1; 1; 1; 1; 1; 1; 1];

```

```

%ode45, ode23s, ode15s
Mytols = odeset('RelTol', 1e-6, 'AbsTol', 1e-7);
[t, y] = ode15s(@(t, y) tearlayers7(t, y, Pc, E, Kbar, delta, A, lambda,
    h10, h20, h30, h40, h50, h60, h70), [tstart tend], y0); Mytols;
h = y(:, 1);
c = y(:, 2) ;
H1 = y(:, 3) ;
H2 = y(:, 4);
H3 = y(:, 5);
H4 = y(:, 6);
H5 = y(:, 7);
H6 = y(:, 8);
H7 = y(:, 9);

hmin = min(h); %Find max values in plots on the y-axis
cmax = max(c);
H1max = min(H1);
H2max = min(H2);
H3max = min(H3);
H4max = min(H4);
H5max = min(H5);
H6max = min(H6);
H7max = min(H7);

%use to graph endpoints
% te = [tend, tend, tend, tend, tend, tend, tend]';
% EndPoints1 = [hmin, H1max, H2max, H3max, H4max, H5max];
% EndPoints2 = [1-hmin, 1-H1max, 1-H2max, 1-H3max, 1-H4max, 1-H5max];

figure
set(gca, 'FontSize', 14)
plot(t, h, '-.r', 'linewidth', 2)
%title('Tear Film Thickness', 'FontSize', 16) %Title for the plot

```

```

xlabel('t', 'FontSize', 15)           %Label the horizontal axis
ylabel('h, \phi', 'FontSize', 15)    %Label the vertical axis

hold on;
plot(t, c, '-.b', 'linewidth', 2)
text(tend-0.1, hmin, 'h(t)', 'FontSize', 13) %label functions on plot
text(tend-0.1, cmax, '\phi(t)', 'FontSize', 13)
hold off;

figure
set(gca, 'FontSize', 12)
plot(t, H1, '-.r', 'linewidth', 2)
%title('Relative Corneal Epithelial Cell Thickness', 'FontSize', 16)
xlabel('t ', 'FontSize', 15)         %Label the horizontal axis
ylabel('h_i(t)', 'FontSize', 15)    %Label the vertical axis

hold on;
plot(t, H1, '-.r', 'linewidth', 2)
plot(t, H2, '-.b', 'linewidth', 2)
plot(t, H3, 'r', 'linewidth', 2)
plot(t, H4, 'b', 'linewidth', 2)
plot(t, H5, '-r', 'linewidth', 2)
plot(t, H6, '-r', 'linewidth', 2)
plot(t, H7, '-r', 'linewidth', 2)
% text(tend-0.1, H1max, 'h_1(t)', 'FontSize', 13) %label functions on plot
% text(tend-0.1, H2max, 'h_2(t)', 'FontSize', 13)
% text(tend-0.1, H3max, 'h_3(t)', 'FontSize', 13)
% text(tend-0.1, H4max, 'h_4(t)', 'FontSize', 13)
% text(tend-0.1, H5max, 'h_5(t)', 'FontSize', 13)
hold off;

% figures to plot endpoints of graph produced from these values

```

```

% plot(te, EndPoints1, 'k*')
% title('Relative Corneal Epithelial Cell Thickness in End', 'FontSize',
% 16) %Title for the plot
% xlabel('t ', 'FontSize', 15) %Label the horizontal axis
% ylabel('%h_i(t) from begining', 'FontSize', 15) %Label the vertical axis
%
% figure
% plot(te, EndPoints2, 'r*')
% title('Relative Corneal Epithelial Cell Thickness Decrease %',
% 'FontSize', 16) %Title for the plot
% xlabel('t ', 'FontSize', 15) %Label the horizontal axis
% ylabel('% Decrease', 'FontSize', 15) %Label the vertical axis
%plot(tend, hmin, 'r*', tend, H1max, 'b*', tend, H2max, 'g*', tend,
% H3max, 'y*', tend, H4max, 'm*', tend, H5max, 'k*')

cumdecepi= (H1max*h10+ H2max*h20+ H3max*h30+ H4max*h40+ H5max*h50 +
H6max*h60 +H7max*h70)/(h10 + h20 + h30 + h40 + h50 + h60 + h70);
cumdectot= (hmin*d + H1max*h10+ H2max*h20+ H3max*h30+ H4max*h40+ H5max*h50
+ H6max*h60 +H7max*h70)/(d+h10 + h20 + h30 + h40 + h50 + h60 + h70);

```

B.5 Multiple Blink Cornea

```

% model problem: Multible Blinks
% uses ode solver to compute
% uses tearlayers3.m as a function

clear all
close all

tstart = 0; tend =30; %time start and end
%vary time intervals
n = 480; %amount of blinks

```

```

h0 = 1; % initial value
c0 = 1;
h10 = 4e-6; % initial h value (cm)
h20 = 4e-6;
h30 = 4e-6;
h40 = 6e-6;
h50 = 6e-6;
h60 = 6e-6;
h70 = 2e-5;

R = 8.314e7; %ideal gas constant
Teye = 308; %corneal surface temperature
PhiA = 3e-4; %osmolarity
Sc = 1.47; %surface area cornea (cm^2)

Rt = 2.15*10^11; %resistance to flow through material
%below film: table 6.2 of F&W

epsilon = 7e-4; % ratio of length (d/L) => (cm/cm)
U = 0.5; % film (cm/ s)
k = 0.68; %thermal conductivity befor 0.68 (W/m/K)
Teye-Ts = 10; %corneal surface temp-saturation temp
p = 1000; % (kg/m^3)
d = 3.5*10^-6; % thickness (m)
Lm = 2.3*10^6; %latent heat of vaporization (J/kg)

K= 2.4*10^5; %length evaporation rate from thermal
%adjusting Kbar, gives 2.5e-5
sigma = 45e-3; %surface tension (N/m)
mu = 1.3e-3;
%mu = 1.3; % Pa s
U0 = 0.005; % (m/s)
a = 3.484*10^-19;

```

```

l = 5*10^-3; % m
alpha = 3.59*10^(-3); %relates evaporative mass flux to
%pressure difference

Pf = 0.045; % (cm/s)
Vw = 18; % (cm^3/mol)
Phii = 0.0003;

J0 = (k*Teye-Ts)/(d*Lm);

%Braun and Smith
Kbar = (k*K)/(d*Lm); %constitutive equ for evapoative rate
x = 0.0168;
Pfbar = (x*Pf*Vw*PhiA)/(epsilon*U0*100); %cgs units
Pc = 2*Pfbar; %Nondim permeability of the
E = (k*Teye-Ts)/(epsilon*p*U0*d*Lm); %energy balance
S = (sigma*(epsilon^3))/(mu*U0); %Normal stress & Kinematic Condition
A = a/(mu*U0*d*l) ; %tangential immobility
delta = (alpha*mu*U0)/((epsilon^2)*l*Teye-Ts); %conservation of solute
%adelta = (A*delta)^(1/3);

lambda = (d/h10)*Pfbar;

%y0 = [h c H1 H2 H3 H4 H5] inital values
y0 = zeros(n+1, 7);
et = zeros(n+1, 7);
Osmo = zeros(n+1, 8);
cumdecepi = zeros (n, 1);
cumdectot = zeros (n, 1);
tft = zeros (n, 1);
y0(1:9, 1) = [h0; c0; 1; 1; 1; 1; 1; 1; 1];
et(1, 1:7) = [1 1 1 1 1 1 1];

```

```

for i=1:n
    Mytols = odeset('RelTol', 1e-6, 'AbsTol', 1e-7);
    [t, y] = ode15s(@(t, y) tearlayers7(t, y, Pc, E, Kbar, delta, A,
        lambda, h10, h20, h30, h40, h50, h60, h70), [tstart tend],
        y0(1:9, i)); Mytols;
    h = y(:, 1);
    c = y(:, 2) ;
    H1 = y(:, 3) ;
    H2 = y(:, 4);
    H3 = y(:, 5);
    H4 = y(:, 6);
    H5 = y(:, 7);
    H6 = y(:, 8);
    H7 = y(:, 9);

    hmin = min(h);           %Find max values in plots on the y-axis
    cmax = max(c);
    H1max = min(H1);
    H2max = min(H2);
    H3max = min(H3);
    H4max = min(H4);
    H5max = min(H5);
    H6max = min(H6);
    H7max = min(H7);

    y0(1:9, i+1) = [h0; c0; H1max; H2max; H3max; H4max; H5max; H6max;
        H7max];
    tft(i) = [hmin];
    et(i+1, 1:7) = [H1max; H2max; H3max; H4max; H5max; H6max; H7max];
    Osmo(i+1, 1:8) = [300/hmin; 300/H1max; 300/H2max; 300/H3max;
        300/H4max; 300/H5max; 300/H6max; 300/H7max];

```

```

    cumdecepi(i) = [(H1max*h10+ H2max*h20+ H3max*h30+ H4max*h40+ H5max*h50
        + H6max*h60 +H7max*h70)/(h10 + h20 + h30 + h40 + h50 + h60 + h70)];
    cumdectot(i) = [(hmin*d + H1max*h10+ H2max*h20+ H3max*h30+ H4max*h40+
        H5max*h50 + H6max*h60 +H7max*h70)/(d + h10 + h20 + h30 + h40 + h50
        + h60 + h70)];

end

p = [1:n]';
figure
for k=1:n
    plot( p(k), et(k, :), '-.k', 'linewidth', 2)
    hold on;
end
xlabel('Blink Number (30 sec intervals)', 'FontSize', 15)
ylabel('h_i(t)', 'FontSize', 15)
hold off;

figure
for s = 1:n
    plot(p(s) , Osmo(s, :), '-.k','linewidth', 2)
    hold on;
end
xlabel('Blink Number (30 sec intervals)', 'FontSize', 15)
ylabel('Osmolarity', 'FontSize', 15)
hold off;

%figure
%plot( p, cumdecepi, '-.k', 'linewidth', 2)

%figure
%plot( p, cumdectot, '-.k', 'linewidth', 2)

```

```
%figure
%plot( p, tft, '-.k', 'linewidth', 2)
```

B.6 Equations for Conjunctiva

```
function f =tearlayers4(t, y, Pc, E, Kbar, delta, A, lambda, y10, y20, y30,
y40)
```

```
h = y(1);
c = y(2) ;
Y1 = y(3) ;
Y2 = y(4);
Y3 = y(5);
Y4 = y(6);
```

```
f(1, 1) = Pc*(c-1) -E/(Kbar + h)*(1-delta*A*h^(-3));
f(2, 1) = (E/(Kbar + h)*(1-delta*A*h^(-3)) -Pc*(c-1))*c/h ;
f(3, 1) = lambda*(4/Y1 - 4*c - 0.5/Y2 + 0.5/Y1);
f(4, 1) = lambda*(.5*y10/y20)*((1/Y2) - 1/(Y1) - (1/(Y3)) + (1/(Y2)));
f(5, 1) = lambda*(.5*y10/y30)*((1/(Y3)) - 1/(Y2) - (1/(Y4)) + (1/(Y3)));
f(6, 1) = lambda*(.5*y10/y40)*((1/Y4) - (1/Y3)) - (y10/y40)*(1 - (1/Y4));
```

B.7 Single Blink Conjunctiva

```
% model problem: Single Blink Model for the Conjunctiva
% uses ode solver to compute
% uses tearlayers4.m as a function

clear all
%close all
```

```

tstart = 0; tend =90;           %time start and end
%vary time check early ones

h0 = 1;                         % initial value
c0 = 1;
y10 = 6e-6;                     % initial h value (cm)
y20 = 8e-6;
y30 = 8e-6;
y40 = 20e-6;

R = 8.314e7;                    %ideal gas constant
Teye = 308;                     %corneal surface temperature
PhiA = 3e-4;                    %osmolarity
Sc = 1.47;                      %surface area cornea (cm^2)

Rt = 2.15*10^11;               %resistance to flow through material
%below film: table 6.2 of F&W

epsilon = 7e-4;                % ratio of length (d/L) => (cm/cm)
%epsillon = 7e8;              % m/m
U = 0.5;                       % film (cm/ s)
%U = 0.005;                   % (m/s)
%k = 0.68;                    %thermal conductivity 0.68 (W/m/K)
k = 1.2143;
Teye-Ts = 10;                  %corneal surface temp-saturation temp
p = 1000;                      % (kg/m^3)
d = 3.5*10^-6;                 % thickness (m)
Lm = 2.3*10^6;                 %latent heat of vaporization (J/kg)

%gives A=0.0616

```

```

%K= 2.4*10^5; %length evaporation rate from thermal
K = 4.2857e5; %adjusting Kbar, gives 2.5e-5
               %adjusting Kbar, gives TR 1.4e-5

sigma = 45e-3; %surface tension (N/m)
mu = 1.3e-3;
%mu = 1.3; % Pa s
U0 = 0.005; % (m/s)
a = 3.484*10^-19;
l = 5*10^-3; % m
alpha = 3.59*10^(-3); %relates evaporative mass flux to
                       %pressure difference

Pf = 0.045; % (cm/s)
Vw = 18; % (cm^3/mol)
Phii = 0.0003;

%Kbar = 1.5*10^4; %Longfei's numbers
%S = 1.5*10^-6;
%E = 328.5;
%A = 6.51*10^-5;
%delta = 153.61; %or 15.36

J0 = (k*Teye-Ts)/(d*Lm);

%Braun and Smith
%Kbar over 2, 4, 8
Kbar = (k*K)/(d*Lm); %constitutive equ for evapoative rate
x = 0.0168;
%Pfbar = 0.009025714285714;
Pfbar = (x*Pf*Vw*PhiA)/(epsilon*U0*100); %cgs units
Pc = 4*Pfbar; %Nondim permeability of the
E = (k*Teye-Ts)/(epsilon*p*U0*d*Lm); %energy balance

```

```

S = (sigma*(epsilon^3))/(mu*U0);           %Normal stress & Kinematic Condition
A = a/(mu*U0*d*1) ;                       %tangential immobility
delta = (alpha*mu*U0)/((epsilon^2)*l*Teye_Ts); %conservation of solute
%adelta = (A*delta)^(1/3);

lambda = (d/y10)*Pfbars;

%y0 = [h c Y1 Y2 Y3 Y4] initial values
y0 = [h0; c0; 1; 1; 1; 1];

%ode45, ode23s, ode15s
Mytols = odeset('RelTol', 1e-6, 'AbsTol', 1e-7);
[t, y] = ode15s(@(t, y) tearlayers4(t, y, Pc, E, Kbar, delta, A, lambda,
    y10, y20, y30, y40), [tstart tend], y0); Mytols;
h = y(:, 1);
c = y(:, 2) ;
Y1 = y(:, 3) ;
Y2 = y(:, 4);
Y3 = y(:, 5);
Y4 = y(:, 6);

hmin = min(h);                             %Find max values in plots on the y-axis
cmax = max(c);
Y1max = min(Y1);
Y2max = min(Y2);
Y3max = min(Y3);
Y4max = min(Y4);

%use to graph endpoints
% te = [tend, tend, tend, tend, tend, tend]';
% EndPoints1 = [hmin, Y1max, Y2max, Y3max, Y4max];

```

```

% EndPoints2 = [1-hmin, 1-Y1max, 1-Y2max, 1-Y3max, 1-Y4max, 1-Y5max];

%figure
subplot(2, 2, 3)
set(gca, 'FontSize', 12)
plot(t, h, '-.r', 'linewidth', 2)
title('(c)', 'FontSize', 11)           %Title for the plot
xlabel('t', 'FontSize', 12)           %Label the horizontal axis
ylabel('h, c', 'FontSize', 12)        %Label the vertical axis

hold on;
plot(t, c, '-.b', 'linewidth', 2)
    %text(tend-0.1, hmin, 'h(t)', 'FontSize', 12)    %label functions on plot
    %text(tend-0.1, cmax, '\phi(t)', 'FontSize', 12)
hold off;

subplot(2, 2, 4)
set(gca, 'FontSize', 12)
plot(t, Y1, '-.r', 'linewidth', 2)
title('(d)', 'FontSize', 11) %Title for the plot
xlabel('t', 'FontSize', 12)           %Label the horizontal axis
ylabel('y-i(t)', 'FontSize', 12)      %Label the vertical axis

hold on;
plot(t, Y1, '-.r', 'linewidth', 2)
plot(t, Y2, '-.b', 'linewidth', 2)
plot(t, Y3, 'r', 'linewidth', 2)
plot(t, Y4, 'b', 'linewidth', 2)
% text(tend-0.1, Y1max, 'y-1(t)', 'FontSize', 13) %label functions on plot
% text(tend-0.1, Y2max, 'y-2(t)', 'FontSize', 13)
% % text(tend-0.1, H3max, 'y-3(t)', 'FontSize', 13)
% % text(tend-0.1, H4max, 'y-4(t)', 'FontSize', 13)

```

```

hold off;

% figures to plot endpoints of graph produced from these values
% plot(te, EndPoints1, 'k*')
% title('Relative Corneal Epithelial Cell Thickness in End', 'FontSize',
% 16) %Title for the plot
% xlabel('t ', 'FontSize', 15) %Label the horizontal axis
% ylabel('%h_i(t) from begining', 'FontSize', 15)%Label the vertical axis
%
% figure
% plot(te, EndPoints2, 'r*')
% title('Relative Corneal Epithelial Cell Thickness Decrease %',
% 'FontSize', 16) %Title for the plot
% xlabel('t ', 'FontSize', 15) %Label the horizontal axis
% ylabel('% Decrease', 'FontSize', 15) %Label the vertical axis

% plot(tend, hmin, 'r*', tend, H1max, 'b*', tend, H2max, 'g*', tend,
% H3max, 'y*', tend, H4max, 'm*', tend, H5max, 'k*')

```

B.8 Multiple Blink Conjunctiva

```

% model problem: Multiple Blink Model for the Conjunctiva
% uses ode solver to compute
% uses tearlayers4.m as a function

clear all
%close all

tstart = 0; tend =30; %time start and end
%vary time check early ones

n = 480; %amount of blinks

```

```

h0 = 1; % initial value
c0 = 1;
y10 = 6e-6; % initial h value (cm)
y20 = 8e-6;
y30 = 8e-6;
y40 = 20e-6;

R = 8.314e7; %ideal gas constant
Teye = 308; %corneal surface temperature
PhiA = 3e-4; %osmolarity
Sc = 1.47; %surface area cornea (cm^2)

Rt = 2.15*10^11; %resistance to flow through material
%below film: table 6.2 of F&W

epsilon = 7e-4; % ratio of length (d/L) => (cm/cm)
%epsillon = 7e8; % m/m
U = 0.5; % film (cm/ s)
%U = 0.005; % (m/s)
k = 0.68; %thermal conductivity befor 0.68 (W/m/K)
Teye_Ts = 10; %corneal surface temp-saturation temp
p = 1000; % (kg/m^3)
d = 3.5*10^-6; % thickness (m)
Lm = 2.3*10^6; %latent heat of vaporization (J/kg)

%gives A=0.0616
%K= 2.4*10^5; %length evaporation rate from thermal
%adjusting Kbar, gives TR 2.5e-5
K = 4.2857e5; %adjusting Kbar, gives TR 1.4e-5

```

```

sigma = 45e-3; %surface tension (N/m)
mu = 1.3e-3;
%mu = 1.3; % Pa s
U0 = 0.005; % (m/s)
a = 3.484*10^-19;
l = 5*10^-3; % m
alpha = 3.59*10^(-3); %relates evaporative mass flux to
%pressure difference

Pf = 0.045; % (cm/s)
Vw = 18; % (cm^3/mol)
Phii = 0.0003;

J0 = (k*Teye-Ts)/(d*Lm);

%Braun and Smith
%Kbar over 2, 4, 8
Kbar = (k*K)/(d*Lm); %constitutive equ for evapoative rate
x = 0.0168;
%Pfbar = 0.009025714285714;
Pfbar = (x*Pf*Vw*PhiA)/(epsilon*U0*100); %cgs units
Pc = 4*Pfbar; %Nondim permeability of the
E = (k*Teye-Ts)/(epsilon*p*U0*d*Lm); %energy balance
S = (sigma*(epsilon^3))/(mu*U0); %Normal stress & Kinematic Condition
A = a/(mu*U0*d*l) ; %tangential immobility
delta = (alpha*mu*U0)/((epsilon^2)*l*Teye-Ts); %conservation of solute
%adelta = (A*delta)^(1/3);

lambda = (d/y10)*Pfbar;

%y0 = [h c Y1 Y2 Y3 Y4] inital values
y0 = zeros(6, n+1);

```

```

et = zeros(n+1, 4);
Osmo = zeros(n+1, 5);
cumdecepi = zeros (n, 1);
cumdectot = zeros (n, 1);
tft = zeros (n, 1);
y0(1:6, 1) = [h0; c0; 1; 1; 1; 1];
et(1, 1:4) = [1 1 1 1];
Osmo(1, 1:5) = [300 300 300 300 300];

for i=1:n
    Mytols = odeset('RelTol', 1e-6, 'AbsTol', 1e-7);
    [t, y] = ode15s(@(t, y) tearlayers4(t, y, Pc, E, Kbar, delta, A,
        lambda, y10, y20, y30, y40), [tstart tend], y0(1:6, i)); Mytols;
    h = y(:, 1);
    c = y(:, 2) ;
    Y1 = y(:, 3) ;
    Y2 = y(:, 4);
    Y3 = y(:, 5);
    Y4 = y(:, 6);

    hmin = min(h); %Find max values in plots on the y-axis
    cmax = max(c);
    Y1max = min(Y1);
    Y2max = min(Y2);
    Y3max = min(Y3);
    Y4max = min(Y4);

    y0(1:6, i+1) = [h0; c0; Y1max; Y2max; Y3max; Y4max];
    et(i+1, 1:4) = [Y1max; Y2max; Y3max; Y4max];
    tft(i) = [hmin];
    Osmo(i+1, 1:5) = [300/hmin; 300/Y1max; 300/Y2max; 300/Y3max;

```

```

    300/Y4max];
cumdecepi(i) = [(Y1max*y10+ Y2max*y20+ Y3max*y30+ Y4max*y40)/(y10 +
    y20 + y30 + y40)];
cumdectot(i) = [(hmin*d + Y1max*y10+ Y2max*y20+ Y3max*y30+ Y4max*y40)/
    (d + y10 + y20 + y30 + y40)];

end

p = [1:n]';
%figure
subplot(4, 2, 7)
for q=1:n
    plot( p(q), et(q, :), '-.k', 'linewidth', 2)
    hold on;
end
title('(g)', 'FontSize', 11)
xlabel('Blink Number', 'FontSize', 12)
ylabel('y_i(t)', 'FontSize', 12)
hold off;

subplot(4, 2, 8)
for s = 1:n
    plot(p(s) , Osmo(s, :), '-.k', 'linewidth', 2)
    hold on;
end
title('(h)', 'FontSize', 11)
xlabel('Blink Number', 'FontSize', 12)
ylabel('Osmolarity', 'FontSize', 12)

```

```
hold off;

%figure
%plot( p, cumdecepi, '-.k', 'linewidth', 2)

%figure
%plot( p, cumdectot, '-.k', 'linewidth', 2)

%figure
%plot( p, tft, '-.k', 'linewidth', 2)
```

Appendix C

PARAMETERS FOR CHAPTER 3

Table C.1: Initial Concentrations in the tear film. These values were taken from the initial concentrations in [3]. The initial osmolarity in the tear film is 300 mOsm. Note: Osmolarity is the sum of the concentrations of sodium, chloride, bicarbonate, and lactate.

Dimensional parameters		
Parameter	Description	Value
$C_{Na,0}(0)$	Initial concentration of sodium	150 mM
$C_{Cl,0}(0)$	Initial concentration of chloride	137.9 mM
$C_{B,0}(0)$	Initial concentration of bicarbonate	12.1 mM
$C_{H,0}(0)$	Initial concentration of hydronium	2.512×10^{-8} mM
$C_{G,0}$	Concentration of glucose	0 mM
$C_{L,0}$	Concentration of lactate	0 mM
$P_{O,0}(0)$	Initial partial pressure of oxygen	155 mm Hg
$P_{C,0}(0)$	Initial partial pressure of carbon dioxide	0.5 mm Hg
$h_0(0)$	Tear Film thickness [28]	3.5 μ m

Table C.2: Henry's Constants and valence values.

Parameters		
Parameter	Description	Value
$k_{H,O}$	Henry's Constant for O ₂	769.23 $\frac{\text{L}\cdot\text{atm}}{\text{mol}}$
$k_{H,C}$	Henry's Constant for CO ₂	29.41 $\frac{\text{L}\cdot\text{atm}}{\text{mol}}$
z_{Na}	valence for sodium	+1
z_{Cl}	valence for chloride	-1
z_B	valence for bicarbonate	-1
z_L	valence for lactate	+1
z_G	valence for glucose	0
z_O	valence for oxygen	0
z_C	valence for carbon dioxide	0
z_H	valence for hydronium	+1

Table C.3: Initial Concentrations in the epithelial cells. Here $j = 1$ to $j = 7$. These values were taken from the steady state results in [3].

Parameters		
Parameter	Description	Value
$C_{Na,j}(0)$	Initial concentration of sodium	143 mM
$C_{Cl,j}(0)$	Initial concentration of chloride	107 mM
$C_{B,j}(0)$	Initial concentration of bicarbonate	19 mM
$C_{H,j}(0)$	Initial concentration of hydronium	2.512×10^{-8} mM
$C_{G,j}(0)$	Initial concentration of glucose	4.4 mM
$C_{L,j}(0)$	Initial concentration of lactate	16.5 mM
$P_{O,j}(0)$	Initial partial pressure of oxygen	130 mm Hg
$P_{C,j}(0)$	Initial partial pressure of carbon dioxide	6 mm Hg
$h_1(0)$	Epithelial $j = 1$ initial thickness	4 μm
$h_2(0)$	Epithelial $j = 2$ initial thickness	4 μm
$h_3(0)$	Epithelial $j = 3$ initial thickness	4 μm
$h_4(0)$	Epithelial $j = 4$ initial thickness	6 μm
$h_5(0)$	Epithelial $j = 5$ initial thickness	6 μm
$h_6(0)$	Epithelial $j = 6$ initial thickness	6 μm
$h_7(0)$	Epithelial $j = 7$ initial thickness	20 μm

Table C.4: Constants concentrations in the stroma. These values were taken from the steady state results in [3].

Parameters		
Parameter	Description	Value
$C_{Na,8}$	Concentration of sodium	142.5 mM
$C_{Cl,8}$	Concentration of chloride	106 mM
$C_{B,8}$	Concentration of bicarbonate	19 mM
$C_{H,8}$	Concentration of hydronium	2.512×10^{-8} mM
$C_{G,8}$	Concentration of glucose	4.4 mM
$C_{L,8}$	Concentration of lactate	16 mM
$P_{O,8}$	Partial pressure of oxygen	100 mm Hg
$P_{C,8}$	Partial pressure of carbon dioxide	11 mm Hg

Table C.5: Parameters in proposed model. These values were taken from [3].

Parameter	Value
D_0k_0 (Barrer)	18.8
D_Ck_C (Barrer)	376
$D_L \times 10^6 \frac{\text{cm}}{\text{s}}$	4.4
$D_G \times 10^6 \frac{\text{cm}}{\text{s}}$	3
$D_H \times 10^6 \frac{\text{cm}}{\text{s}}$	0.19
$D_B \times 10^6 \frac{\text{cm}}{\text{s}}$	0.22
$D_{Na} \times 10^6 \frac{\text{cm}}{\text{s}}$	9
$D_{Cl} \times 10^6 \frac{\text{cm}}{\text{s}}$	9
$\frac{K}{\mu} \times 10^{15} \frac{\text{cm}^2}{\text{dyne s}}$	27
$Q_O^{max} \times 10^9 \frac{\text{mol}}{\text{cm}^2 \text{s}}$	11.6
$Q_O^{min} \times 10^9 \frac{\text{mol}}{\text{cm}^2 \text{s}}$	4.83
$L_p \times 10^9 \frac{\text{cm}^3}{\text{dyne s}}$	6.1
σ_{Na}	0.79
σ_{Cl}	0.79
σ_L	0.1
σ_B	0.79
σ_O	0.79
σ_C	0.79
σ_H	0.79
σ_G	1
$\omega_{Na}RT \times 10^5 \frac{\text{cm}}{\text{s}}$	0.019
$\omega_{Cl}RT \times 10^5 \frac{\text{cm}}{\text{s}}$	0.019
$\omega_LRT \times 10^5 \frac{\text{cm}}{\text{s}}$	0
$\omega_BRT \times 10^5 \frac{\text{cm}}{\text{s}}$	0.019
$\omega_HRT \times 10^5 \frac{\text{cm}}{\text{s}}$	0.019
$\omega_GRT \times 10^5 \frac{\text{cm}}{\text{s}}$	0
$\omega_O \frac{\text{mol O}_2 \text{cm}}{\text{s mm Hg cm}^3}$	$\frac{D_Ok_O}{\Delta x}$
$\omega_C \frac{\text{mol O}_2 \text{cm}}{\text{s mm Hg cm}^3}$	$\frac{D_Ck_C}{\Delta x}$
$J_a \times 10^{10} \frac{\text{mol}}{\text{cm}^2 \text{s}}$	0.16 (chloride)
$\rho_d (\frac{\text{g}}{\text{cm}^3})$	1.49
γ (Pa)	2.41×10^6
K_O^O (mm Hg)	2.2
K_O^L (mm Hg)	2.2
K_G^O (mM)	0.4
K_G^L (mM)	0.4
K_{pH}	0.1
pK_B	6.04
$s_C \frac{\text{mM}}{\text{mm Hg}}$	0.0258

BIBLIOGRAPHY

- [1] K. N. Winter, D. M. Anderson, and R. J. Braun. A model for wetting and evaporation of a post-blink precorneal tear film. *Math. Med. Biol.*, 27:211–25, 2010.
- [2] V.S. Ajaev and G.M. Homsy. Steady vapor bubbles in rectangular microchannels. *J. Coll. Interface Sci.*, 240:259–71, 2001.
- [3] B. K. Leung, J. A. Bonanno, and C. J. Radke. Oxygen-deficient metabolism and corneal edema. *Prog. Ret. Eye. Res.*, 30:471–492, 2011.
- [4] National Eye Institute. Ref number: Nea05, 2013.
- [5] P. E. King-Smith, P. Ramamoorthy, K. K. Nichols, R. J. Braun, and J. J. Nichols. If tear evaporation is so high, why is tear osmolarity so low? *6th International Conference on the Tear Film and Ocular Surface: Basic Science and Clinical Relevance*, Poster 43:(abstract), 2010.
- [6] M. H. Levin and A. S. Verkman. Aquaporin-dependent water permeation at the mouse ocular surface: In vivo microfluorometric measurements in cornea and conjunctiva. *Invest. Ophthalmol. Vis. Sci.*, 45:4423–32, 2004.
- [7] R. J. Braun. Dynamics of the tear film. *Annu. Rev. Fluid Mech.*, 44:267–97, 2012.
- [8] A Lens. *Ocular Anatomy and Physiology*. SLACK, 1999.
- [9] Tiffany-J.M. Gouveia S.M. Yokoi N. Bron, A.J. and L.W. Voon. Functional aspects of the tear film lipid layer. *Exp Eye Res*, 78:347–360, 2004.
- [10] M. A. Lemp et al. The definition and classification of dry eye disease: Report of the Definition and Classification Subcommittee of the International Dry Eye WorkShop. *Ocul. Surf.*, 5:75–92, 2007.
- [11] H. Liu, C. Begley, M. Chen, A. Bradley, J. Bonanno, N. A. McNamara, J. D. Nelson, and T. Simpson. A link between tear instability and hyperosmolarity in dry eye. *Invest. Ophthalmol. Vis. Sci.*, 50:3671–79, 2009.
- [12] I.K. Gipson. The ocular surface: The challenge to enable and protect vision. *Investigative Ophthalmology and Visual Science*, 48(10):4391–98, 2007.

- [13] D.A. Dartt. Regulation of mucin and fluid secretion by conjunctival epithelial cells. *Progress in retinal and eye research*, 21(6):555–576, 2002.
- [14] B. Govindarajan and I.K. Gipson. Membrane-tethered mucins have multiple functions on the ocular surface. *Exp. Eye Res.*, 90:655–93, 2010.
- [15] Tripathi-R. Bron, A. and B. Tripathi. *Wolff’s anatomy of the eye and orbit*. Chapman and Hall Medical, 8th edition, 1997.
- [16] Karamoko-I. Baudouin C. Francoz, M. and A. Labbe. Ocular surface epithelial thickness evaluation with spectra domain optical coherence tomography. *Investigative Ophthalmology and Visual Science*, 52(12):9116–123, November 2011.
- [17] C.W. Oyster. *The Human Eye: Structure and Function*. Sinauer Associates, 1999.
- [18] Eds Moses, R.A. *Alder’s Physiology of the eye*. St. Louis: C.V. Mosby, 7 edition, 1981.
- [19] Z. Chen, L. Tong, Z. Li, K.-C. Yoon, H. Qi, W. Farley, D.-Q. Li, and S. C. Plugfelder. Hyperosmolarity-induced cornification of human corneal epithelial cells is regulated by JNK MAPK. *Invest. Ophthalmol. Vis. Sci.*, 49:539–49, 2008.
- [20] D.L. Nelson and M.M. Cox. *Lehninger: Principles of Biochemistry*. W.H. Freeman and Company, 5 edition, 2008.
- [21] I. Fatt and B.A. Weissman. *Physiology of the eye – An introduction to the vegetative functions*. Butterworth-Heinemann, Boston, 2nd edition, 1992.
- [22] E. A. Gaffney, J. M. Tiffany, N. Yokoi, and A. J. Bron. A mass and solute balance model for tear volume and osmolarity in the normal and the dry eye. *Prog. Retinal Eye Res.*, 29:59–78, 2010.
- [23] C.W. Oyster. *The Human Eye – Structure and Function*. Sinauer, Sunderland, MA, 1999.
- [24] D. A. Dartt. Regulation of mucin and fluid secretion by conjunctival epithelial cells. *Prog. Ret. Eyt Res.*, 21:555–76, 2002.
- [25] L. Li and R. J. Braun. A model for the tear film including heat transfer from the eye. *Phys. Fluids*, 24:062103, 2012.
- [26] B. R. Masters and A. A. Thaer. In vivo human corneal confocal microscopy of identical fields of subepithelial nerve plexus, basal epithelial , and wing cells at different times. *Microscopy Research and Technique*, 29:350–356, 1994.
- [27] B. Nichols, C. R. Dawson, and B. Togni. Surface features of the conjunctiva and cornea. *Invest. Ophthalmol. Vis. Sci.*, 24:570–6, 1983.

- [28] P.E. King-Smith, B.A. Fink, R.M. Hill, K.W. Koelling, and J.M. Tiffany. The thickness of the tear film. *Curr. Eye Res.*, 29:357–68, 2004.
- [29] O. Kedem and A. Katchalsky. Thermodynamic analysis of the permeability of biological membranes to non-electrolytes. *Biochim Biophys Acta*, 27:229–246, 1958.
- [30] K. L. Miller, K. A. Polse, and C. J. Radke. Black line formation and the “perched” human tear film. *Curr. Eye Res.*, 25:155–62, 2002.
- [31] M. A. Lemp, A. J. Bron, C. Baudouin, J. M. Benítez del Castillo, , D. Geffen, G. N. Foulks J. Tauber, J. S. Pepose, and B. D. Sullivan. Tear osmolarity in the diagnosis and management of dry eye disease. *Am. J. Ophthalmol.*, 151:792–8, 2011.
- [32] B. D. Sullivan, D. Whitmer, K. K. Nichols, A. Tomlinson, G. N. Foulks, G. Geerling, J. S. Pepose, V. Kosheleff, A. Porreco, and M. A. Lemp. An objective approach to dry eye disease severity. *Invest. Ophthalmol. Vis. Sci.*, 51:6125–30, 2010.
- [33] V. Zubkov, C. J. W. Breward, and E. A. Gaffney. Surfactant and osmolarity transport in the tear film. (*in preparation*), 2011.
- [34] J.M. Tiffany. The viscosity of human tears. *Intl. Ophthalmol.*, 15:371–6, 1991.
- [35] B. Nagyová and J. M. Tiffany. Components of tears responsible for surface tension. *Curr. Eye Res.*, 19:4–11, 1999.
- [36] J. A. Scott. A finite element model of heat transport in the human eye. *Phys. Med. Biol.*, 33:227–41, 1988.